SKF®

The Bearing Axial Cracks Root Cause Hypothesis of

Frictional Surface Crack Initiation and Corrosion Fatigue Driven Crack Growth

Presented at the NREL 2011 Wind Turbine Tribology Seminar, Broomfield/CO

Presented by Jürgen Gegner and Wolfgang Nierlich

2011-11-16

SKF

Contents

1

Appearance and Analysis of WEC Premature Bearing Failures

Visual Failure Pattern

axial raceway cracks of <1 mm to >20 mm length

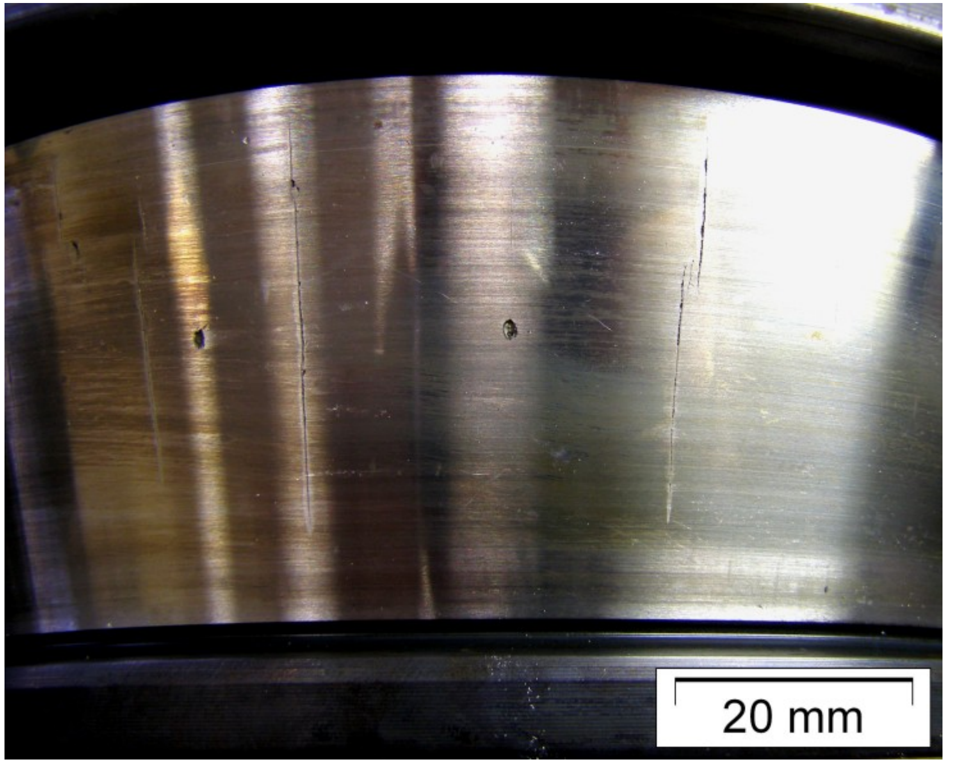

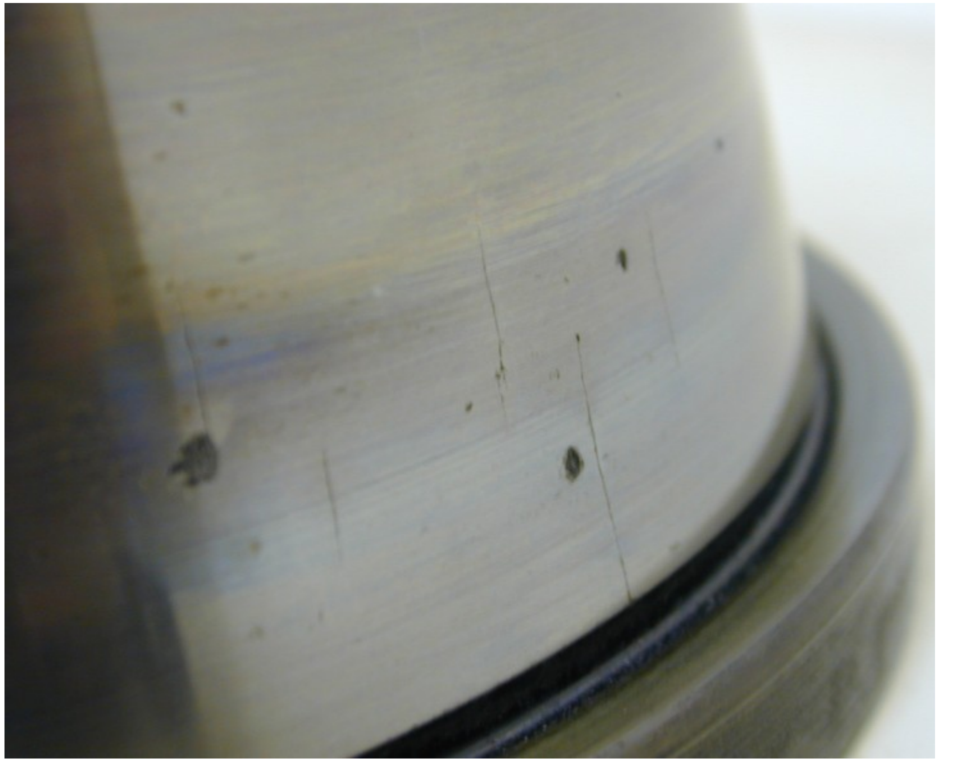

Visual Failure Pattern

axial raceway cracks of <1 mm to >20 mm length

Ÿ partly with shell-shaped spallings

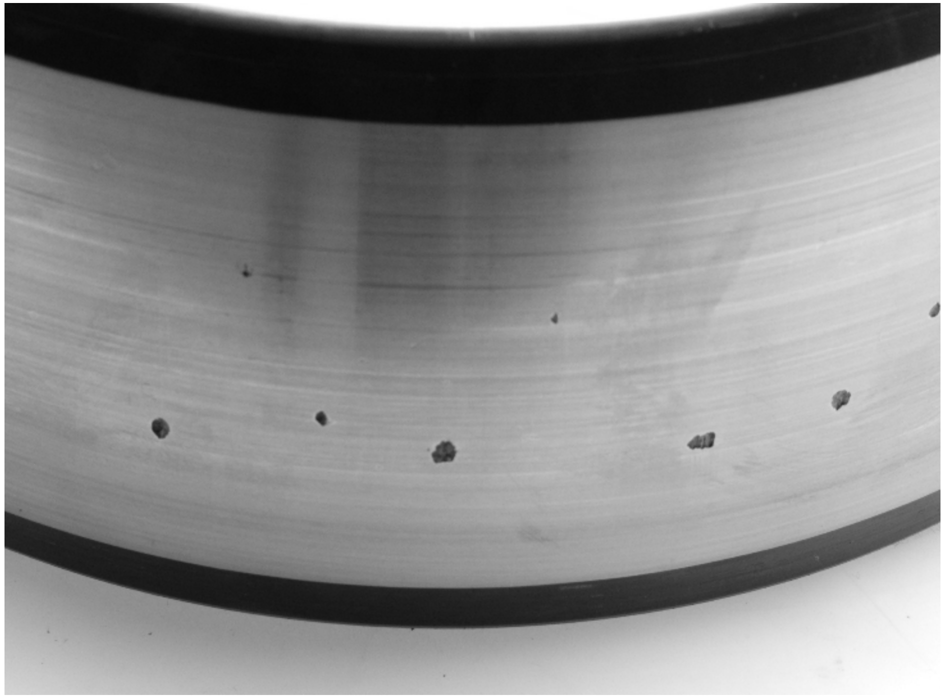

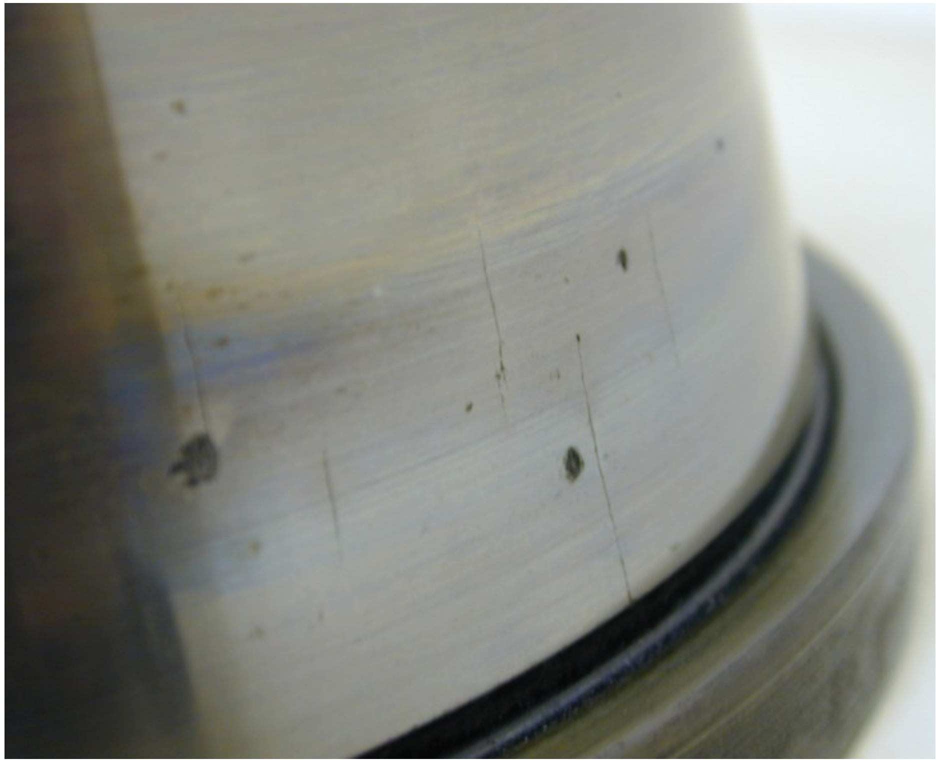

Visual Failure Pattern

axial raceway cracks of <1 mm to >20 mm length

Ÿ partly with shell-shaped spallings from crack returns

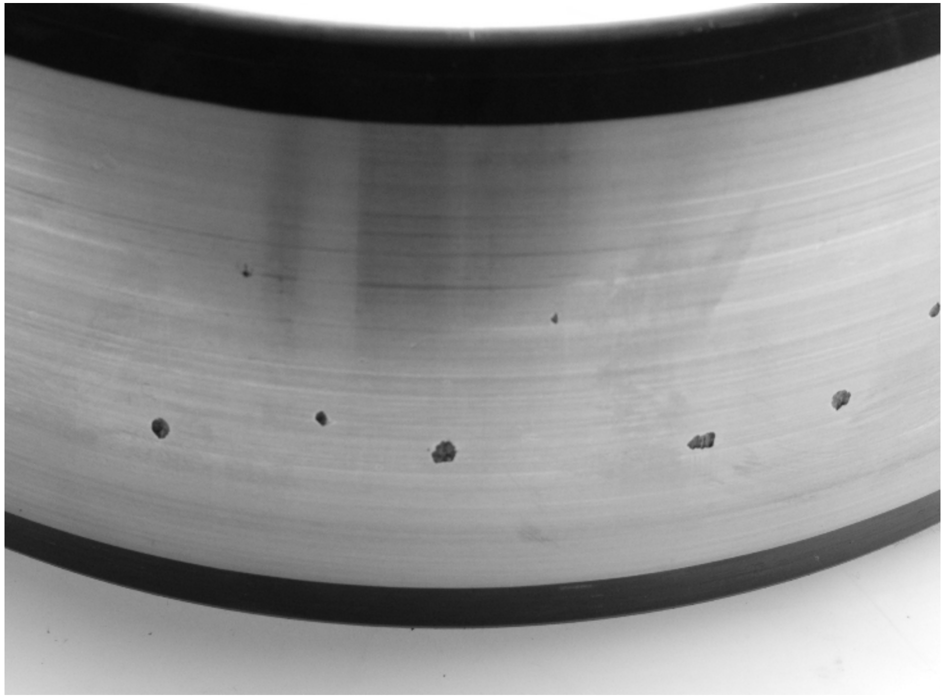

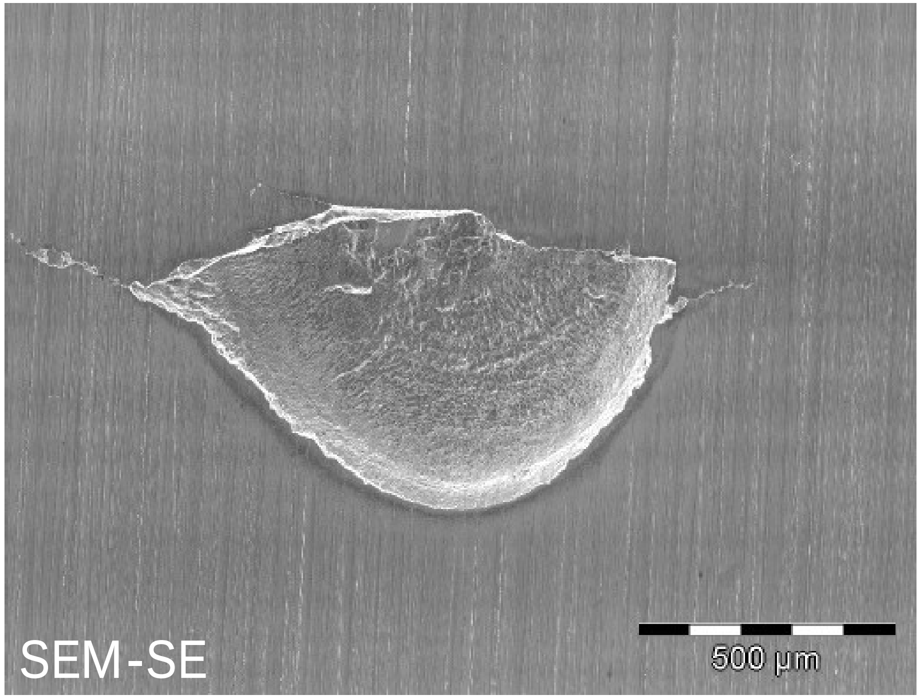

Visual Failure Pattern

axial raceway cracks of <1 mm to >20 mm length

Ÿ partly with shell-shaped spallings from crack returns

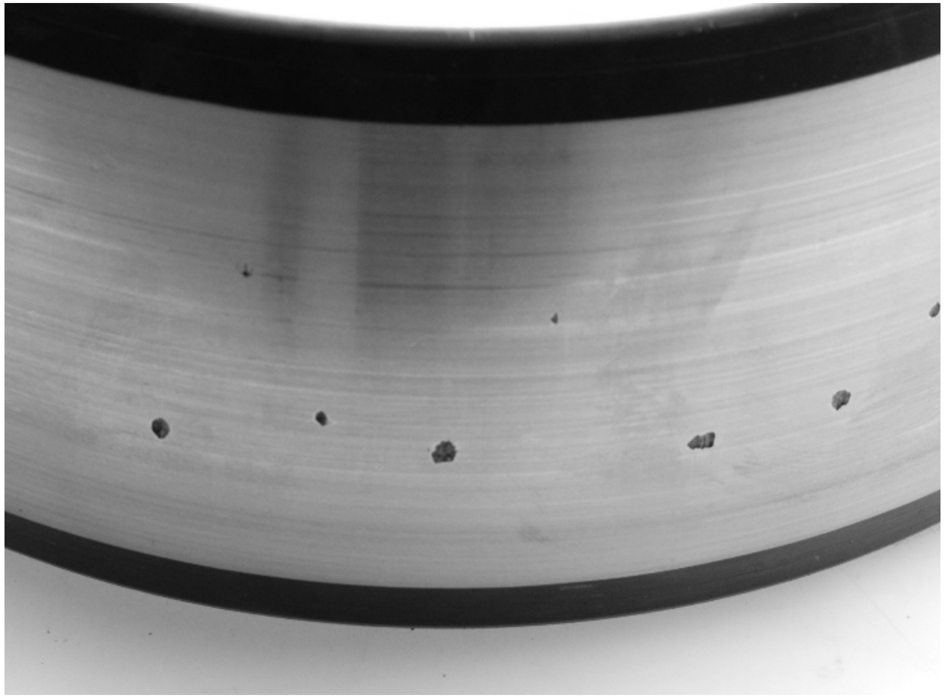

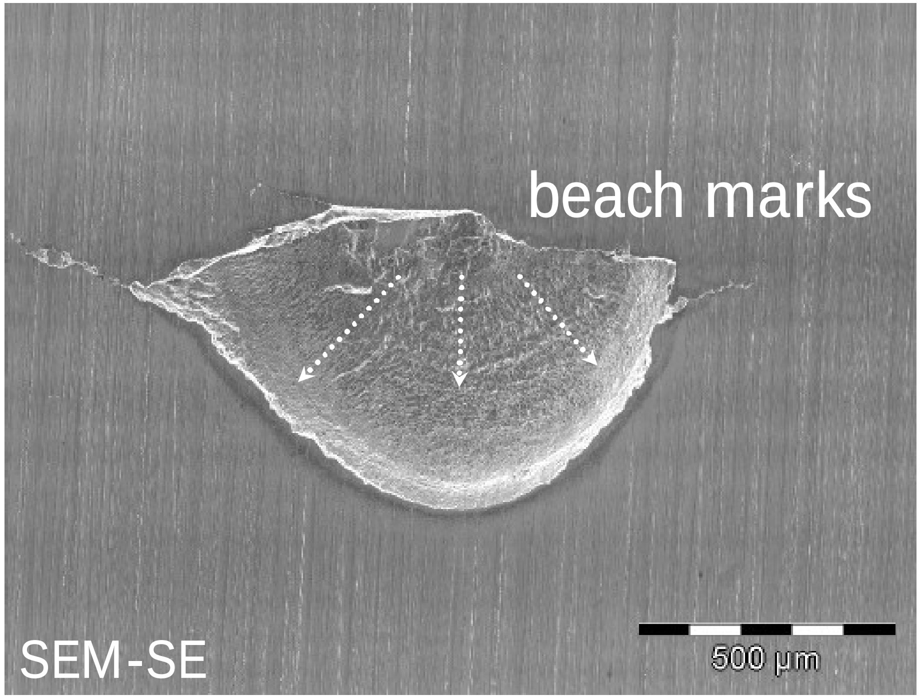

Visual Failure Pattern

axial raceway cracks of <1 mm to >20 mm length

Ÿ partly with shell-shaped spallings

Ÿ ... to advanced spallings

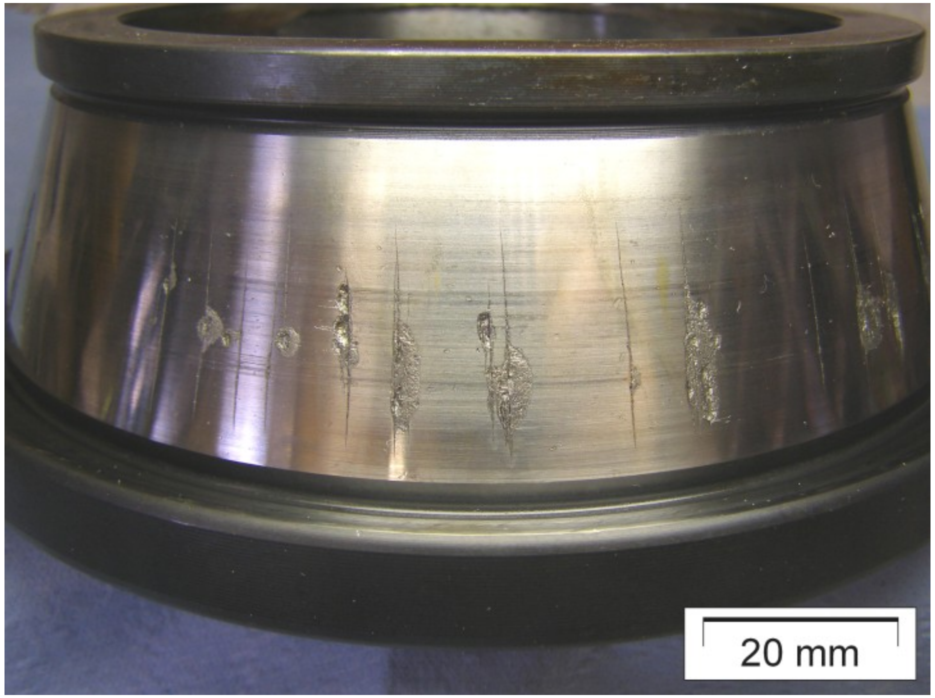

Failure Occurrence

White etching cracks (WEC) bearing failures occur ...

Ÿ at 1% to 20% of L_{10}^{nom}, i.e. before the *failure-free* time
ú *premature* bearing failures $\Rightarrow$ not ordinary RCF as root cause

Ÿ in industrial gearboxes, cranes, paper making machines, dryers, ship drives, mill drives, coal pulverizers, generators, ...
ú not restricted to wind turbines

Ÿ by trend increasingly with enhanced power of the wind turbine
ú solution most important for offshore wind energy generation

Ÿ rarely but in all wind turbine gearbox locations

Ÿ basically independent of heat treatment and bearing type

Failure Occurrence

case hardening – CARB

Ÿ tends to spalling rather than through cracking

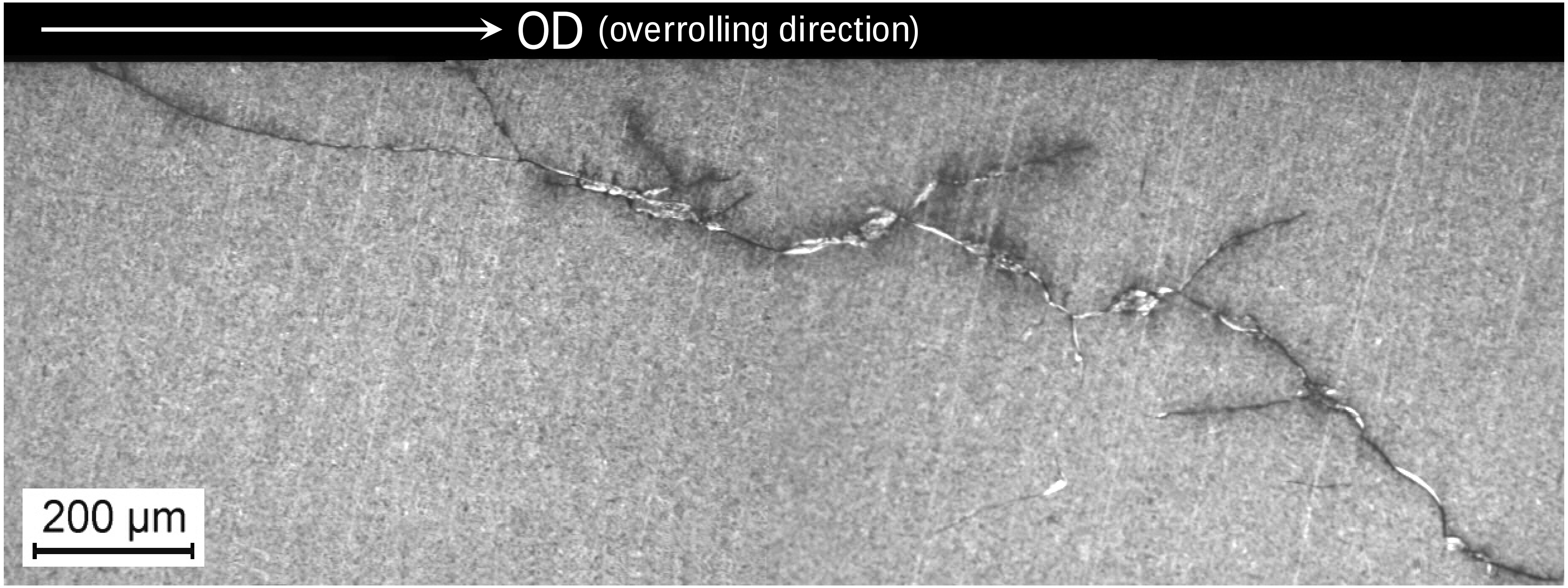

Ÿ basically independent of heat treatment and bearing type

Failure Occurrence

bainite hardening – SRB

Ÿ tends to spalling rather than through cracking

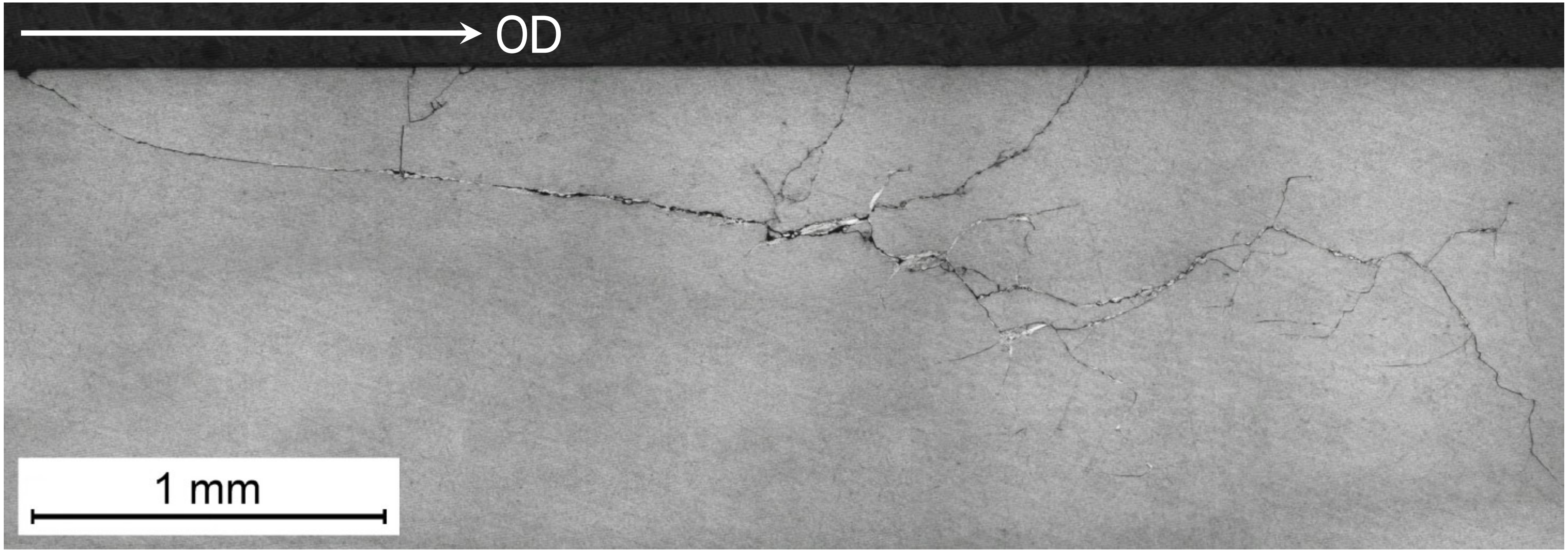

Ÿ basically independent of heat treatment and bearing type

Failure Occurrence

bainite hardening – CRB

Ÿ development of the crack system on the raceway

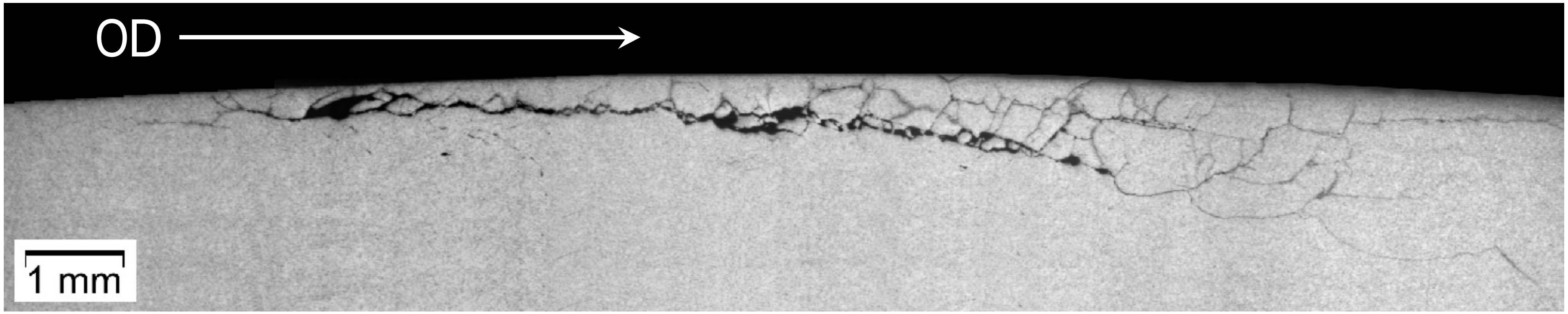

Ÿ basically independent of heat treatment and bearing type

Failure Occurrence

bainite hardening – CRB

Ÿ development of the crack system on the raceway

ú crack returns indicated

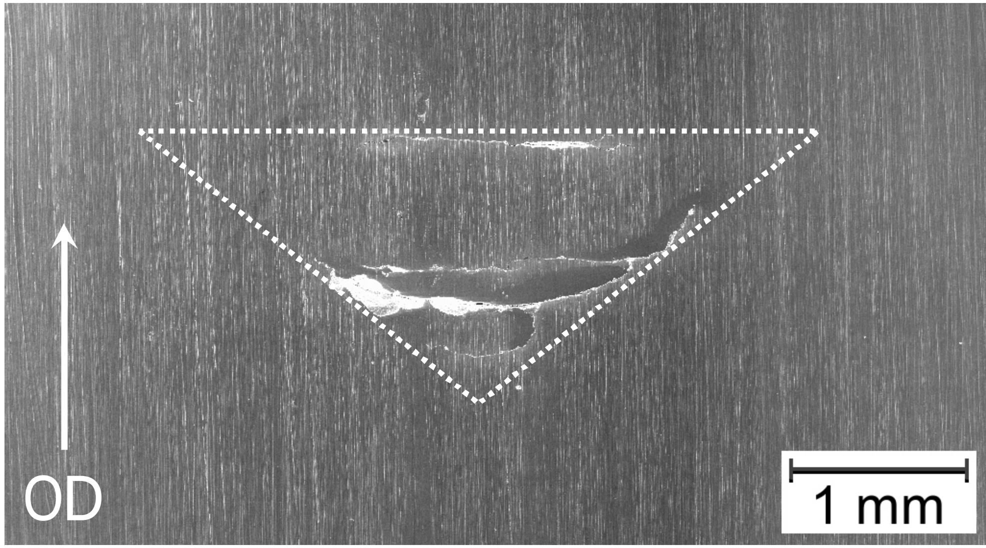

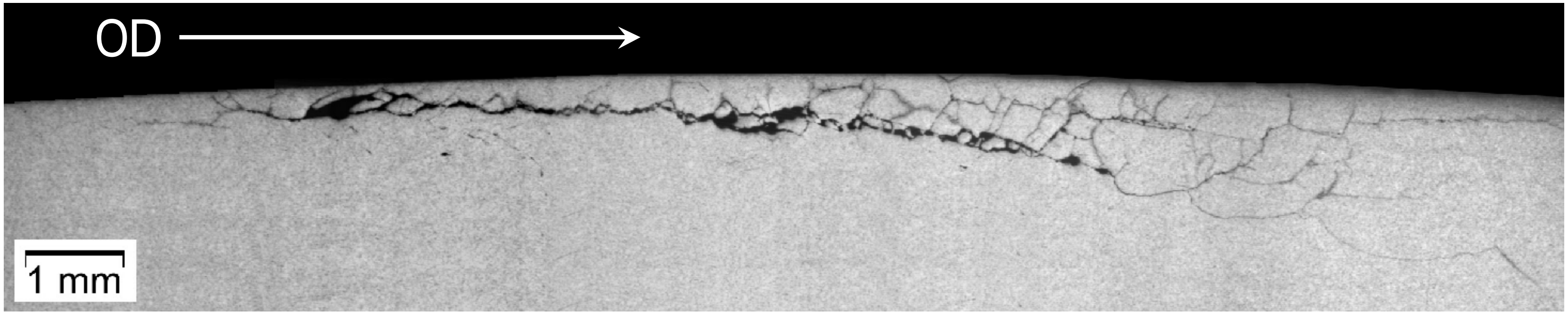

Ÿ basically independent of heat treatment and bearing type

Failure Occurrence

bainite hardening – CRB

- strongly branching & spreading deep transgranular crack systems at moderate permanent loads
  - chemically assisted RCF ⇒ corrosion fatigue cracking (CFC)
- ... in overrolling direction ⇒ surface initiation indicated

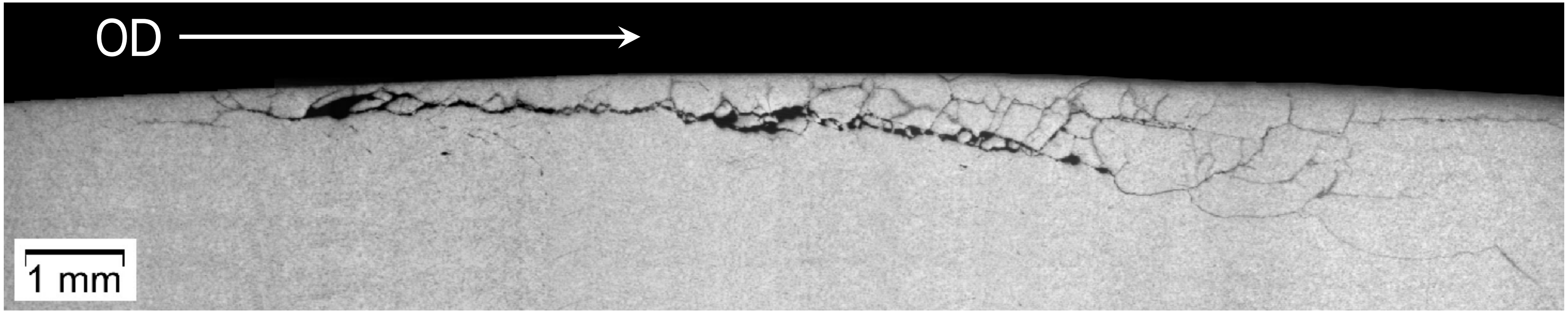

- basically independent of heat treatment and bearing type

Failure Occurrence

martensite hardening – TRB

- tends to through cracking rather than spalling
  - top-down growth

unetched

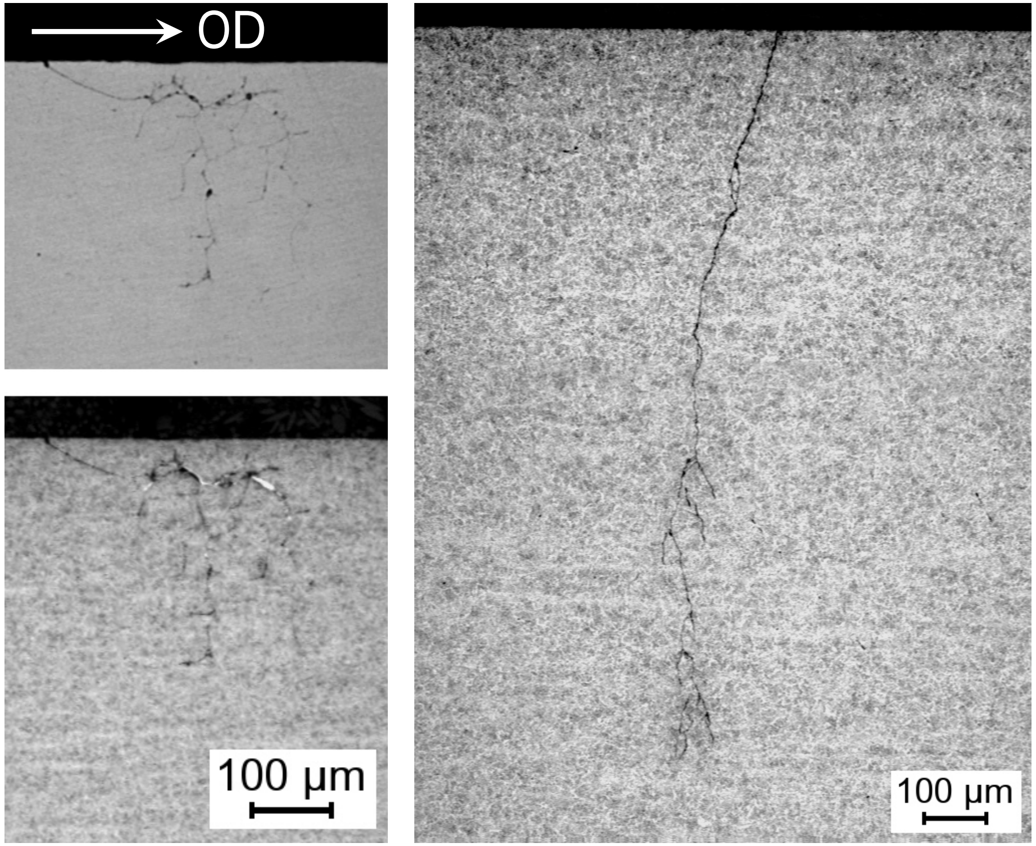

etched microsection

- basically independent of heat treatment and bearing type

Failure Analysis

methods to study material loading and WEC damage mechanisms

- visual and SEM raceway inspection
  - surface condition, tracing of crack paths, *crack detection*
- preparative crack opening
  - fractographic SEM investigation and microchemical analysis
- metallography (incl. SEM): axial & <u>circumferential</u> microsections
  - characterization of crack systems and microstructural changes
- spatially resolved determination of the hydrogen content
- X-ray diffraction residual stress material response analysis
  - clarification of the loading conditions

SKF

2

WEC Root Cause Hypotheses – A Commented Literature Survey

WEC Root Cause Hypotheses

prevailing opinions in the literature

- subsurface failure due to
  - continuous hydrogen absorption through the rolling contact
  - abnormal butterfly growth
- adiabatic shear band formation

WEC Root Cause Hypotheses

prevailing opinions in the literature

- subsurface failure due to
  - continuous hydrogen absorption through the rolling contact
  - abnormal butterfly growth
- adiabatic shear band formation

WEC Root Cause Hypotheses – Subsurface Failure

subsurface cracks tend to develop large fatigue spallings when reaching the raceway surface

Ÿ extended spalling-free crack systems not to be expected

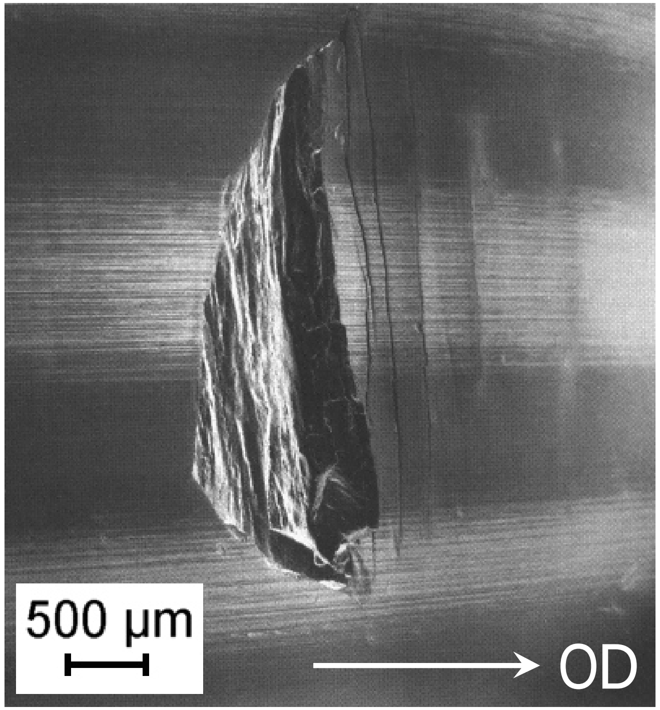

WEC Root Cause Hypotheses – Subsurface Failure

virtually undetectable hairline cracks

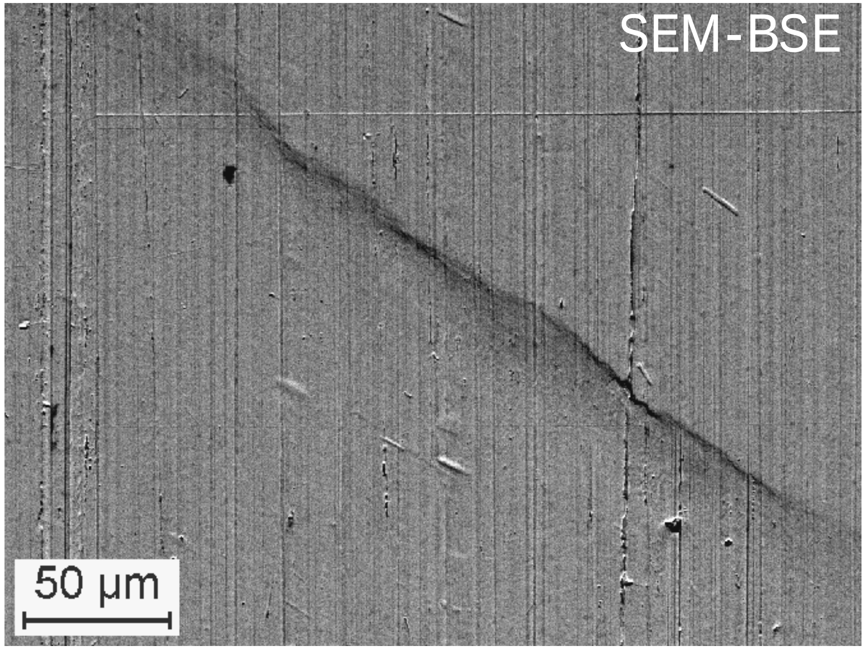

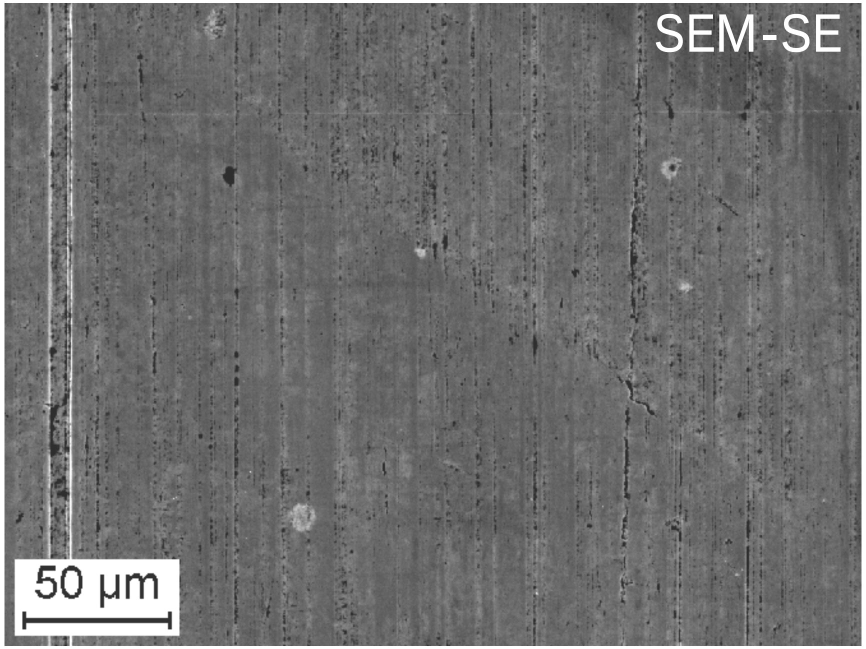

local surface smoothing reveals raceway hairline crack in the SEM

WEC Root Cause Hypotheses – Subsurface Failure

virtually undetectable hairline cracks can cause large WEC systems

Ÿ *negative* way of conclusion from surface connection not found to not there is inconsistent due to limited detection probability

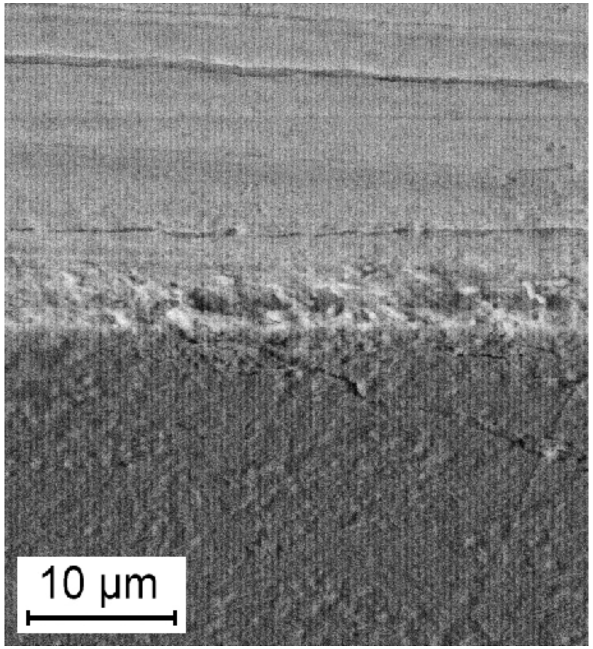

SEM-BSE

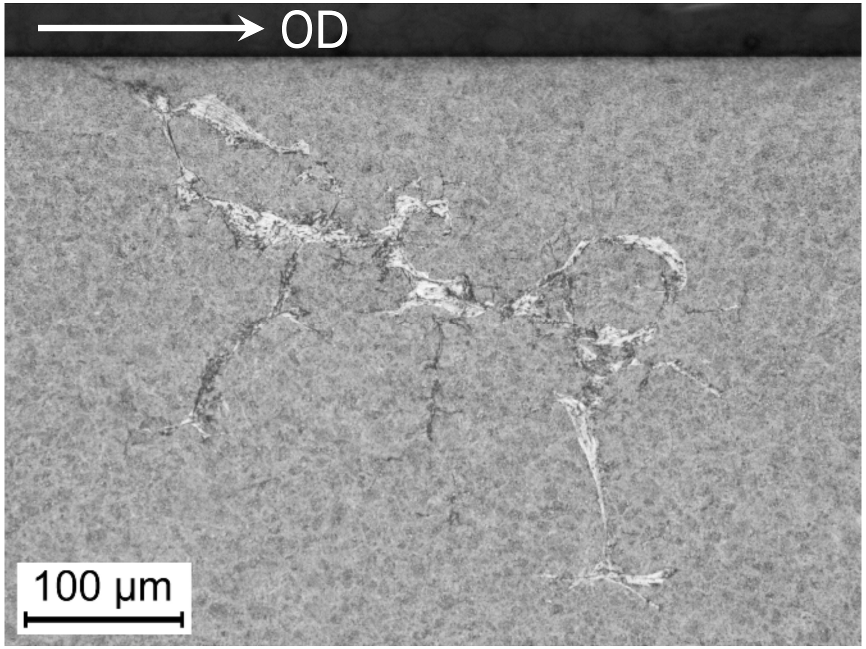

OD shows surface initiation – but no raceway crack visible

WEC Root Cause Hypotheses – Subsurface Failure

virtually undetectable hairline cracks can cause large WEC systems

Ÿ *negative* way of conclusion from surface connection not found to not there is inconsistent due to limited detection probability

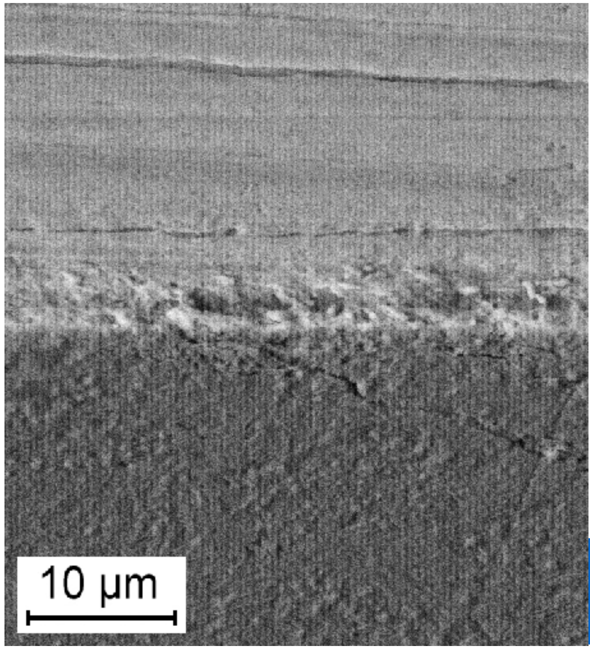

SEM-BSE

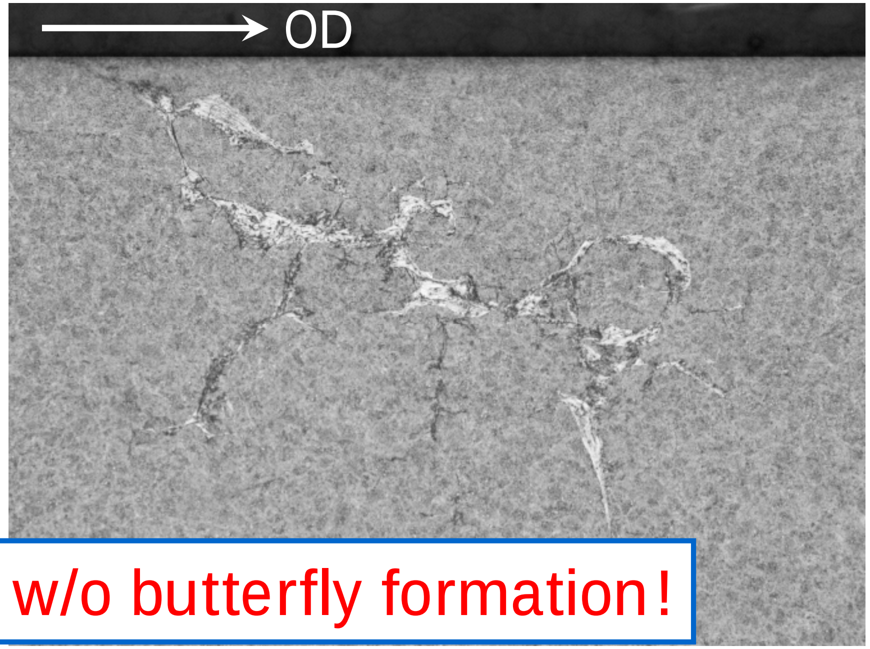

Note: WEC w/o butterfly formation!

OD shows surface initiation – but no raceway crack visible

WEC Root Cause Hypotheses – Subsurface Failure

virtually undetectable hairline cracks can cause large WEC systems

- *negative* way of conclusion from surface connection not found to not there is inconsistent due to limited detection probability
- *positive* way of conclusion from surface initiation verified via CFC to resulting crack-WEA arrangements is more comprehensible

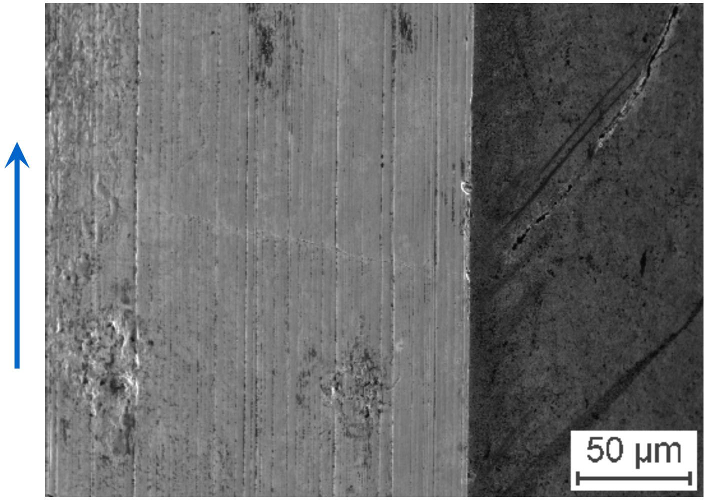

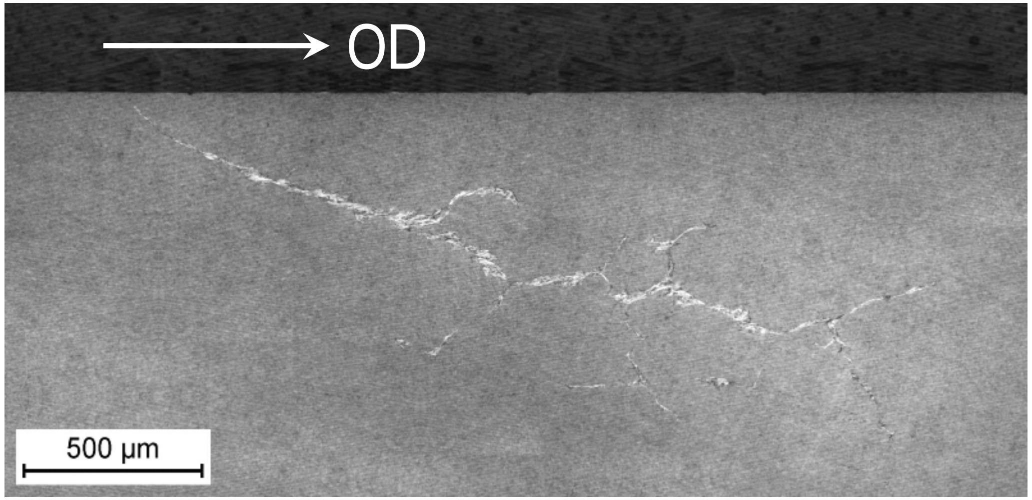

OD shows surface initiation – crack opened during preparation

WEC Root Cause Hypotheses – Subsurface Failure

virtually undetectable hairline cracks can cause large WEC systems

- *negative* way of conclusion from surface connection not found to not there is inconsistent due to limited detection probability
- *positive* way of conclusion from surface initiation verified via CFC to resulting crack-WEA arrangements is more comprehensible

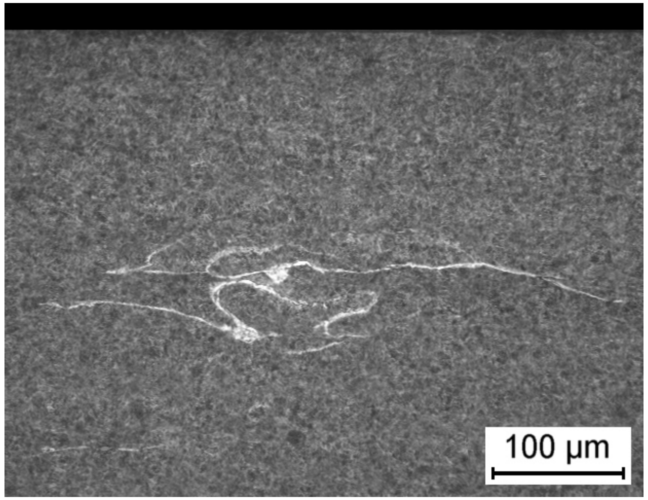

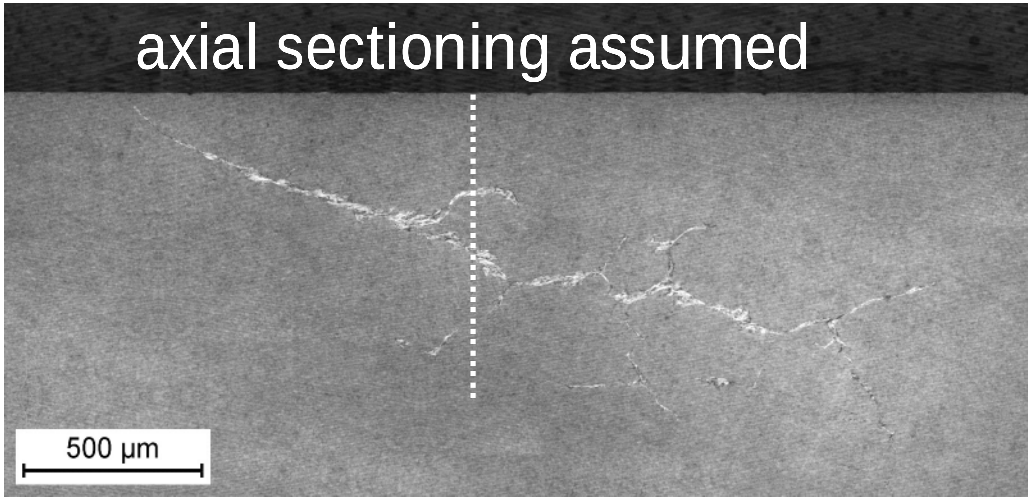

e.g. *spidery* WEA patterns: crack growth prior to phase change

WEC Root Cause Hypotheses – Hydrogen Absorption

hydrogen absorption unlikely through an undamaged RC surface

Ÿ effect known from HF current passage or dense raceway cracks

ú HT (case hardening)

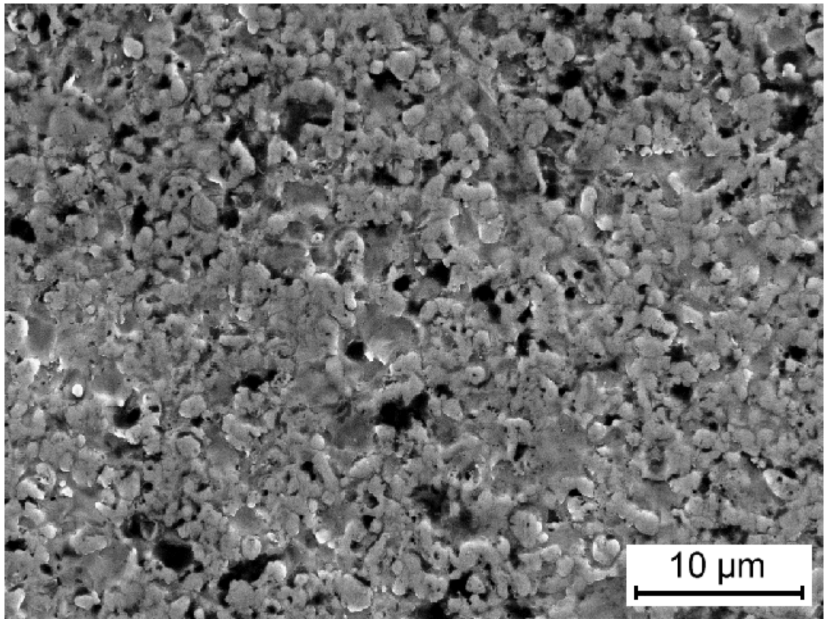

raceway in the contact zone

OR-DGBB from alternator rig

CGHE: $c_H > 3^{\pm 0.2}$ ppm

WEC Root Cause Hypotheses – Hydrogen Absorption

hydrogen absorption unlikely through an undamaged RC surface

Ÿ effect known from HF current passage or dense raceway cracks

ú H-RCF: SWB @ *b*/*B*≈0.71, microcracking

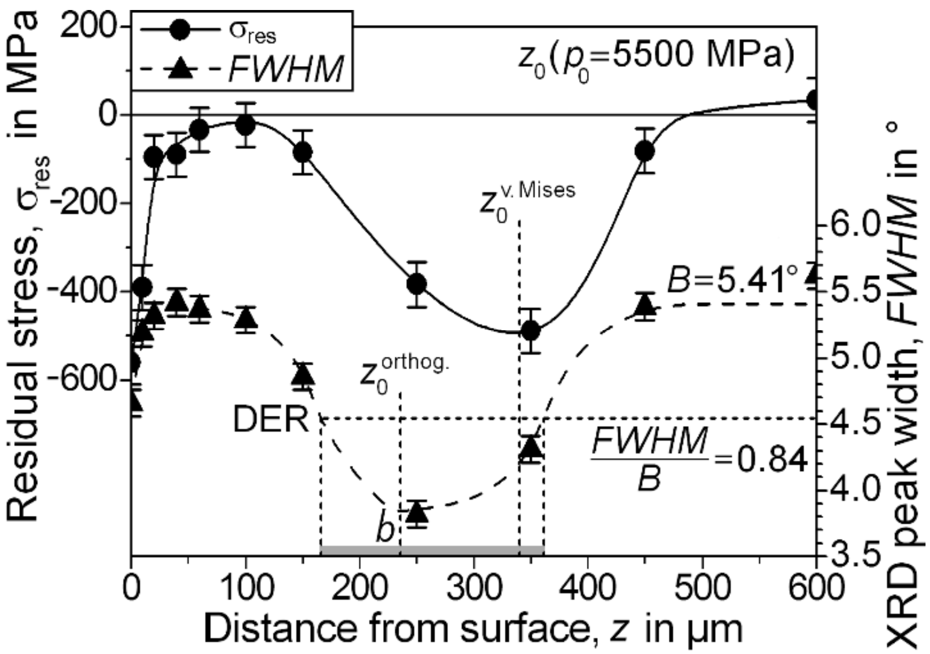

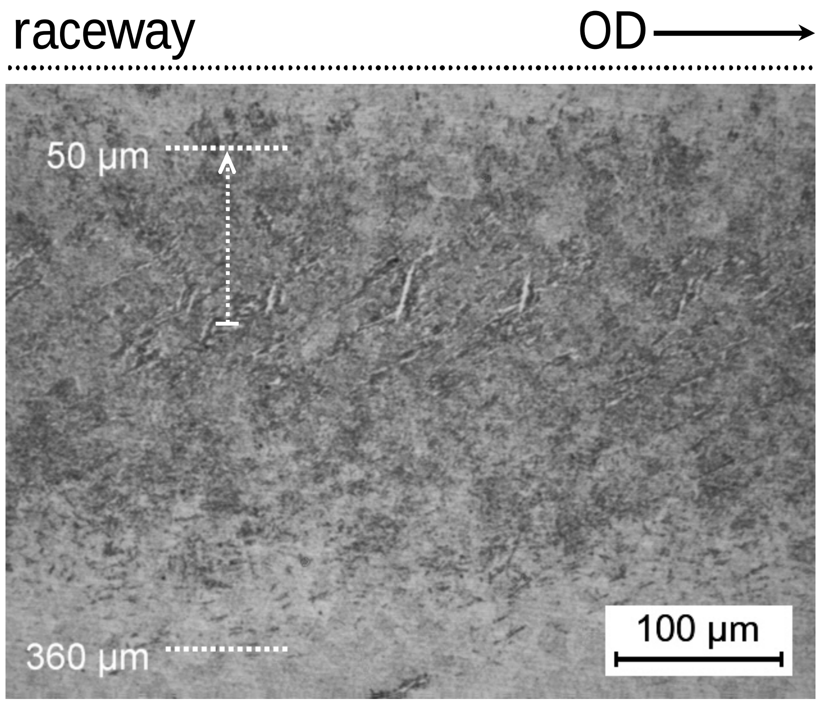

OR-DGBB from alternator rig

WEC Root Cause Hypotheses – Hydrogen Absorption

hydrogen absorption unlikely through an undamaged RC surface

- effect known from HF current passage or dense raceway cracks
  - H-RCF: SWB @ $b/B \approx 0.71$, microcracking
  - accelerated increase of dislocation density and glide mobility
    $\Rightarrow$ DGSL mechanism & HELP

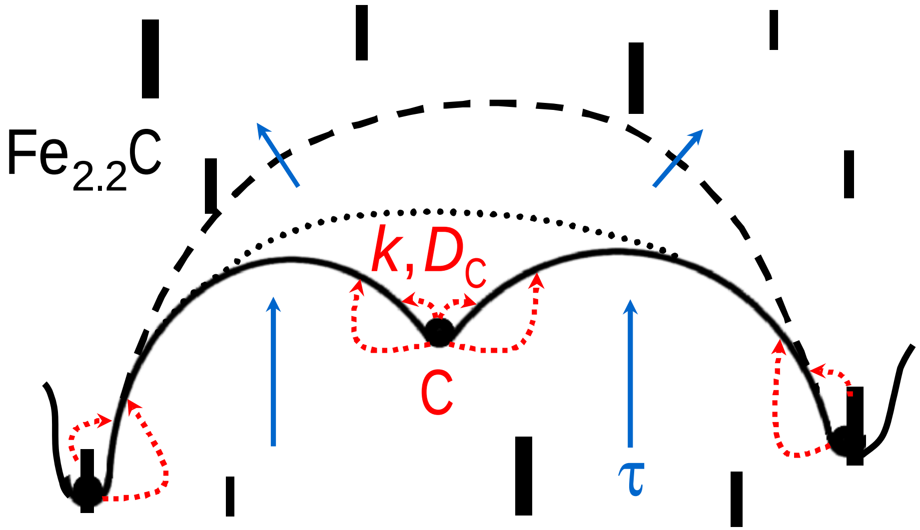

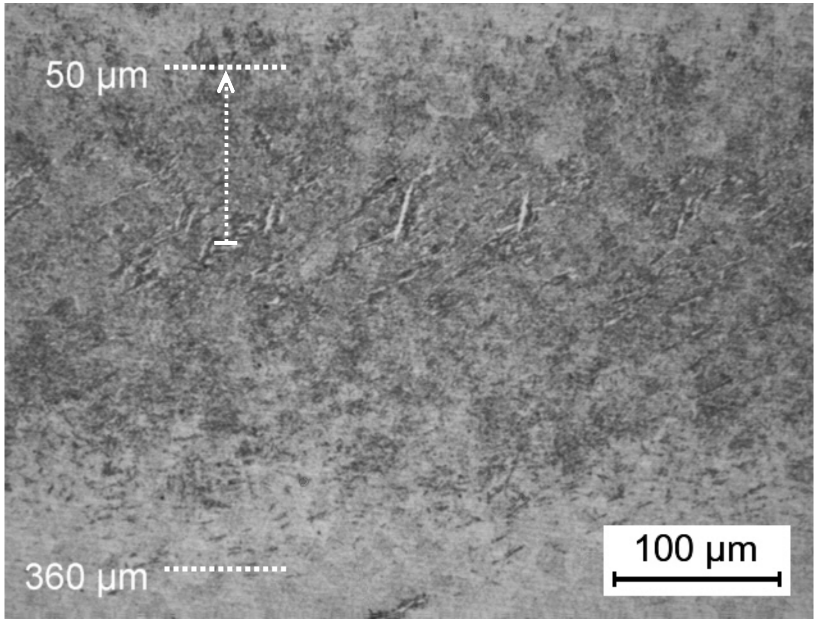

dislocation-carbide interaction

WEC Root Cause Hypotheses – Hydrogen Absorption

hydrogen absorption occurs rapidly not until raceway cracking

Raceway	2.2 ppm H
Center	1.0 ppm H
Bore	1.0 ppm H

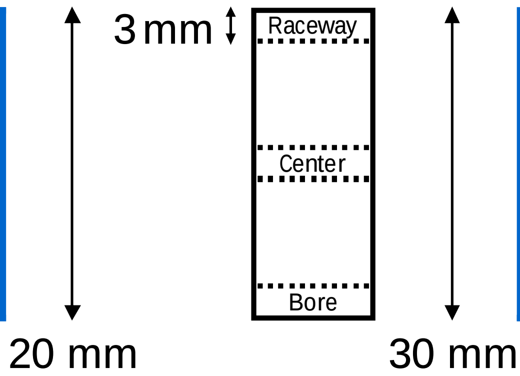

Raceway	1.8 ppm H
Center	1.4 ppm H
Bore	0.6 ppm H

- $D_{eff} \approx 10^{-7}$ cm^2/s $\Rightarrow$ just several weeks to few months of inward diffusion after crack initiation and growth
- hydrogen released from aging products of penetrating lubricant
- intergranular hydrogen embrittlement of opened fracture faces is restricted to the forced rupture around original cracks

WEC Root Cause Hypotheses – Butterfly Formation

butterfly formation is included in the bearing life theory

Ÿ rapid generation at $p_0 \geq 1400$ MPa but slow growth

ú distribution follows the (alternating) orthogonal shear stress

Ÿ the rare failures occur in the upper life range above L_{10}^{nom}

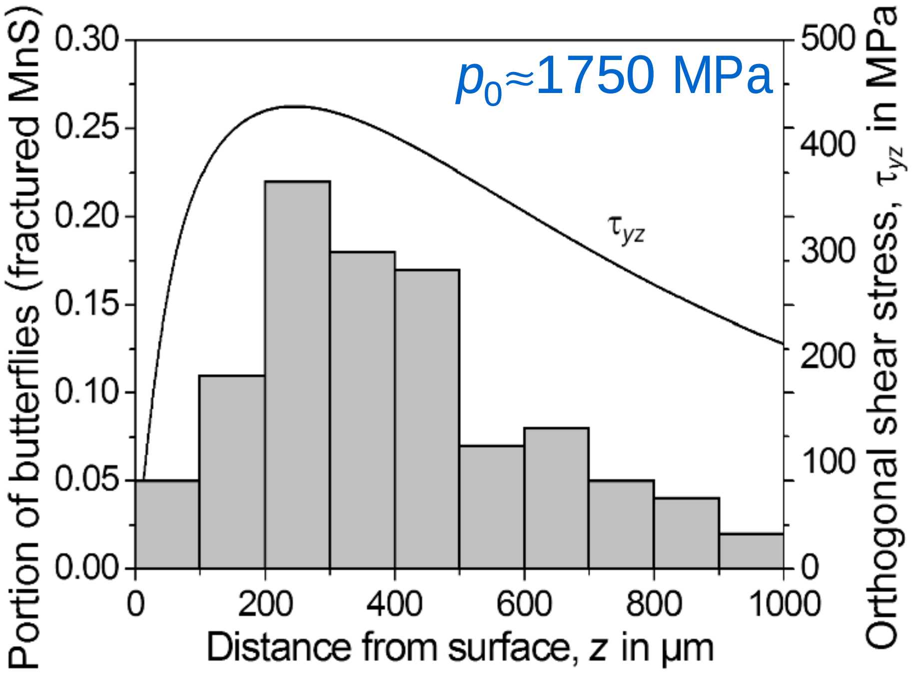

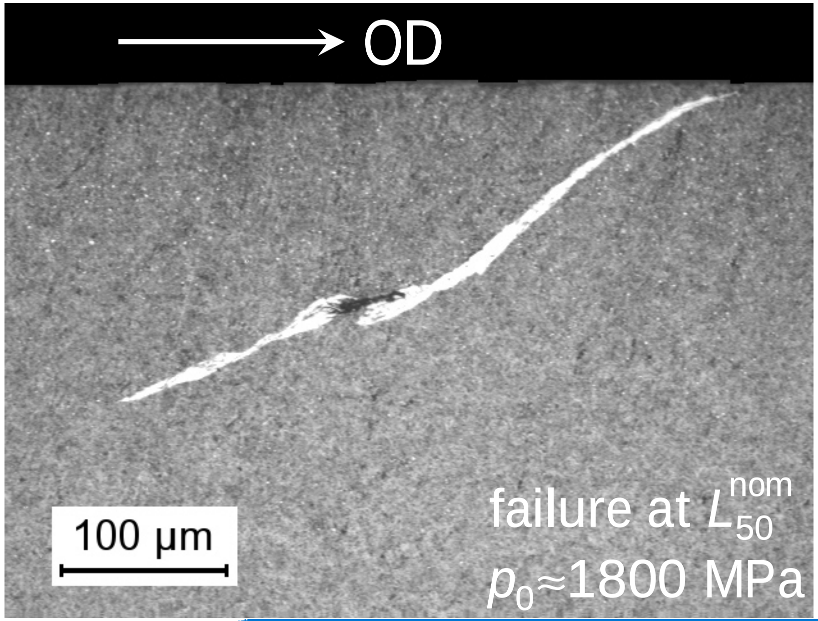

WEC Root Cause Hypotheses – Butterfly Formation

WEC occur with or without butterflies: p_0>/<1400 MPa

Ÿ evolution of butterfly population up to WEC must be traceable

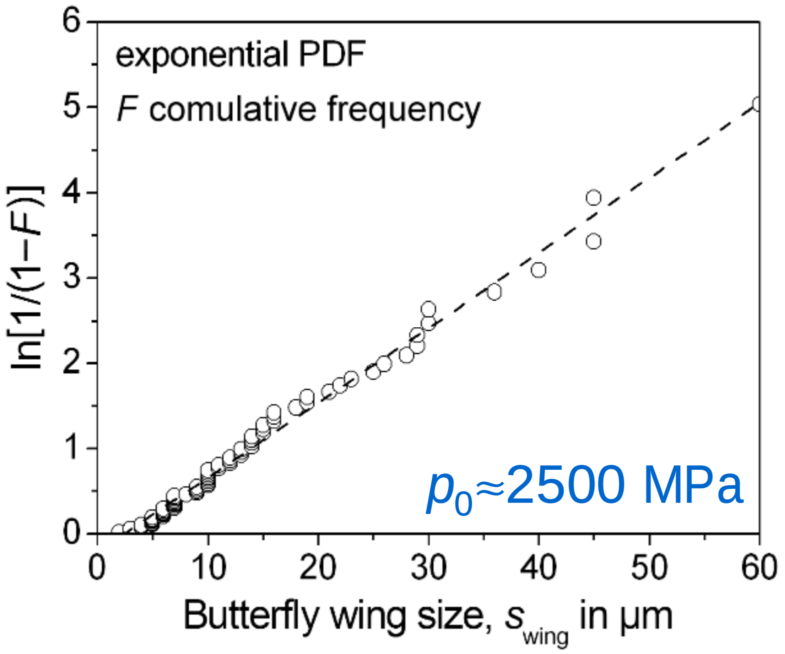

evaluation of 101 butterflies

ú exponential PDF describes natural growth

WEC Root Cause Hypotheses – Butterfly Formation

WEC occur with or without butterflies: $p_0 >/< 1400$ MPa

Ÿ evolution of butterfly population up to WEC must be traceable

butterflies reveal no DER precursor structure of WEA formation

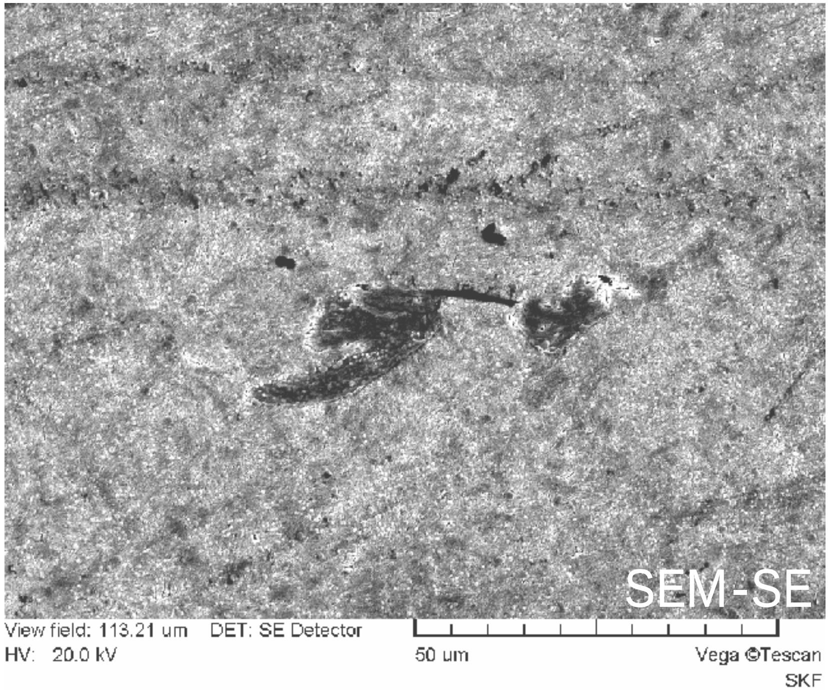

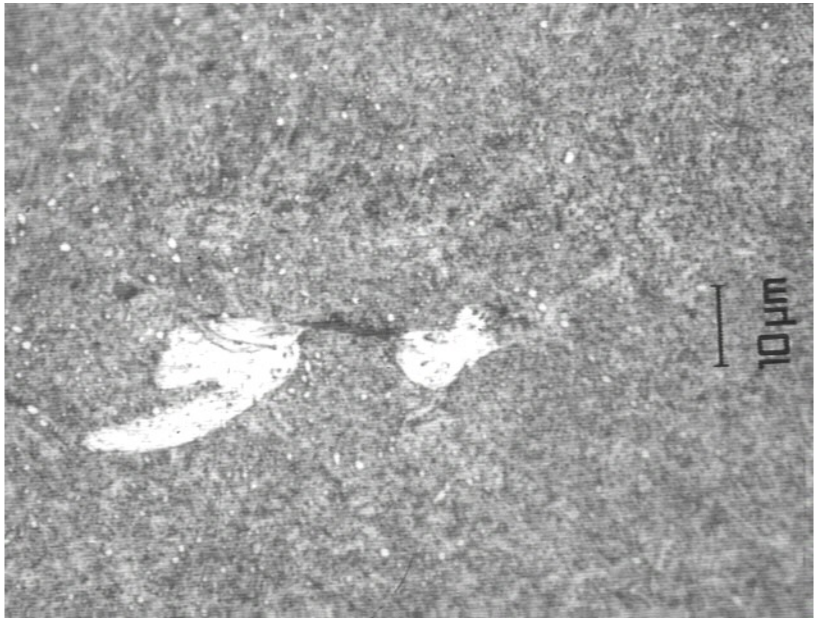

WEC Root Cause Hypotheses – Butterfly Formation

WEC occur with or without butterflies: p_0 >/< 1400 MPa

Ÿ evolution of butterfly population up to WEC must be traceable

butterflies reveal no DER precursor structure of WEA formation

Ÿ ... but WEA of WEC do (hydrogen from aging oil in CFC cracks)

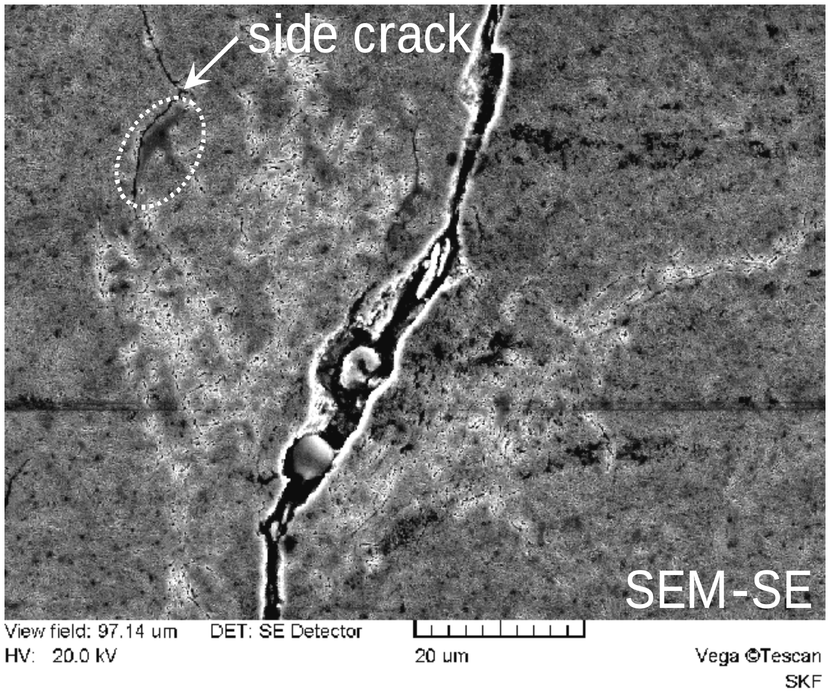

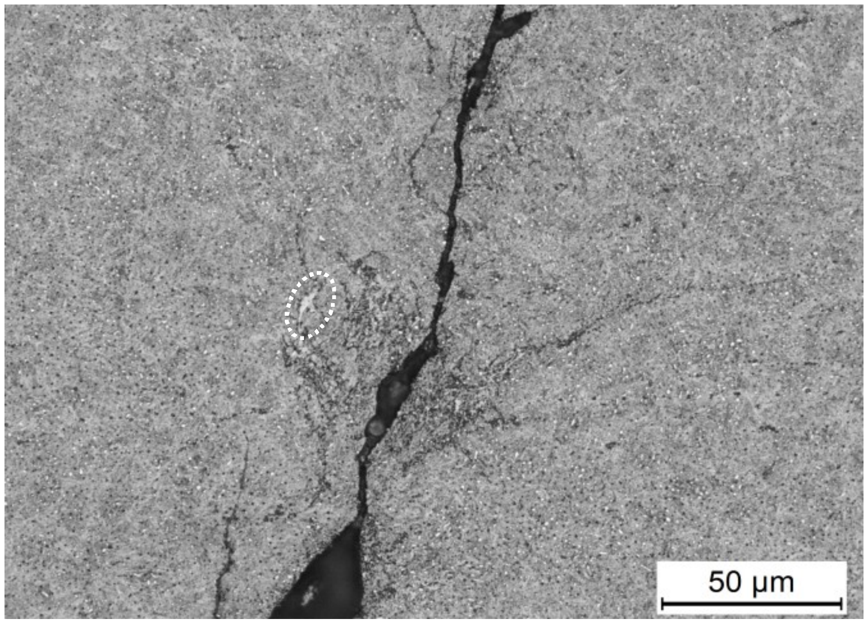

WEC Root Cause Hypotheses – Butterfly Formation

WEC occur with or without butterflies: $p_0 > / < 1400$ MPa

⇒ WEC and butterflies are independent microstructural changes

butterflies reveal no DER precursor structure of WEA formation

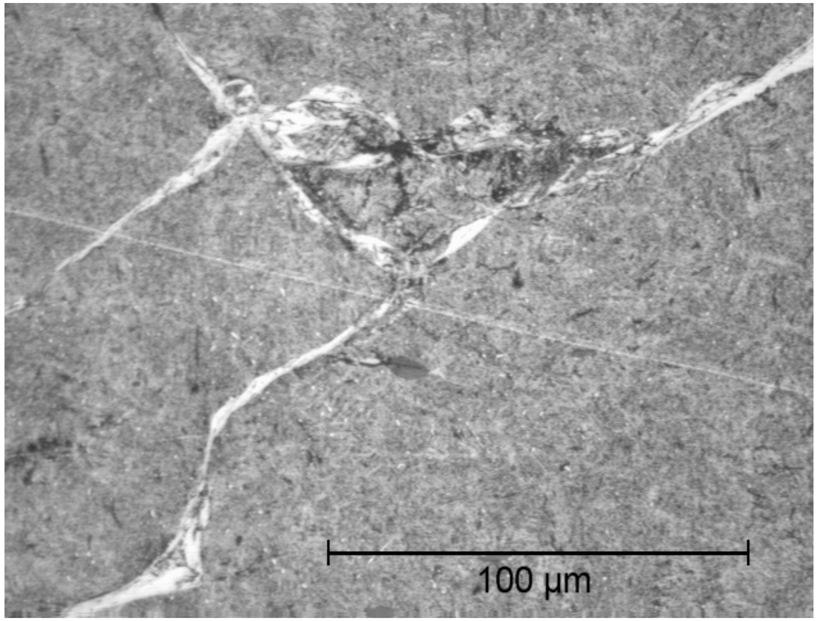

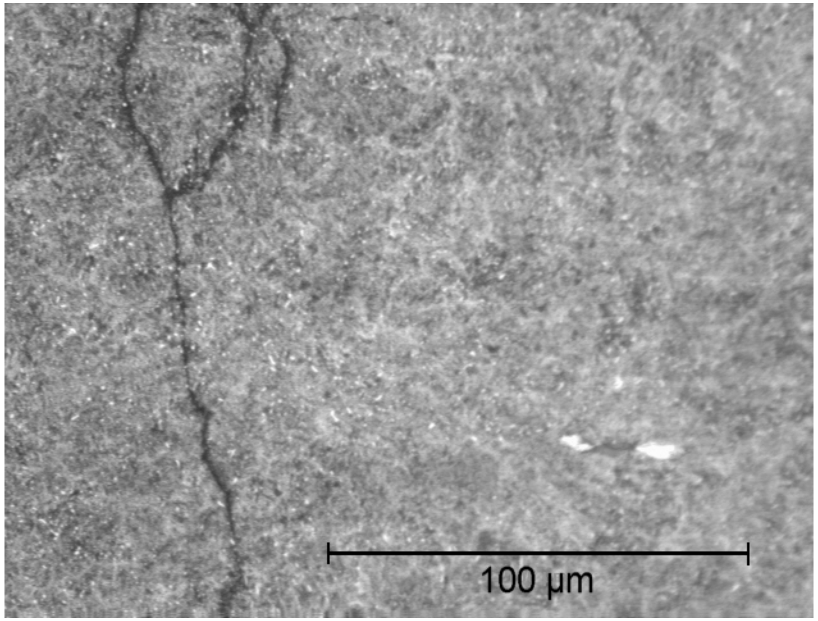

WEC Root Cause Hypotheses – Butterfly Formation

WEC occur with or without butterflies: p_0 >/< 1400 MPa

⇒ WEC and butterflies are independent microstructural changes

butterflies reveal no DER precursor structure of WEA formation

Note: butterflies on operationally broken MnS inclusions
ú M. Brückner et al.: Proc. VHCF-5, pp. 101-106

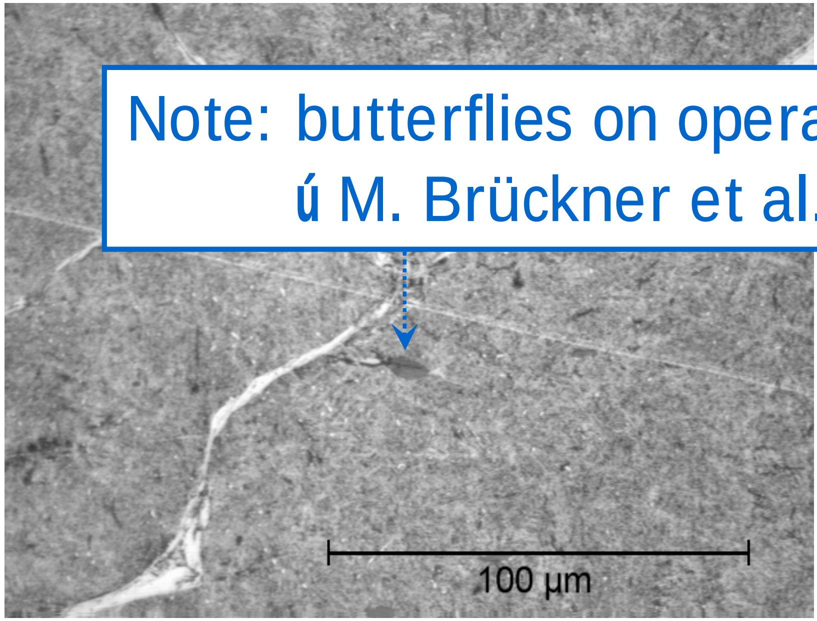

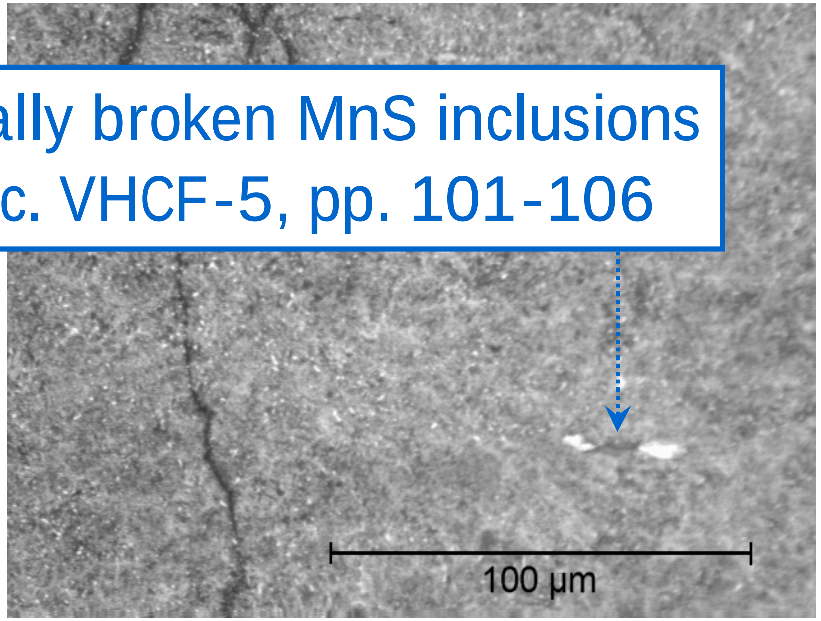

WEC Root Cause Hypotheses – Adiabatic Shearing

local flash austenitizing by very rapid large plastic deformation

Ÿ shock straining conditions do not occur in bearing operation

Ÿ real bearing dynamics do not create critical EHL pressure peaks

  ú impact loads act like small Hertzian contacts or indentations

  ú w/o frictional surface traction, no tensile stress occurs

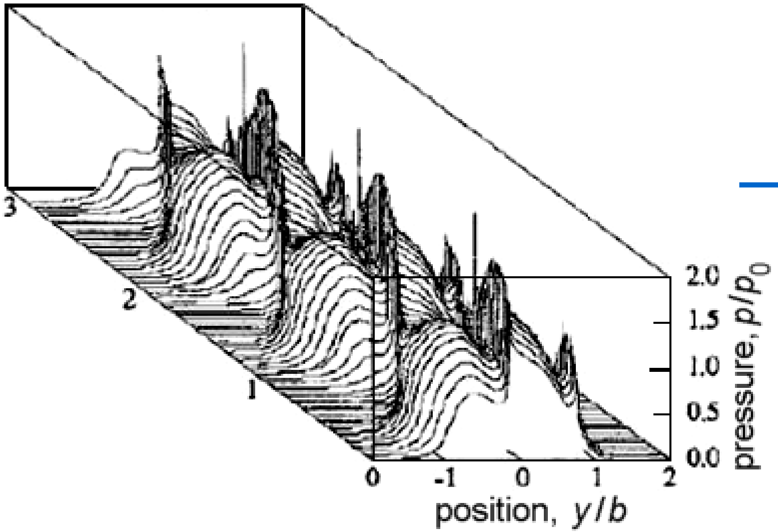

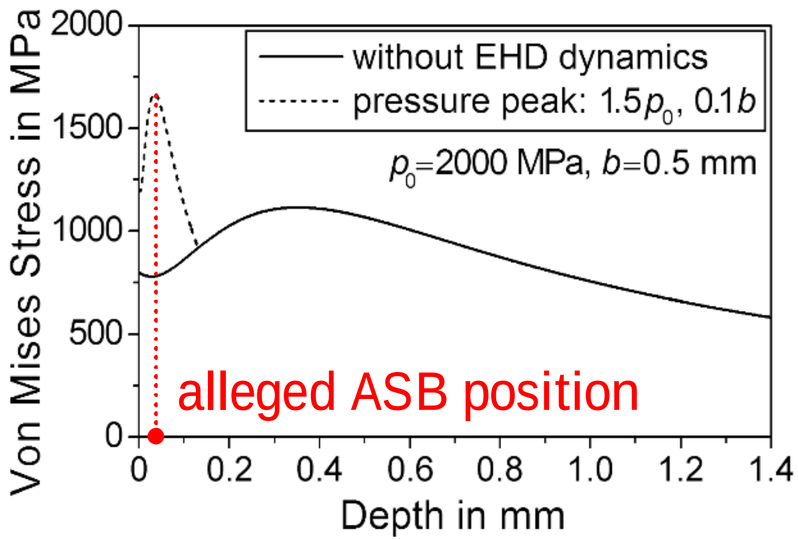

Luyckx, 2011 acc. to Dowson, 2003

WEC Root Cause Hypotheses – Adiabatic Shearing

local flash austenitizing by very rapid large plastic deformation

- shock straining conditions do not occur in bearing operation
- real bearing dynamics do not create critical EHL pressure peaks
  - impact loads act like small Hertzian contacts or indentations
  - w/o frictional surface traction, no tensile stress occurs
- ASB are formed by primary phase transformation to WEA
  - ... but WEC occur by primary CFC crack growth
- ASB represent essentially straight regular ribbons of mm length

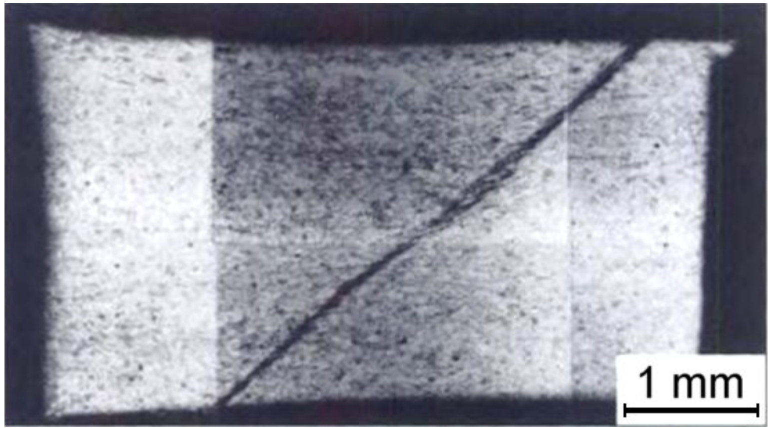

WEC Root Cause Hypotheses – Adiabatic Shearing

local flash austenitizing by very rapid large plastic deformation

- shock straining conditions do not occur in bearing operation
- real bearing dynamics do not create critical EHL pressure peaks
  - impact loads act like small Hertzian contacts or indentations
  - w/o frictional surface traction, no tensile stress occurs
- ASB are formed by primary phase transformation to WEA
  - ... but WEC occur by primary CFC crack growth
- ASB represent essentially straight regular ribbons of mm length
  - ... but WEC reveal strikingly branched crack paths

OD

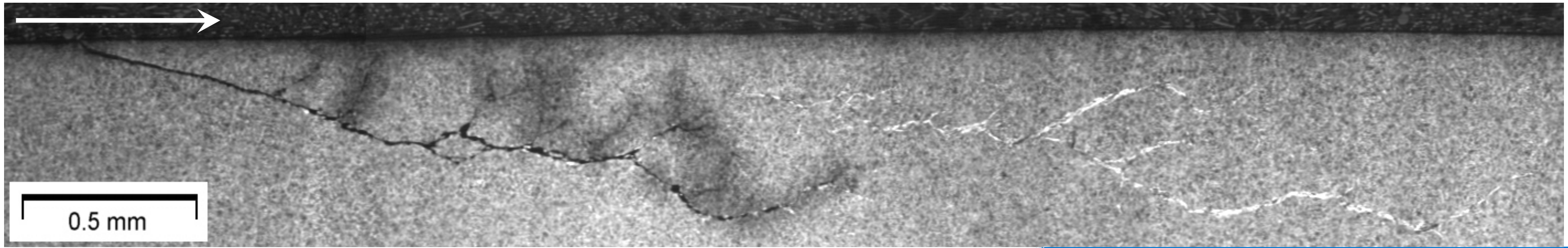

WEC Root Cause Hypotheses – Adiabatic Shearing

local flash austenitizing by very rapid large plastic deformation

Ÿ shock straining conditions do not occur in bearing operation

Ÿ real bearing dynamics do not create critical EHL pressure peaks

  ú impact loads act like small Hertzian contacts or indentations

  ú w/o frictional surface traction, no tensile stress occurs

Ÿ ASB are formed by primary phase transformation to WEA

  ú … but WEC occur by primary CFC crack growth

Ÿ ASB represent essentially straight regular ribbons of mm length

  ú … but WEC reveal strikingly branched crack paths

Note: adiabatic shearing also presumed to cause the regular SWB

Ÿ gradual development of SWB rather indicates RCF damage

Schlicht, 2008

SKF

3

Spontaneous Axial Surface Cracking and Corrosion Fatigue WEC Growth

Preparative Crack Opening and Macrofractography

Typical raceway cracks to be opened for fractography

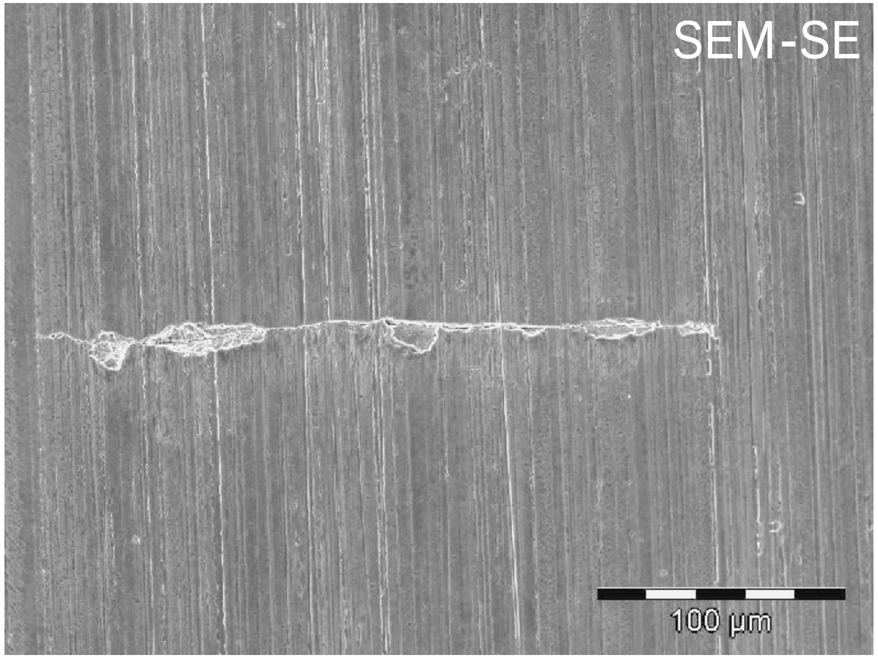

small crack
< 1mm

...

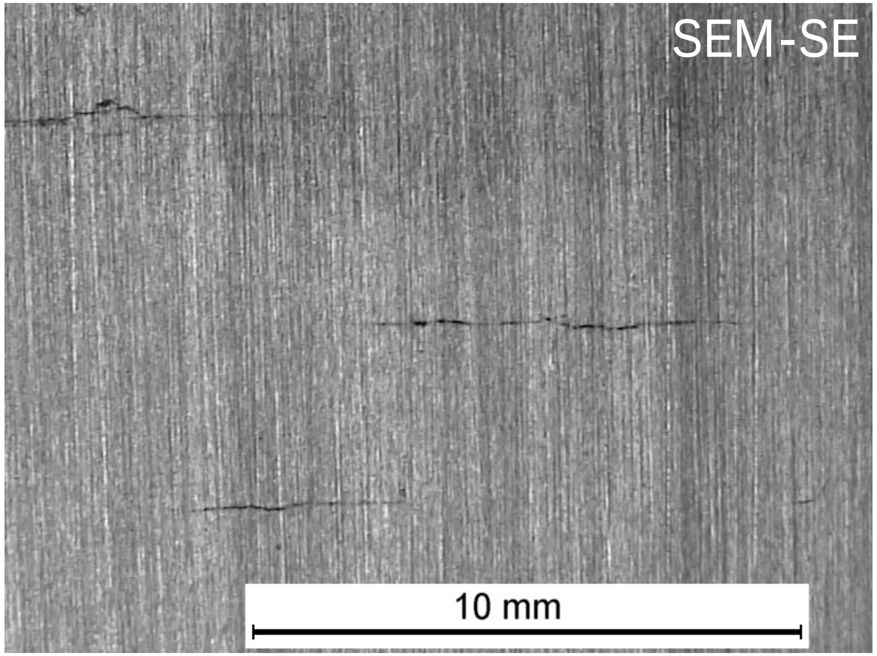

large cracks
> 20 mm

Preparative Crack Opening and Macrofractography

Small raceway crack

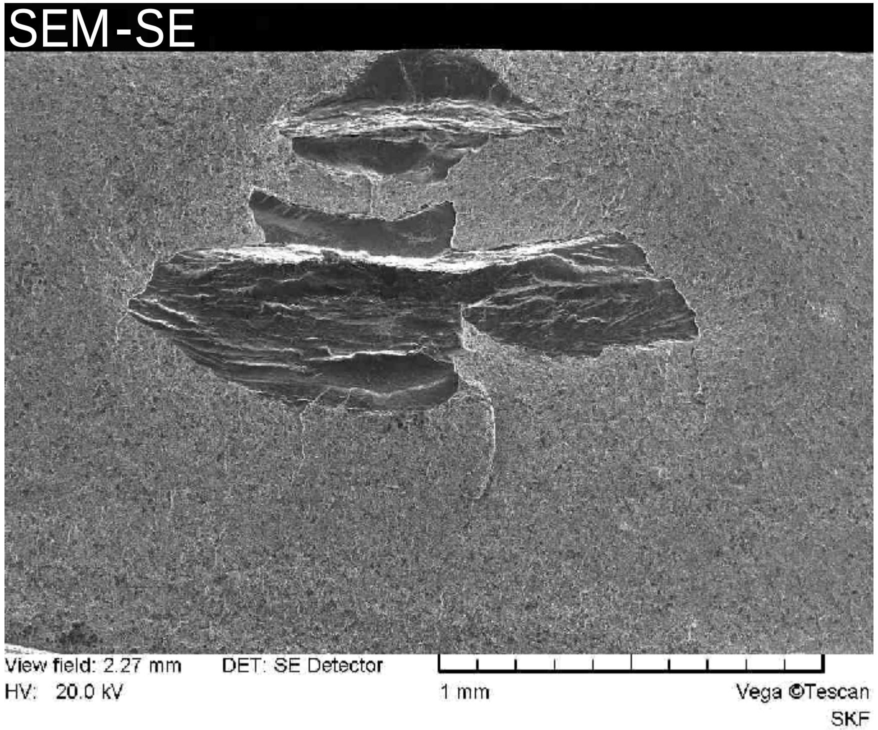

- original fracture surface clearly distinguishable

Preparative Crack Opening and Macrofractography

Small raceway crack

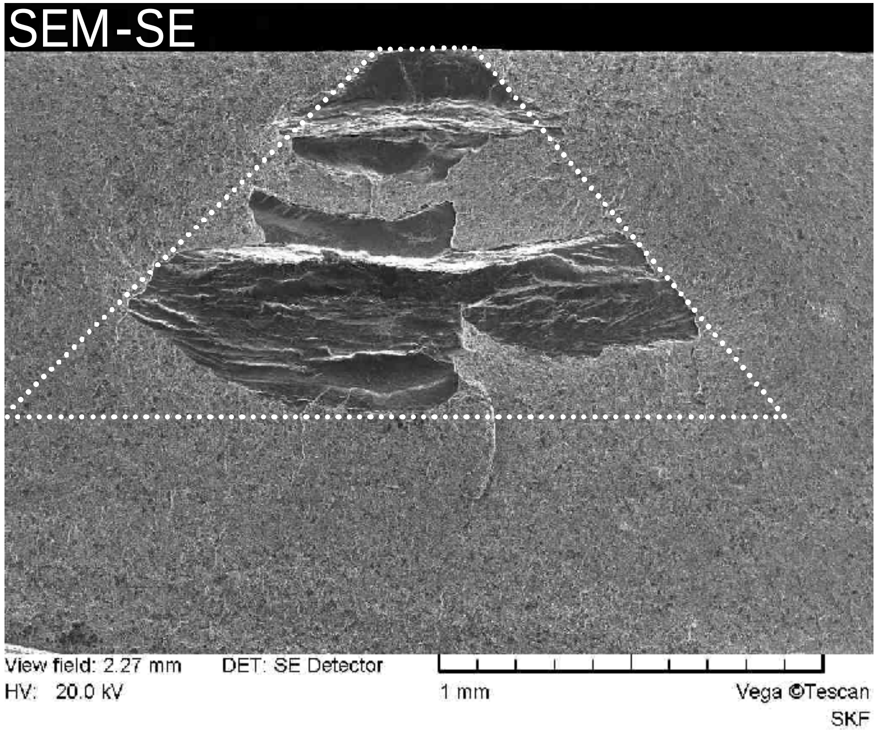

- original fracture surface clearly distinguishable
- trapezoid shape of the spreading crack reveals top-down growth

Preparative Crack Opening and Macrofractography

Small raceway crack

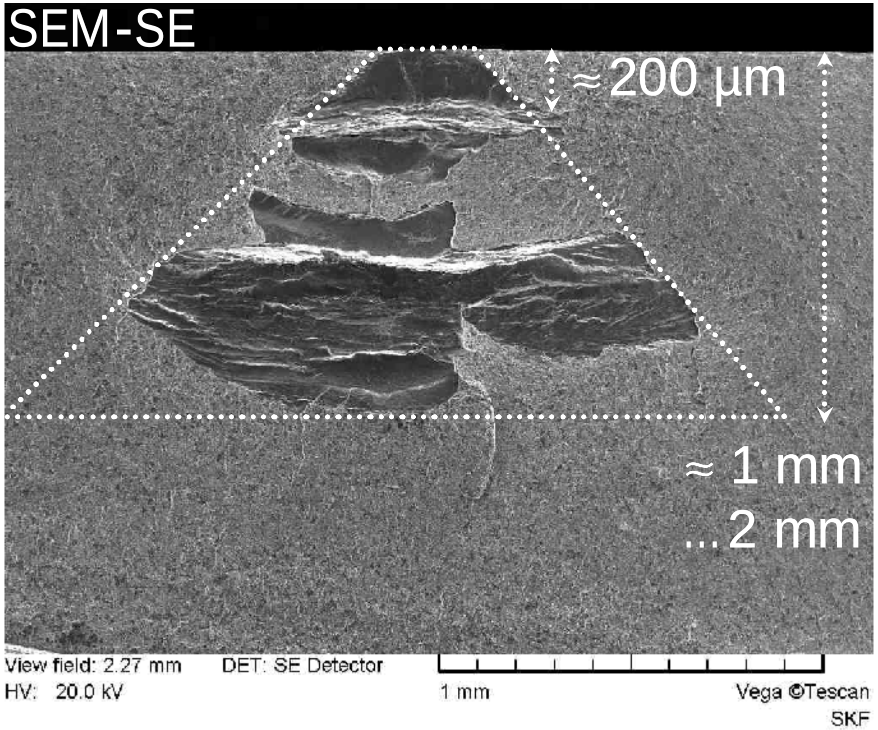

- original fracture surface clearly distinguishable
- trapezoid shape of the spreading crack reveals top-down growth

Preparative Crack Opening and Macrofractography

Small raceway crack

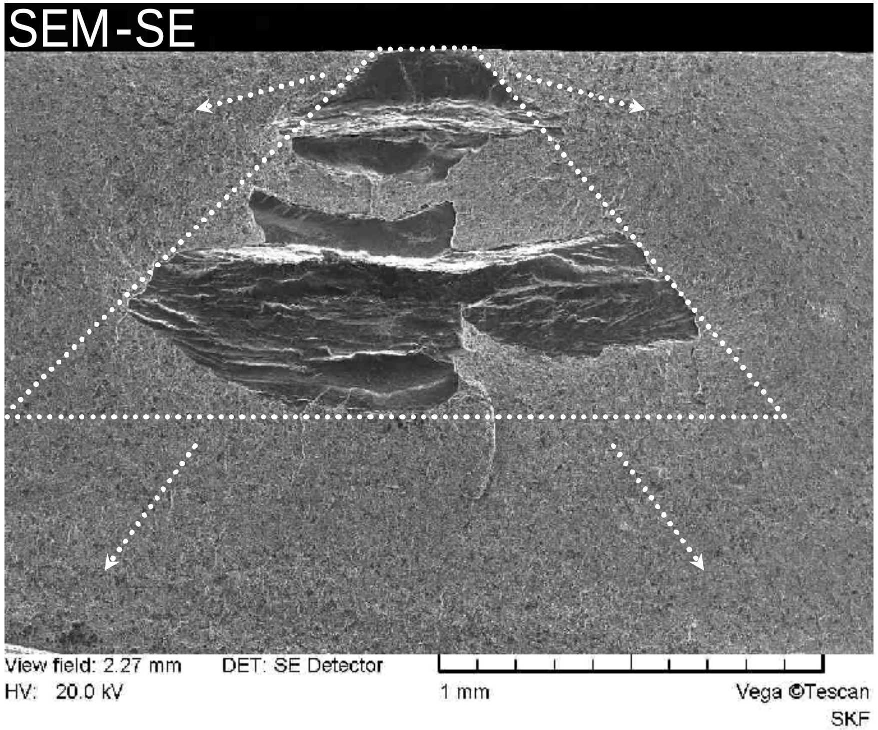

... further crack growth by corrosion fatigue

Preparative Crack Opening and Macrofractography

Small raceway crack

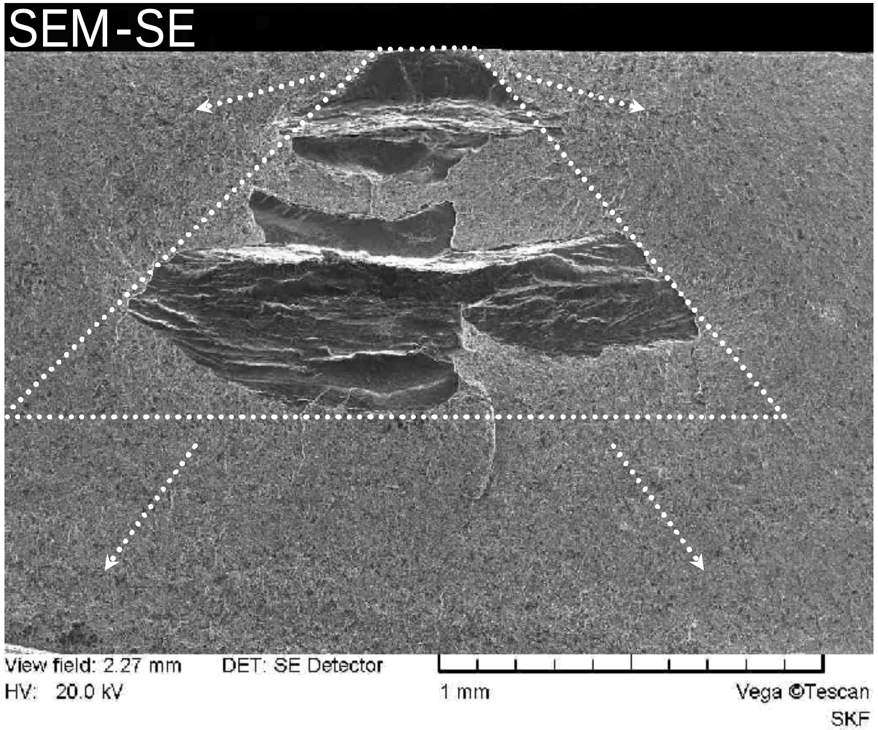

Large raceway crack

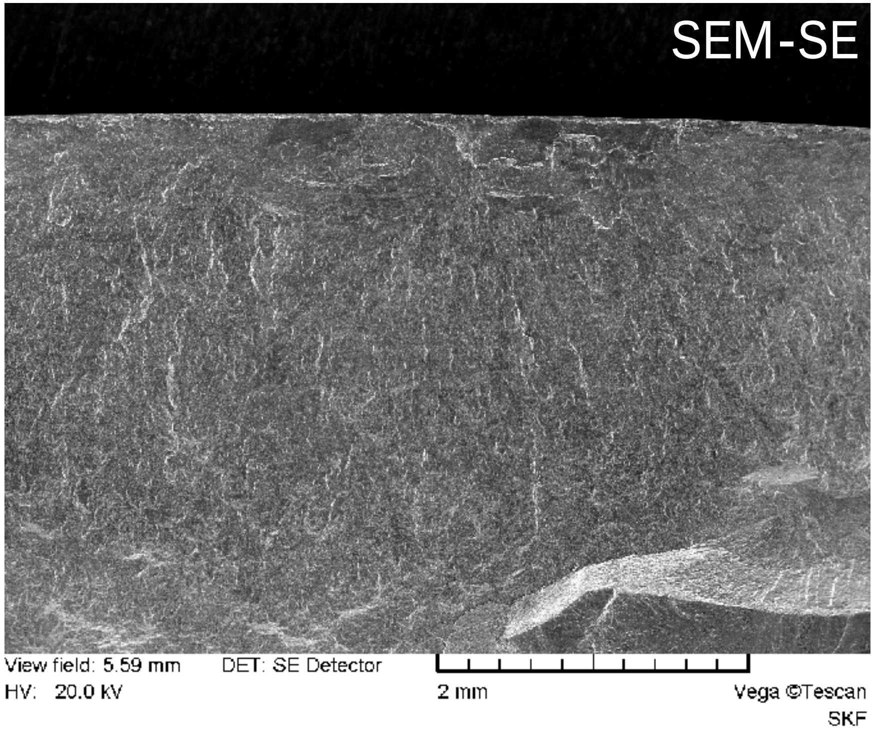

Preparative Crack Opening and Macrofractography

Small raceway crack

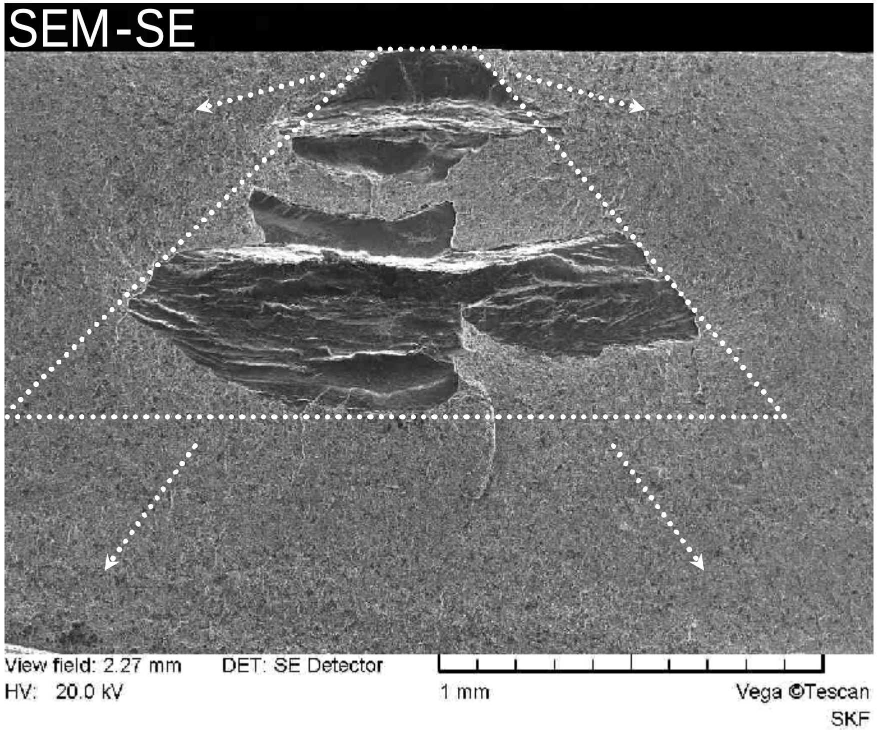

Large raceway crack

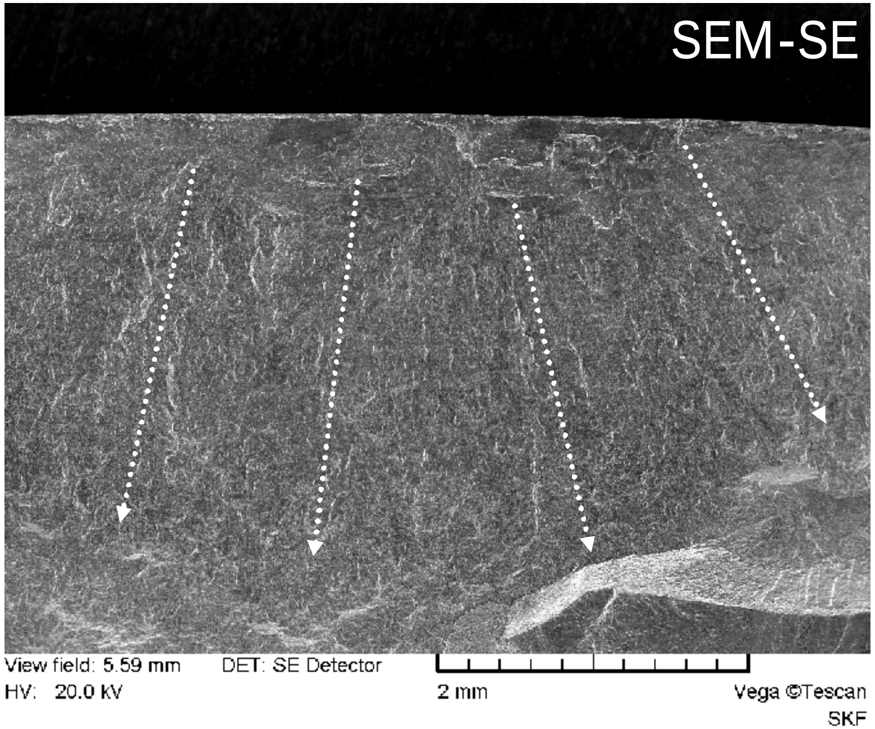

- radial propagation lines $\Rightarrow$ top-down growth, surface initiation

Preparative Crack Opening and Macrofractography

Description of the cracks

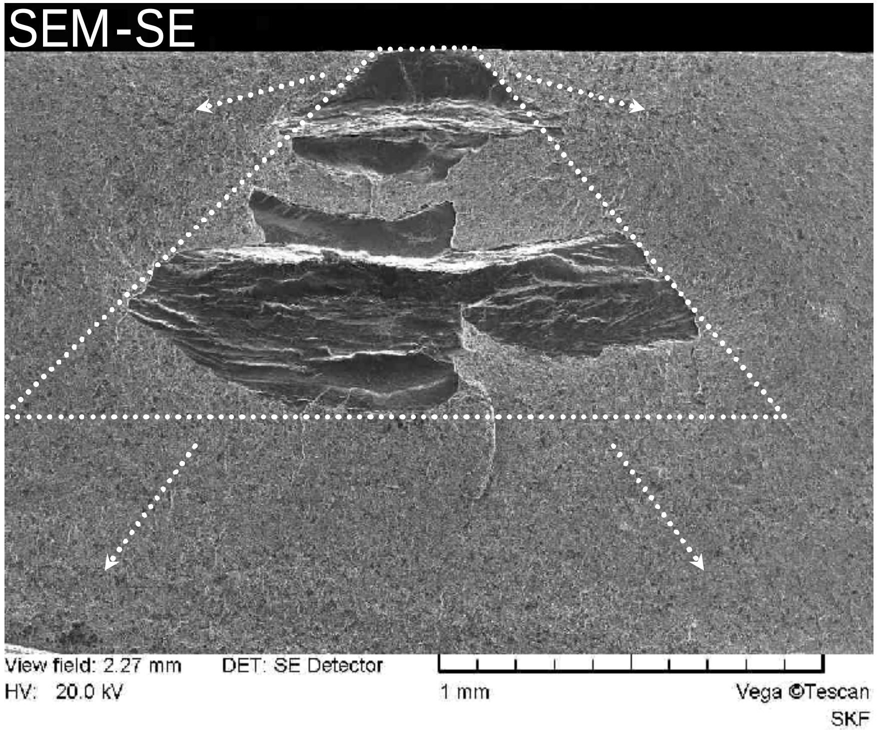

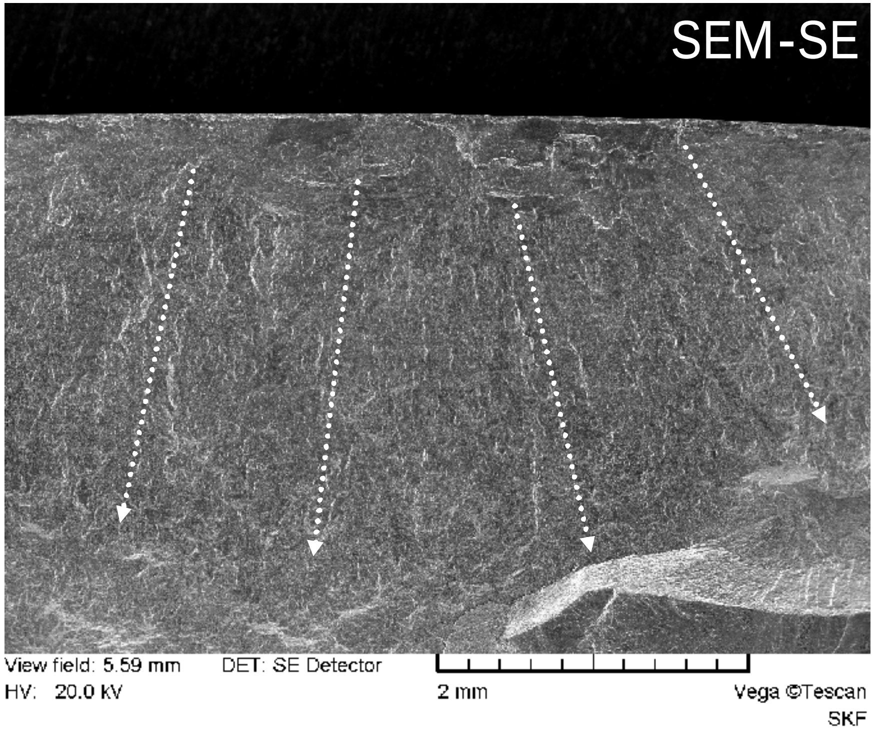

- step 1: cleavage-like fractures → normal stress hypothesis
- step 2: corrosion fatigue cracking (CFC)

→ microfractography, phase changes

(Semi-) Circular Brittle Spontaneous Incipient Cracks
1. Initiation from Near-Surface Inhomogeneities

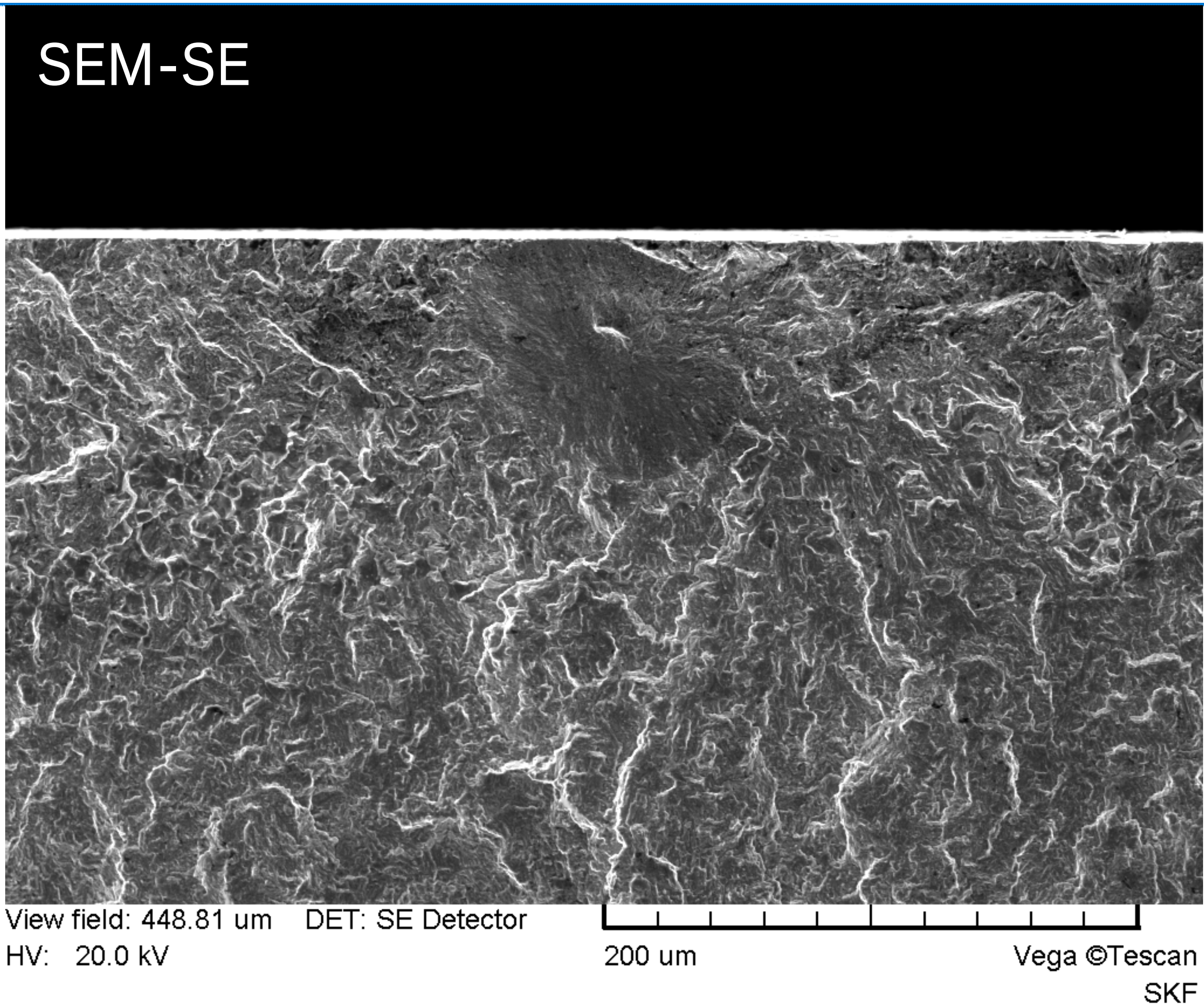

inhomogeneity:
small butterfly
on MnS inclusion

cleavage fracture as initiation of CFC

(Semi-) Circular Brittle Spontaneous Incipient Cracks
1. Initiation from Near-Surface Inhomogeneities

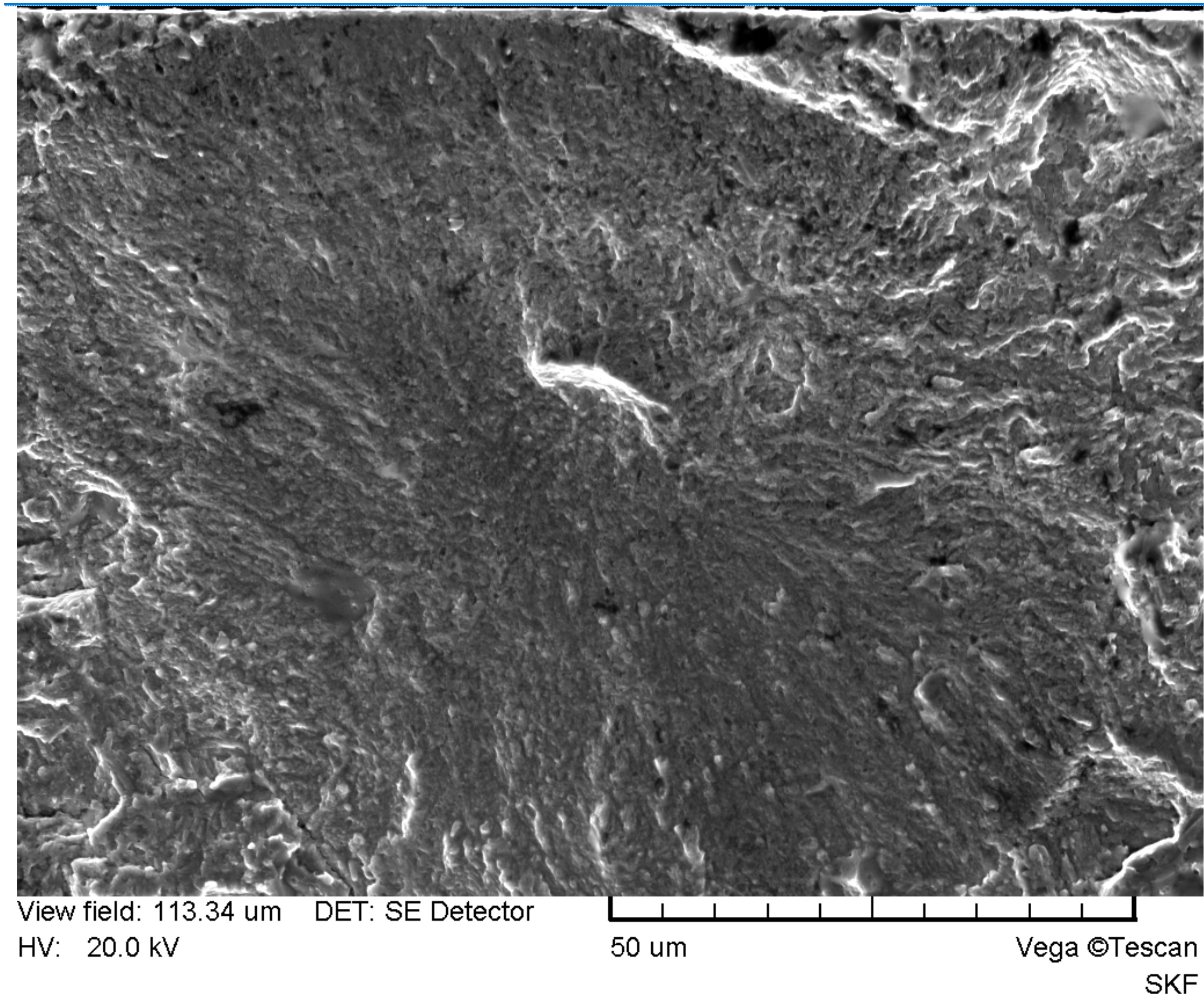

partly radial
fan structure

to the right of the
butterfly: CFC

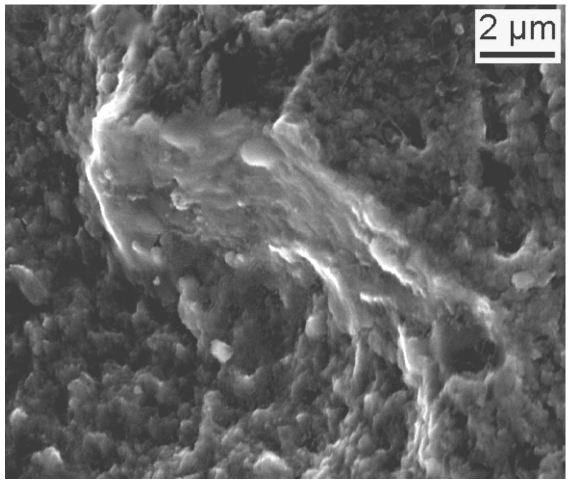

detail

(Semi-) Circular Brittle Spontaneous Incipient Cracks
1. Initiation from Near-Surface Inhomogeneities

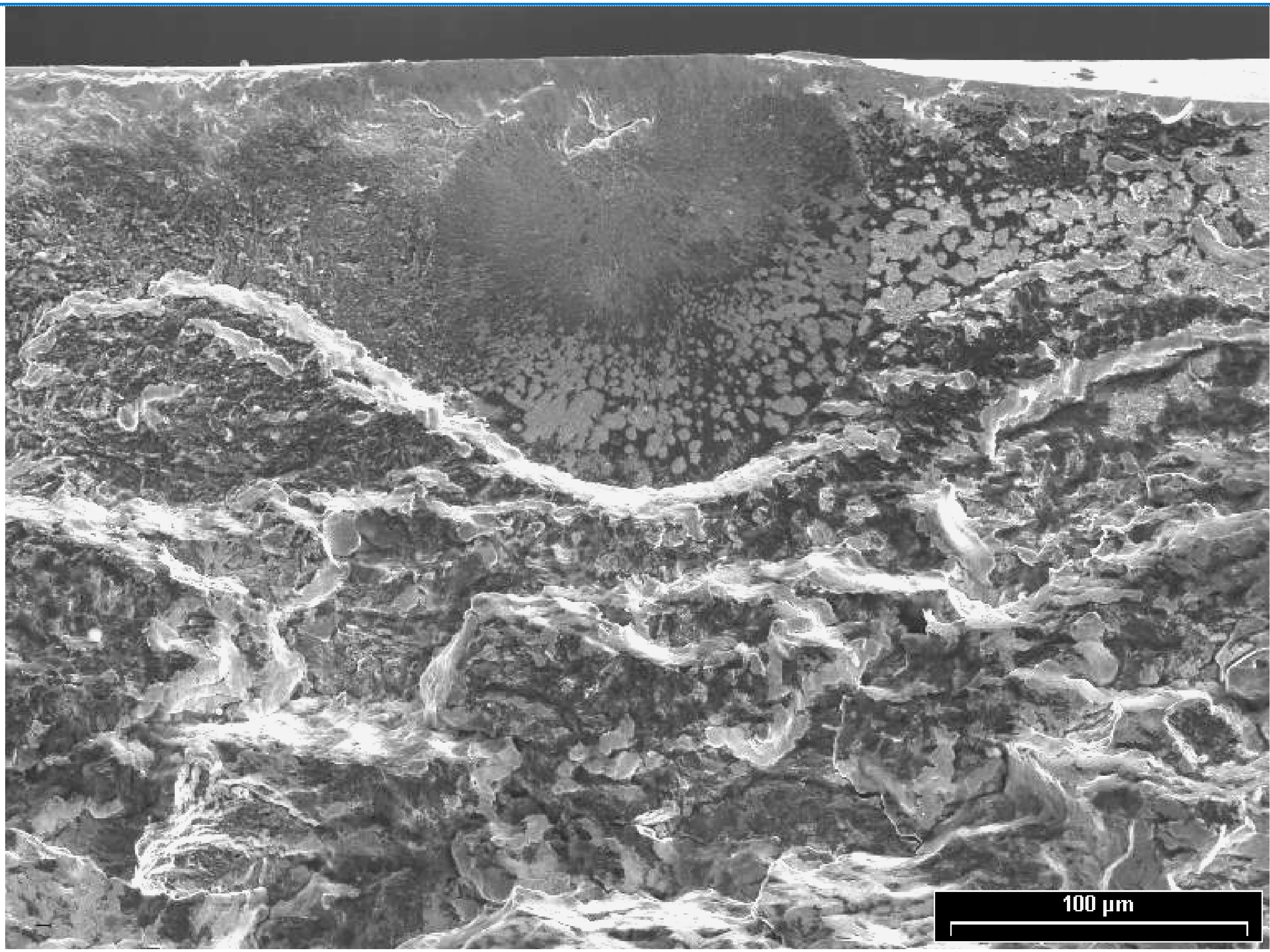

inhomogeneity:

inclusion

TiCN + MnS

cleavage fracture as initiation of CFC

(Semi-) Circular Brittle Spontaneous Incipient Cracks
1. Initiation from Near-Surface Inhomogeneities

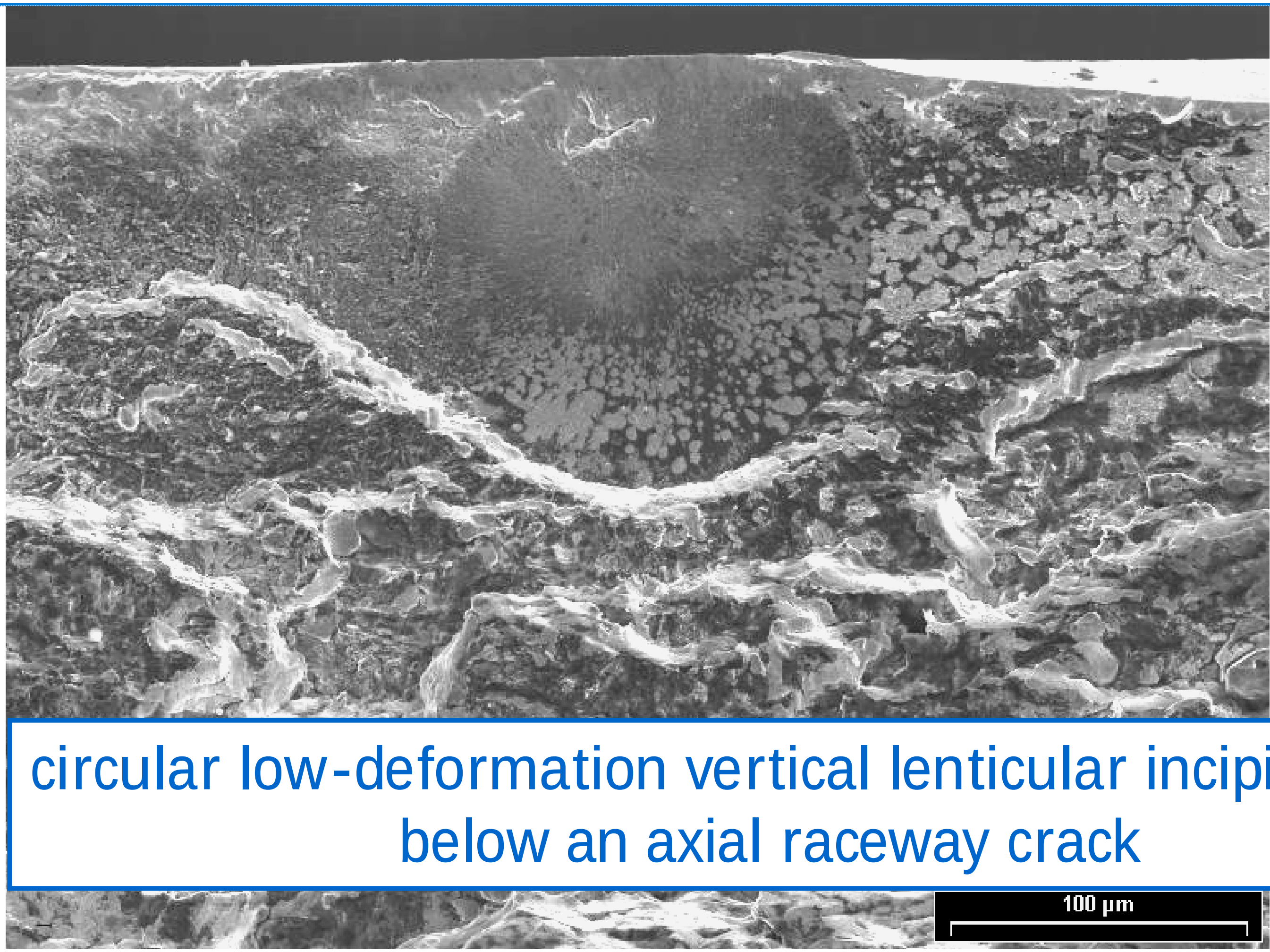

inhomogeneity:

inclusion

TiCN + MnS

circular low-deformation vertical lenticular incipient crack
below an axial raceway crack

cleavage fracture as initiation of CFC

(Semi-) Circular Brittle Spontaneous Incipient Cracks
1. Initiation from Near-Surface Inhomogeneities

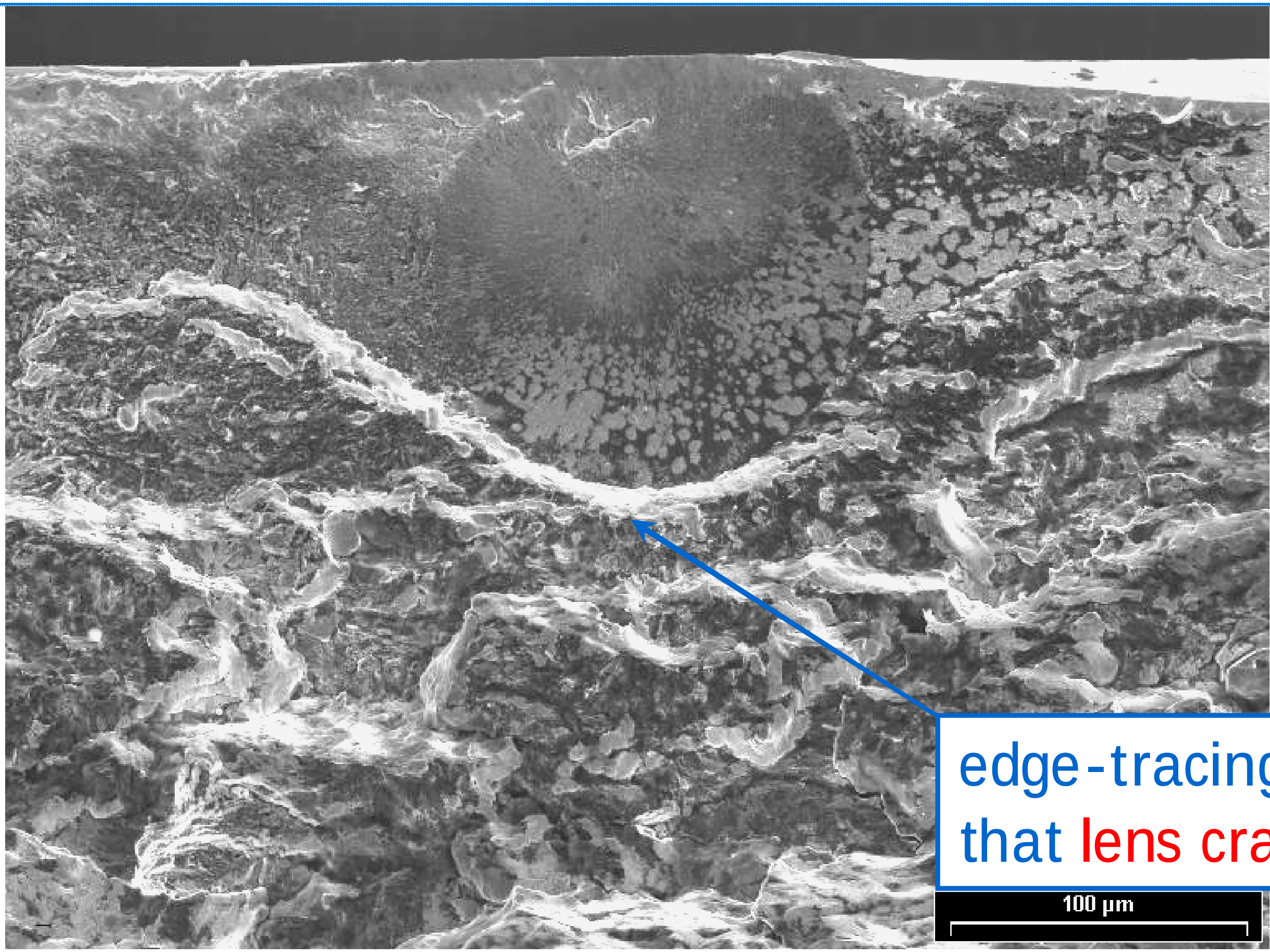

inhomogeneity:

inclusion

TiCN + MnS

edge-tracing bulge verifies that lens crack occurs first

cleavage fracture as initiation of CFC

(Semi-) Circular Brittle Spontaneous Incipient Cracks
1. Initiation from Near-Surface Inhomogeneities

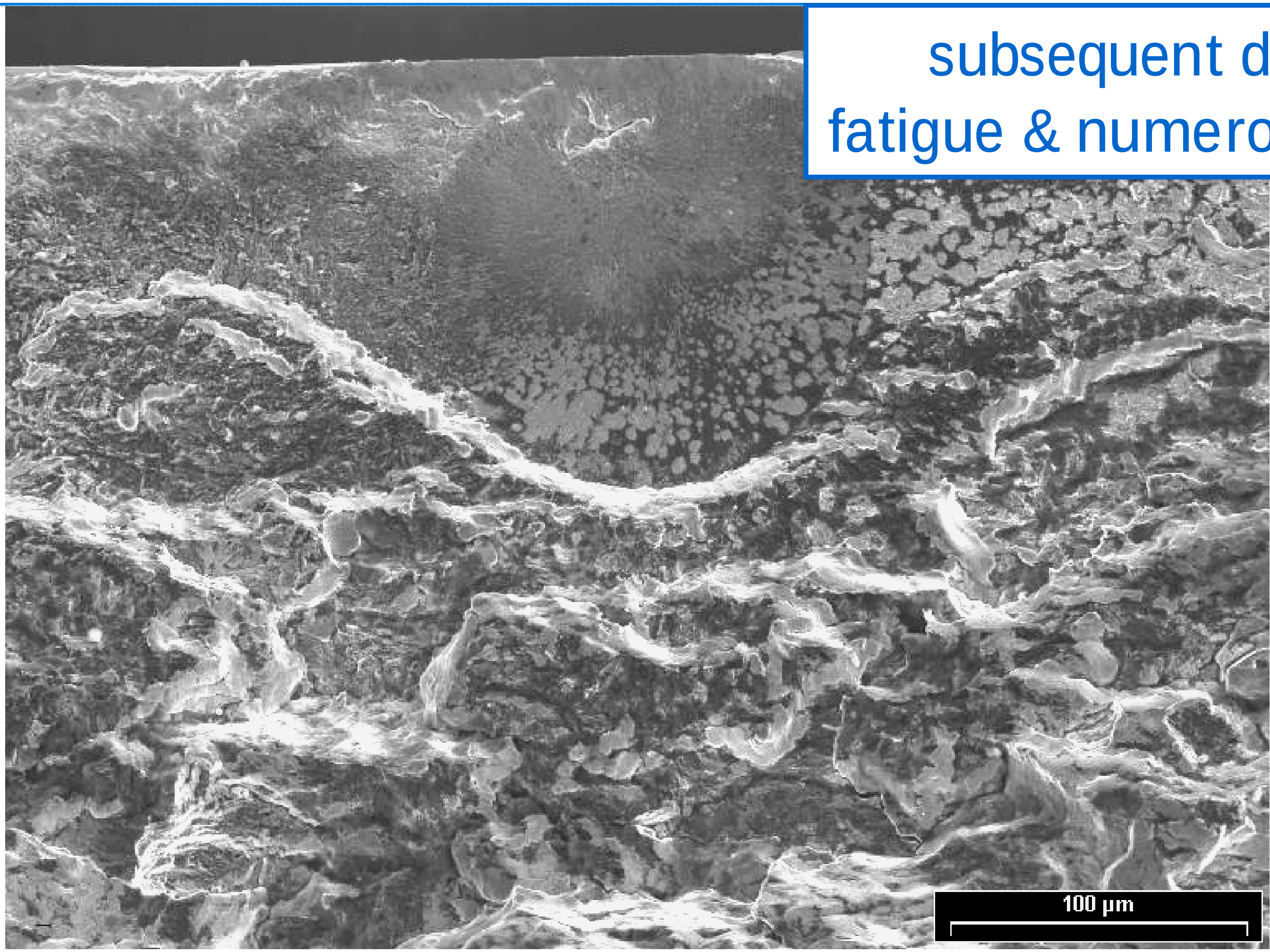

subsequent deep crack:
fatigue & numerous side cracks

inhomogeneity:
inclusion
TiCN + MnS

cleavage fracture as initiation of CFC

(Semi-) Circular Brittle Spontaneous Incipient Cracks
1. Initiation from Near-Surface Inhomogeneities

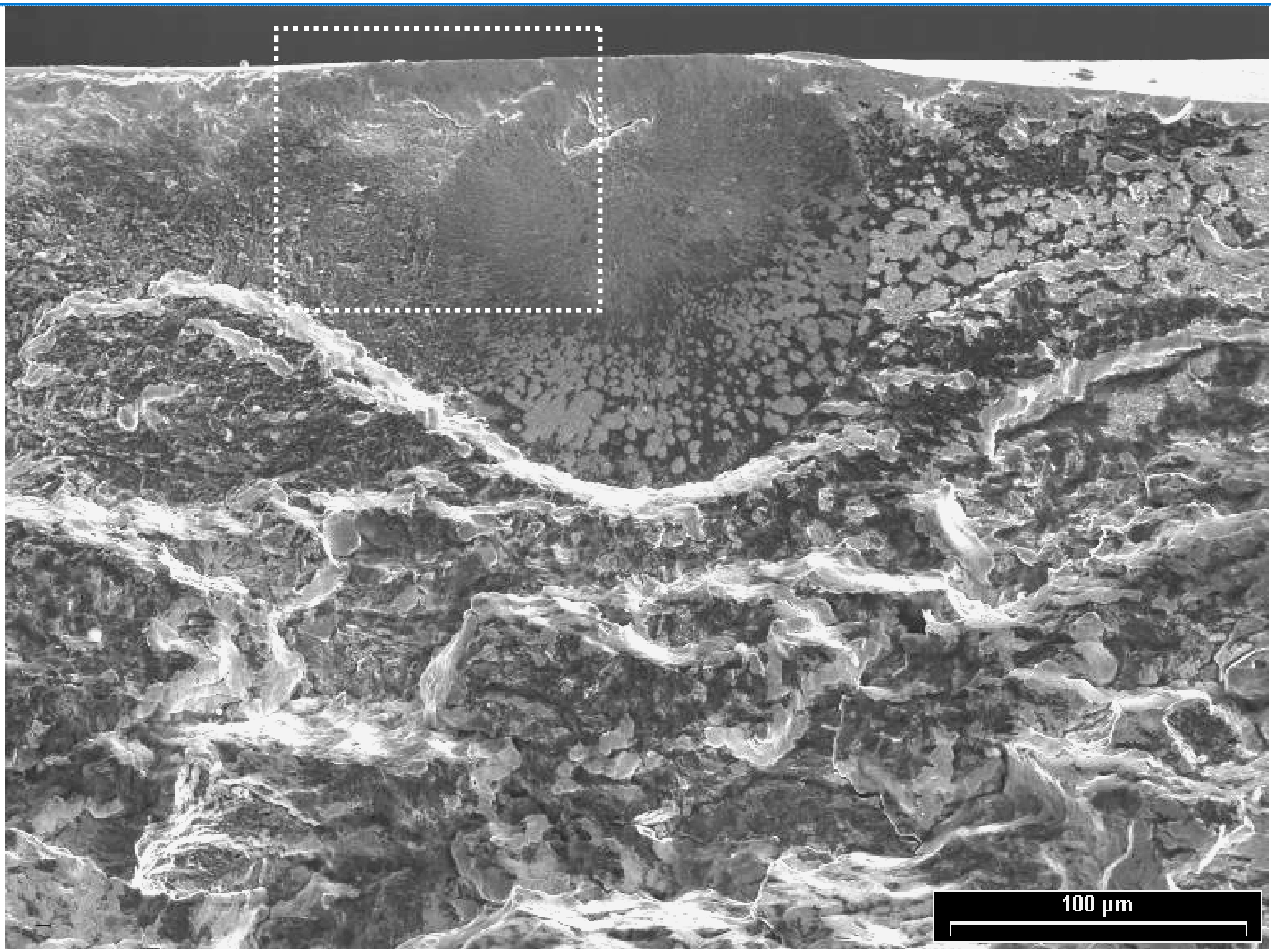

inhomogeneity:

inclusion

TiCN + MnS

cleavage fracture as initiation of CFC

SKF

(Semi-) Circular Brittle Spontaneous Incipient Cracks
1. Initiation from Near-Surface Inhomogeneities

distinct change of the fracture pattern also on the left of the *lens*

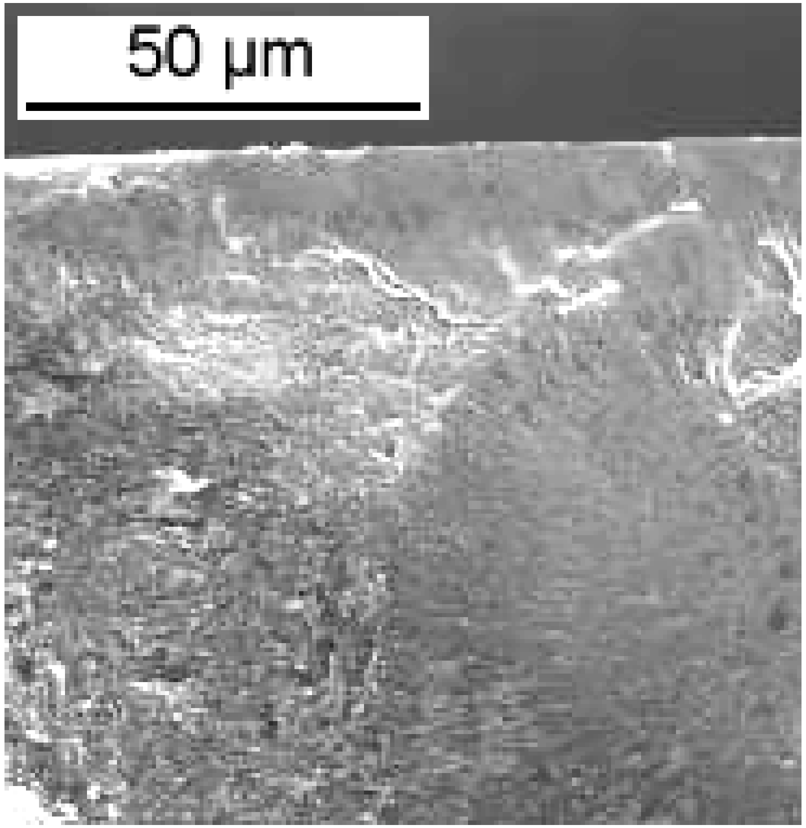

fan structure on *cleavage* area

faint side cracks outside

detail 1

(Semi-) Circular Brittle Spontaneous Incipient Cracks
1. Initiation from Near-Surface Inhomogeneities

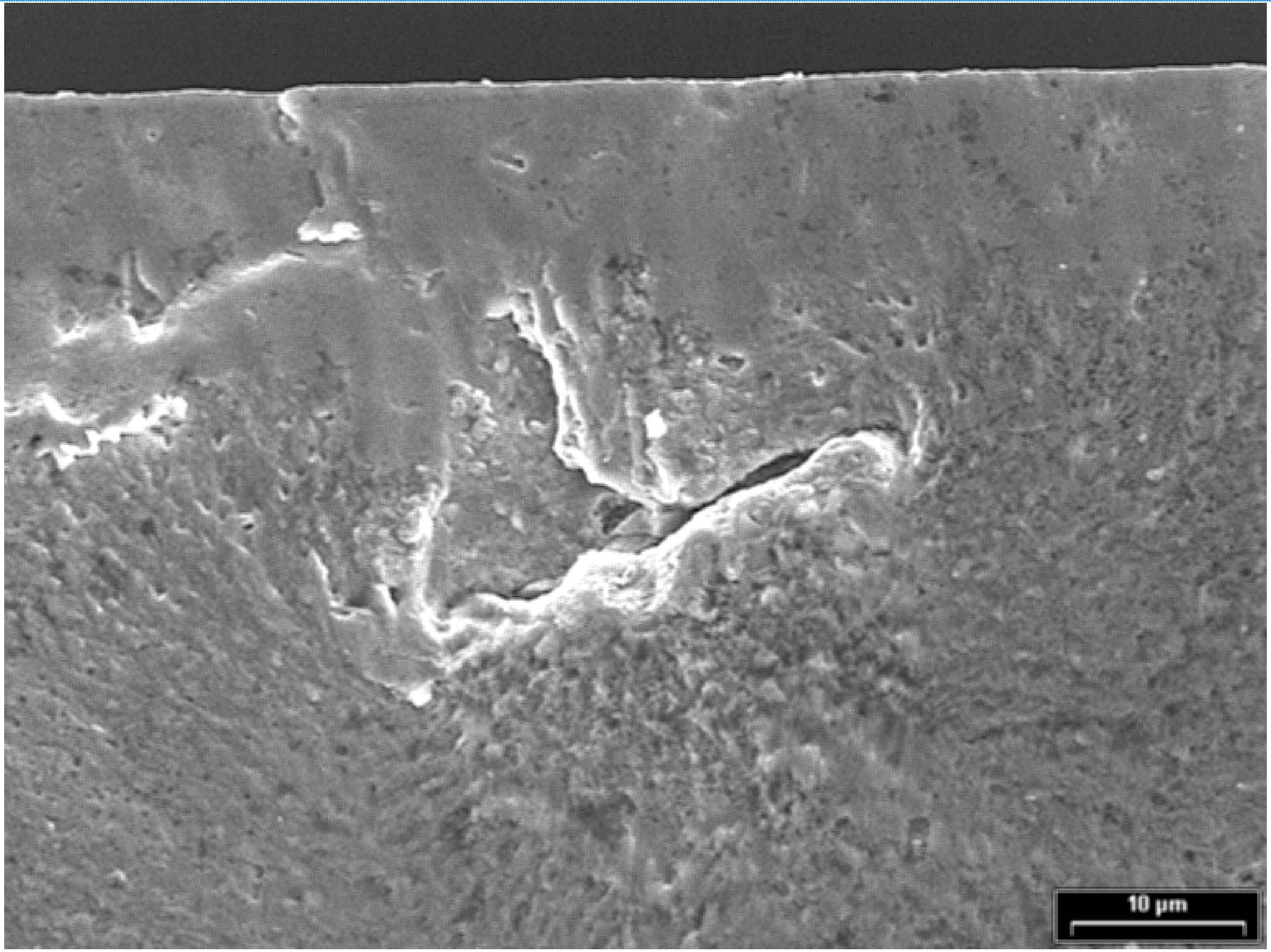

inclusion,
no butterfly

start of
fan structure

detail 2

(Semi-) Circular Brittle Spontaneous Incipient Cracks
1. Initiation from Near-Surface Inhomogeneities

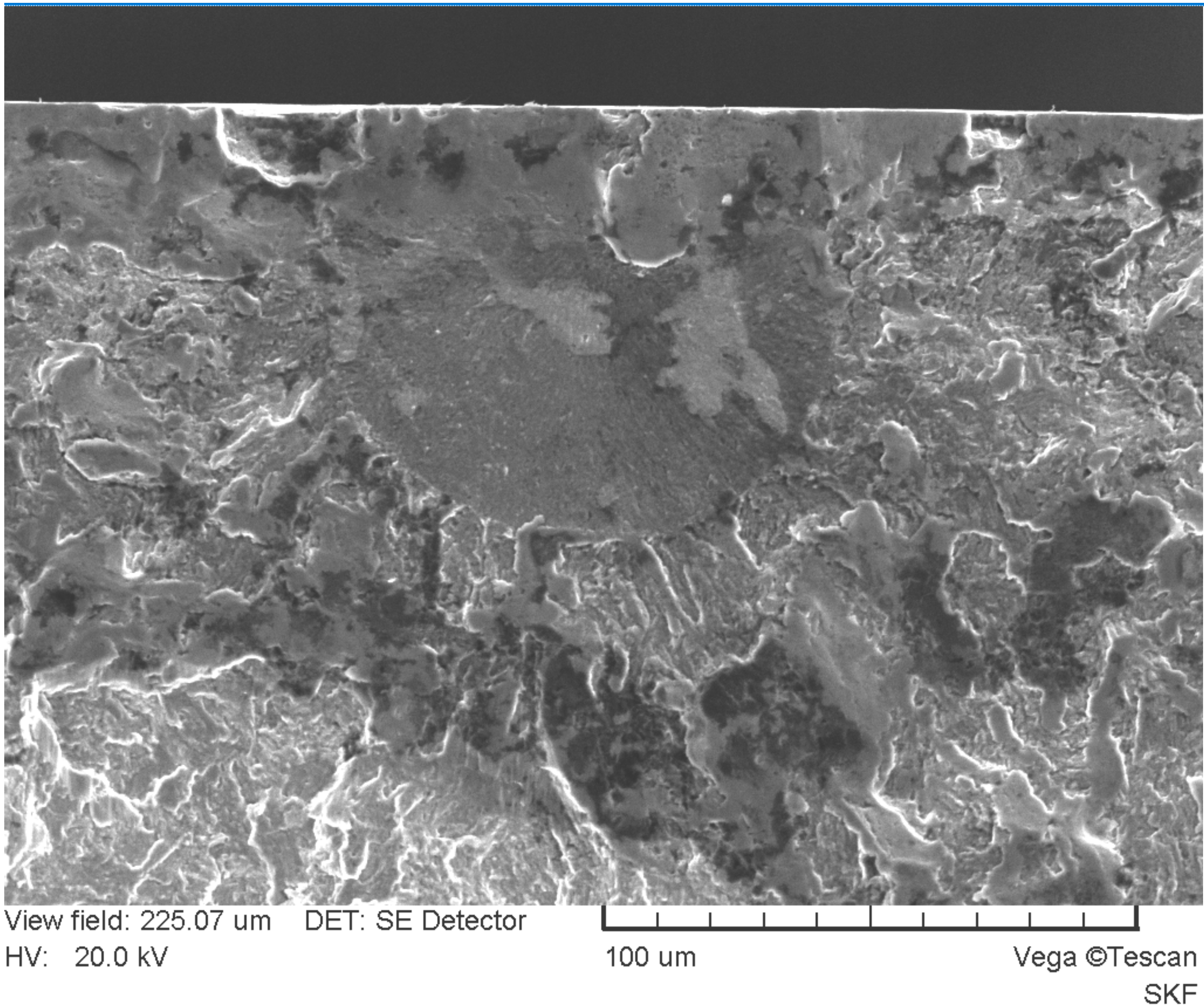

inhomogeneity:

near-surface

tensile residual stress

cleavage fracture as initiation of CFC

(Semi-) Circular Brittle Spontaneous Incipient Cracks
1. Initiation from Near-Surface Inhomogeneities

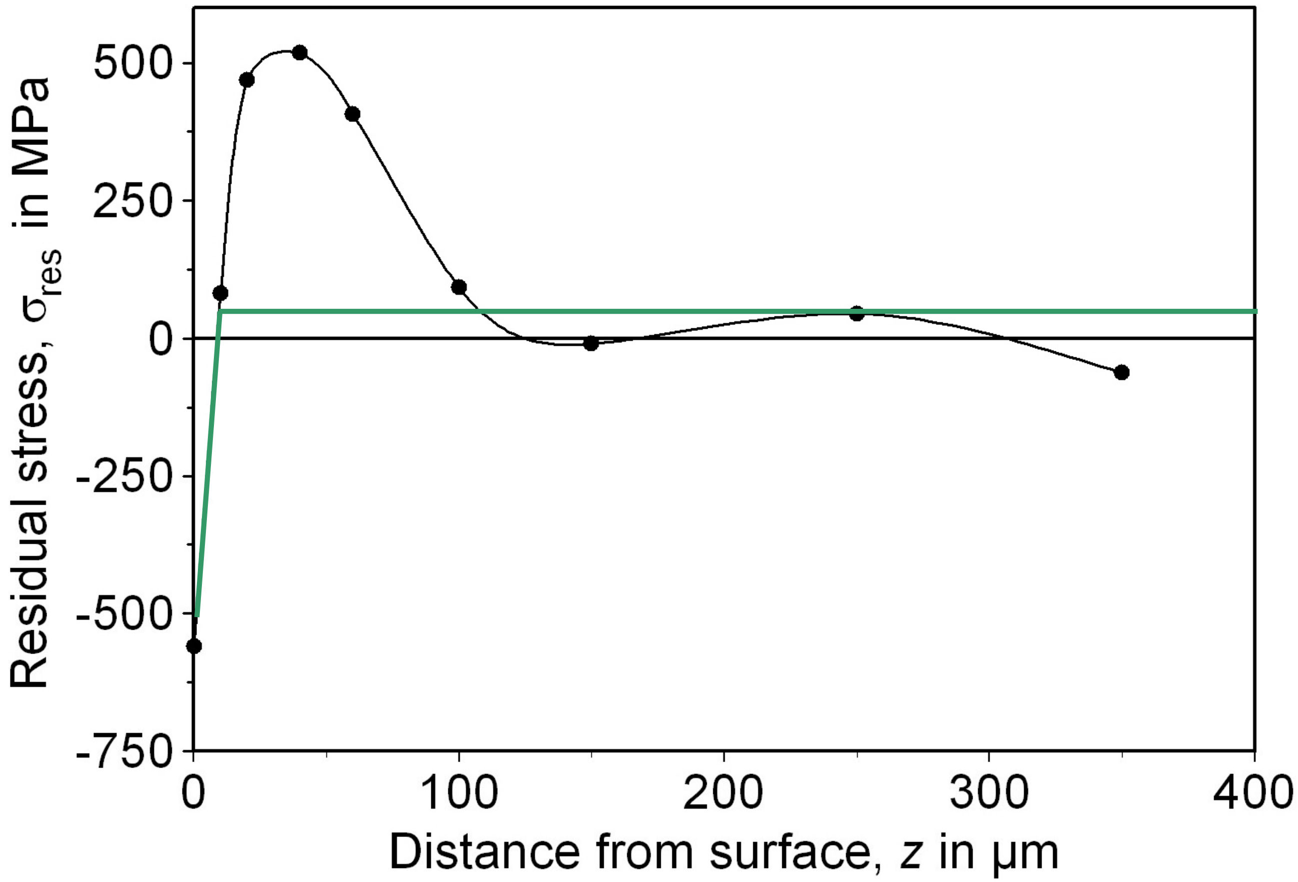

inhomogeneity:

near-surface

tensile residual stress

typical distribution
for martensitically
through hardened
and finished parts

XRD residual stress analysis

(Semi-) Circular Brittle Spontaneous Incipient Cracks
1. Initiation from Near-Surface Inhomogeneities

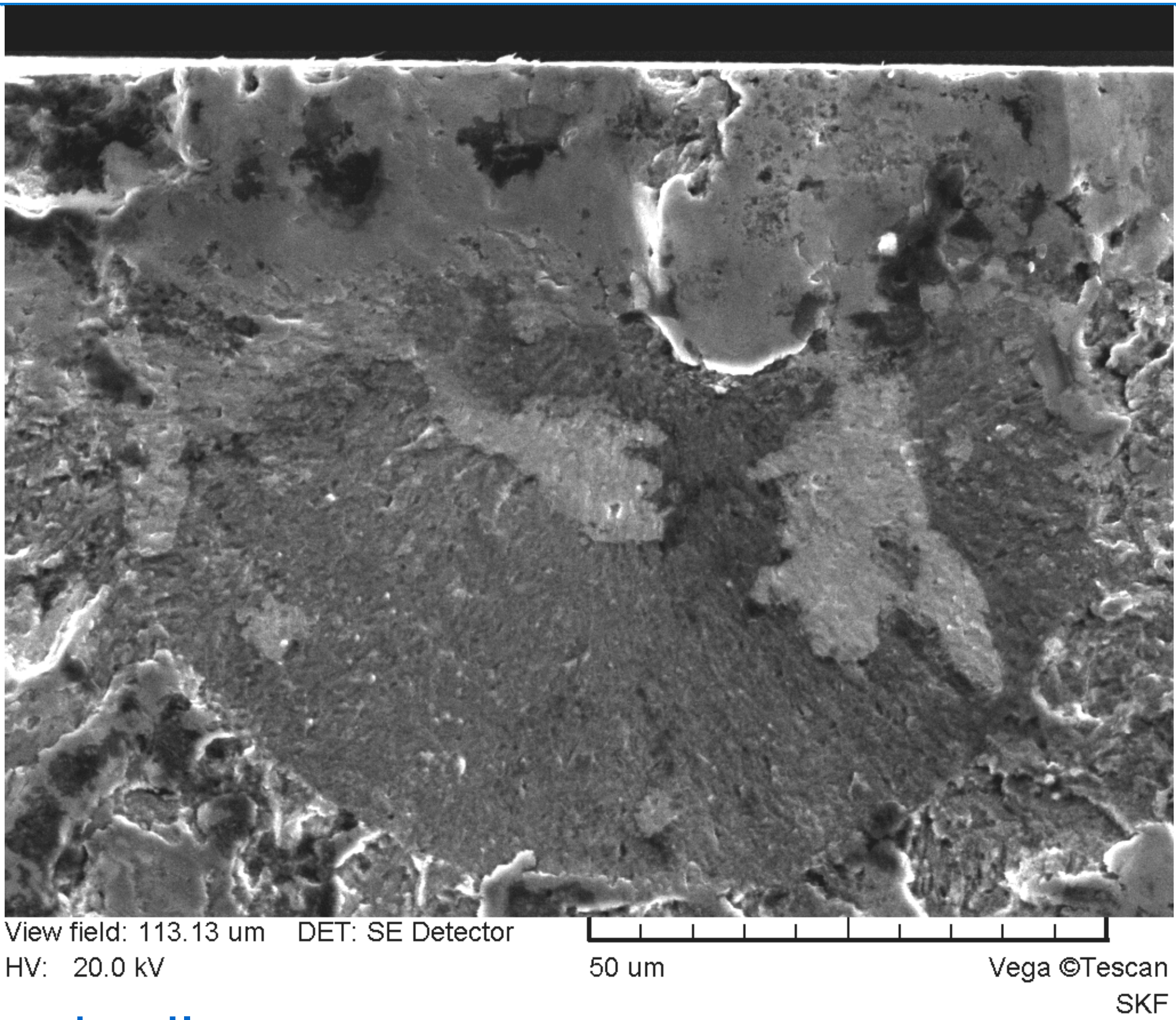

faint radial
fan structure

outside of *cleavage*:

side cracks,
martensite micro-
structure partly
visible

detail

(Semi-) Circular Brittle Spontaneous Incipient Cracks
2. No Distinct Crack Nuclei

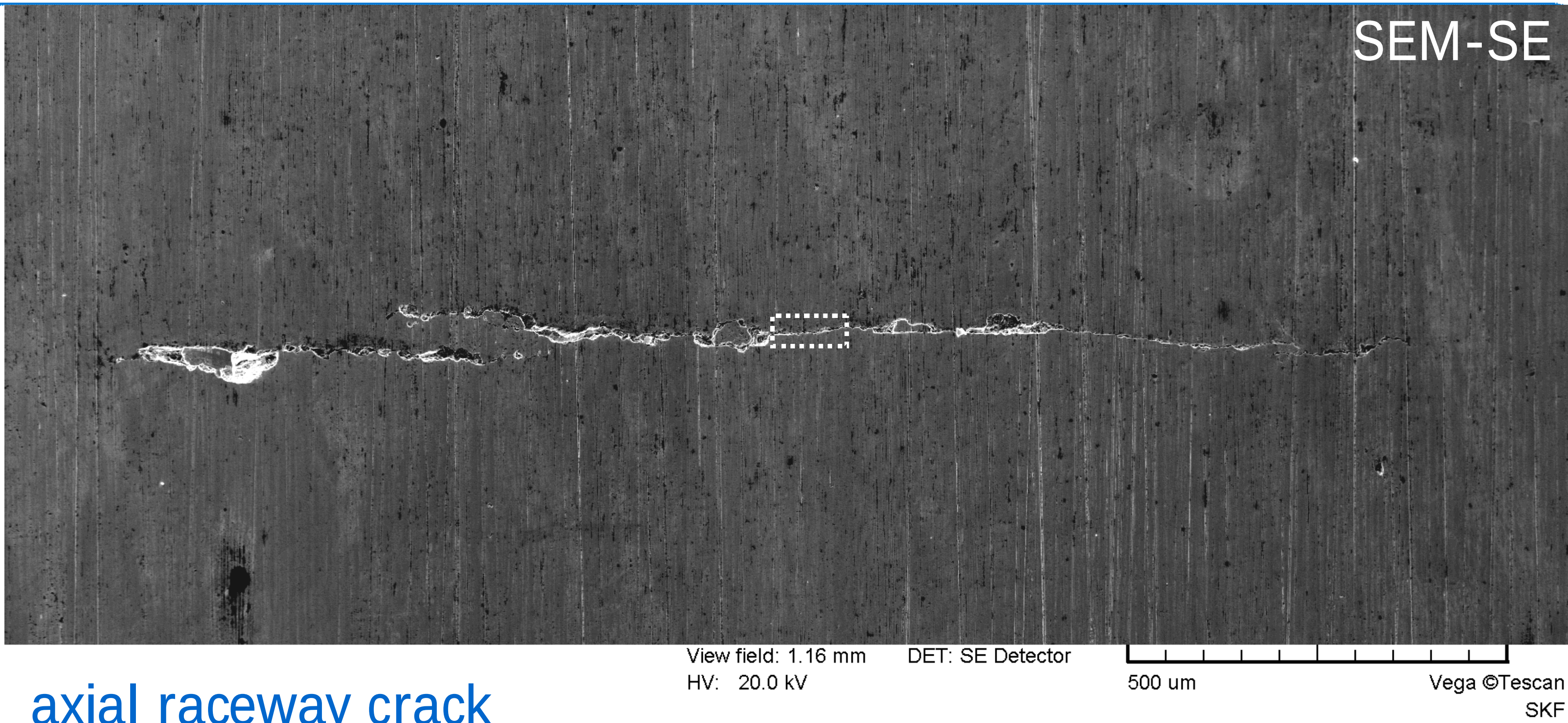

axial raceway crack

Ÿ distinctly smoothed honing structure ⇒ mixed friction conditions

Ÿ brittle spontaneous incipient crack below sharp-edged segment

ú clearly distinguishable from adjacent serrated branching CFC

(Semi-) Circular Brittle Spontaneous Incipient Cracks

2. No Distinct Crack Nuclei

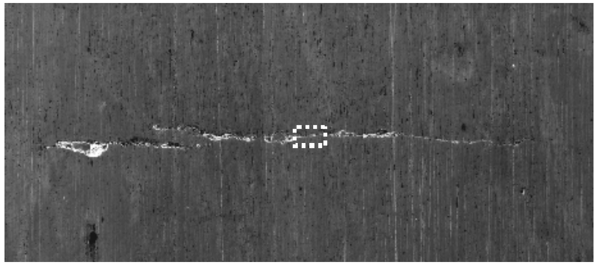

overview of the opened crack

- crack depth about 900 µm
- preparative forced fracture clearly distinguishable

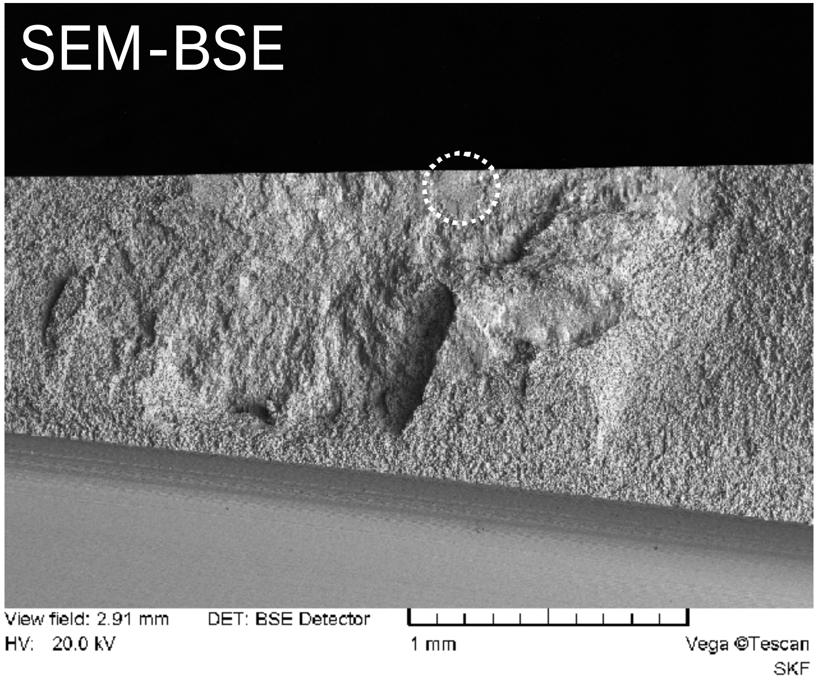

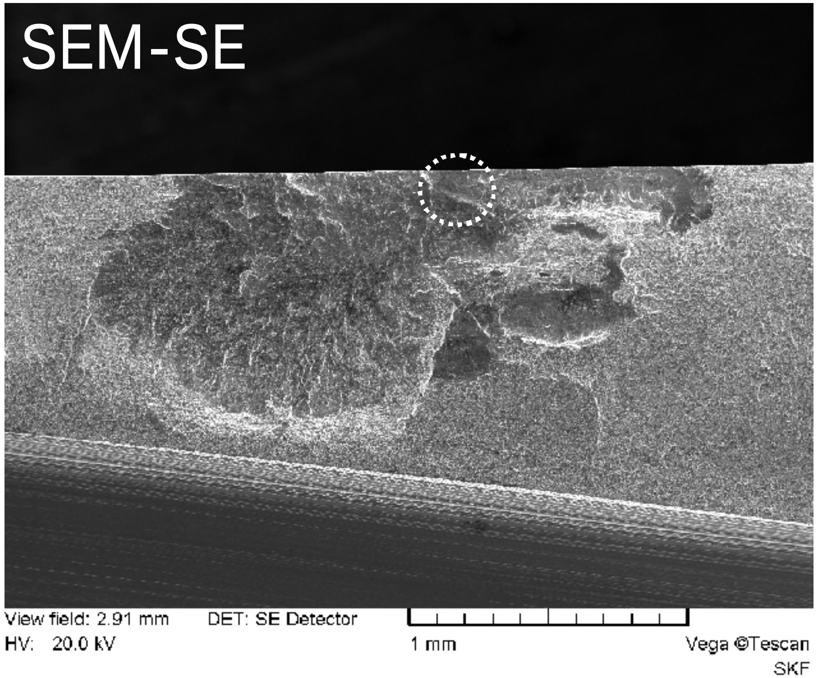

... brittle incipient *cleavage* crack

(Semi-) Circular Brittle Spontaneous Incipient Cracks
2. No Distinct Crack Nuclei

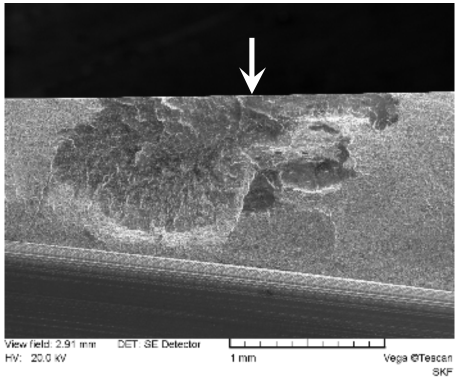

different crack mechanisms inside and outside the flat *cleavage* fracture surface

- 130 µm deep brittle vertical incipient crack
- surrounded by striation-like lines of CFC

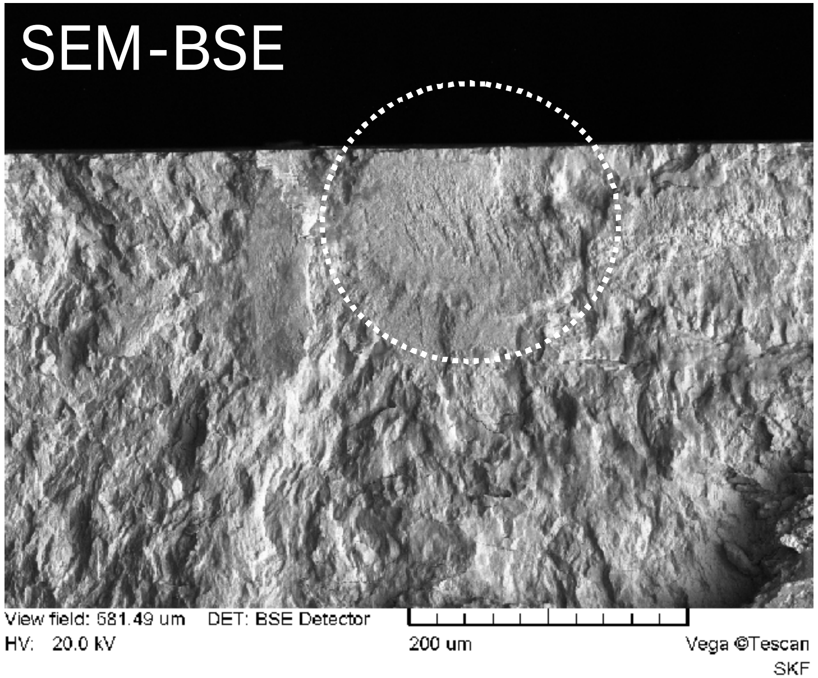

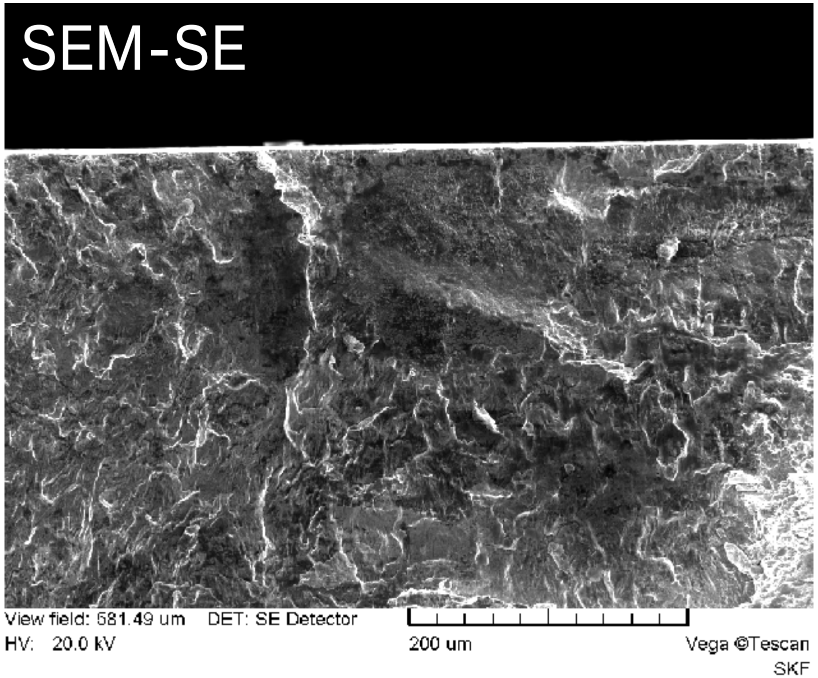

(Semi-) Circular Brittle Spontaneous Incipient Cracks

2. No Distinct Crack Nuclei

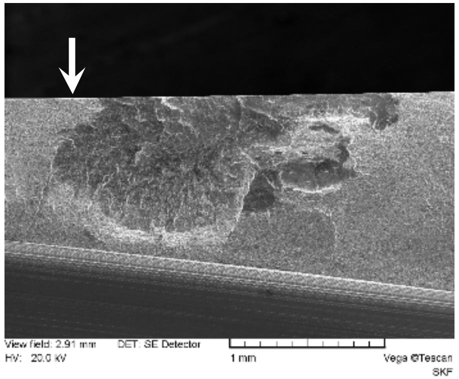

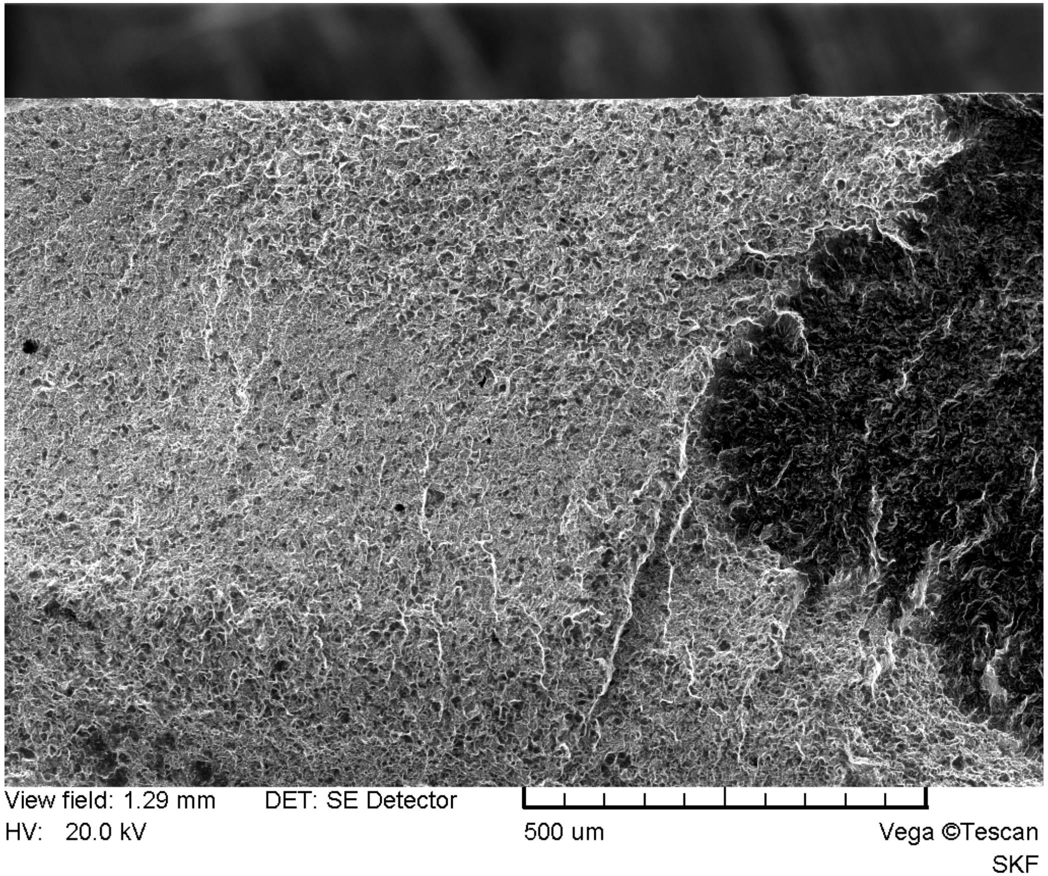

preparatively generated forced fracture face reveals local hydrogen embrittlement adjacent to the original CFC crack

(Semi-) Circular Brittle Spontaneous Incipient Cracks
2. No Distinct Crack Nuclei

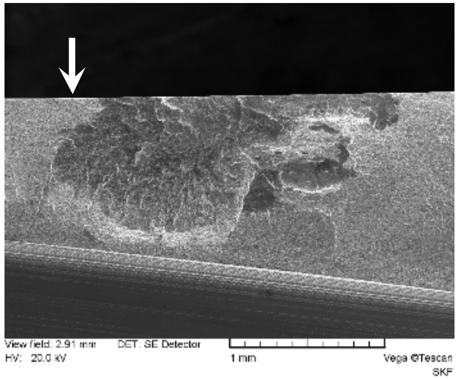

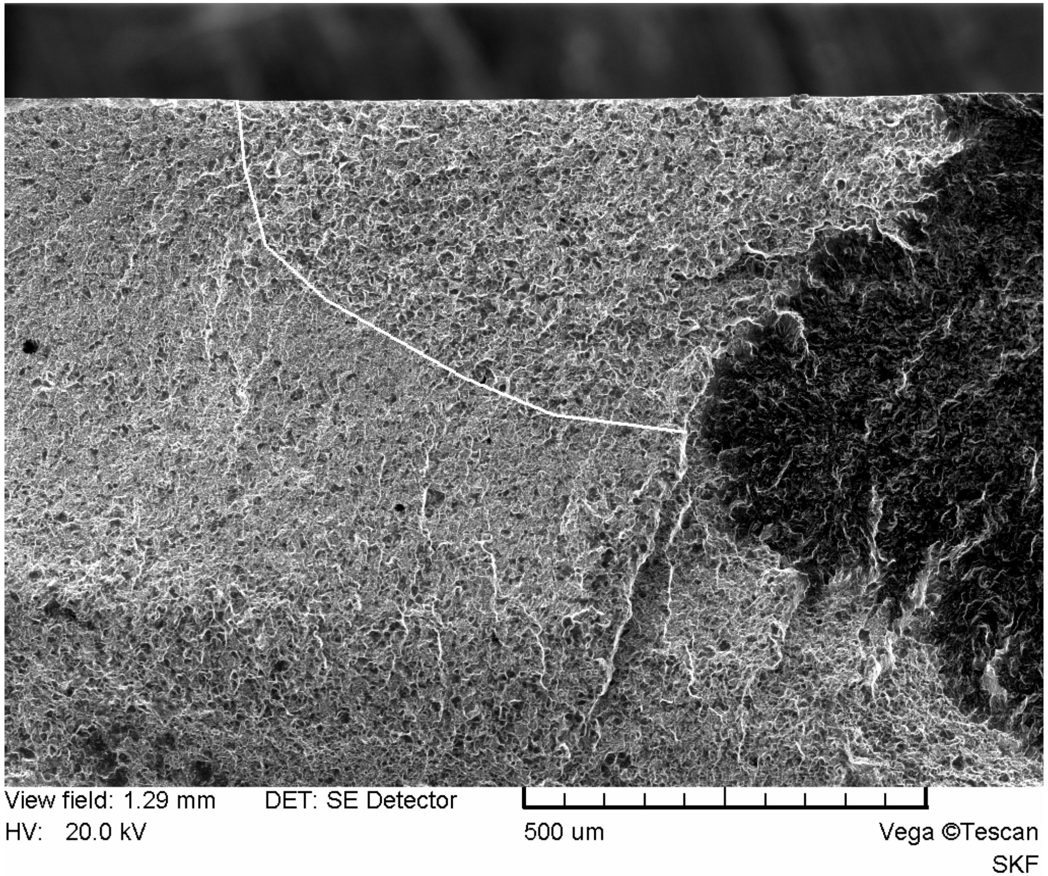

preparatively generated forced fracture face reveals local hydrogen embrittlement adjacent to the original CFC crack

Ÿ increased intergranular fraction

SKF

(Semi-) Circular Brittle Spontaneous Incipient Cracks
2. No Distinct Crack Nuclei

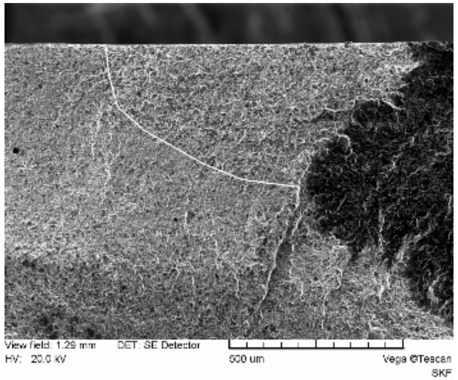

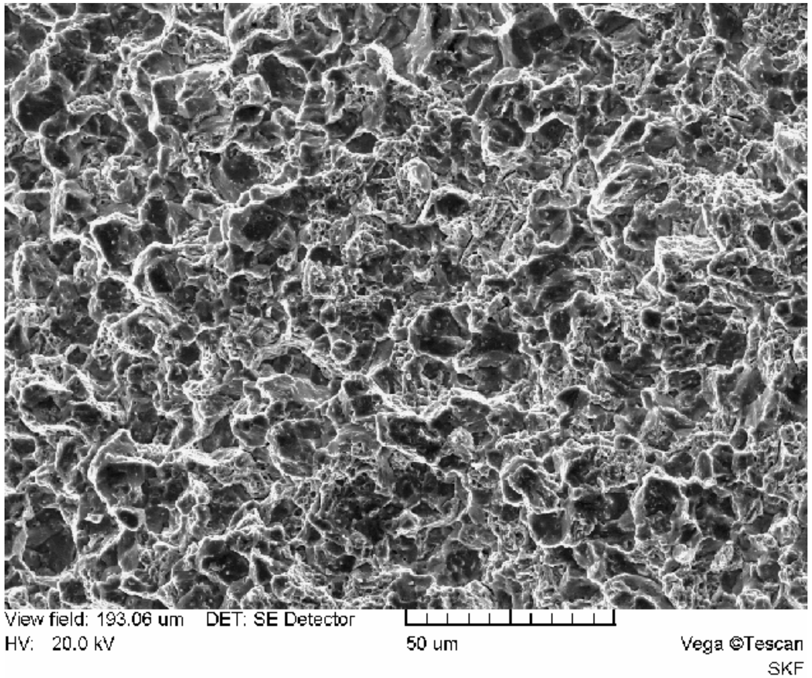

near the original crack

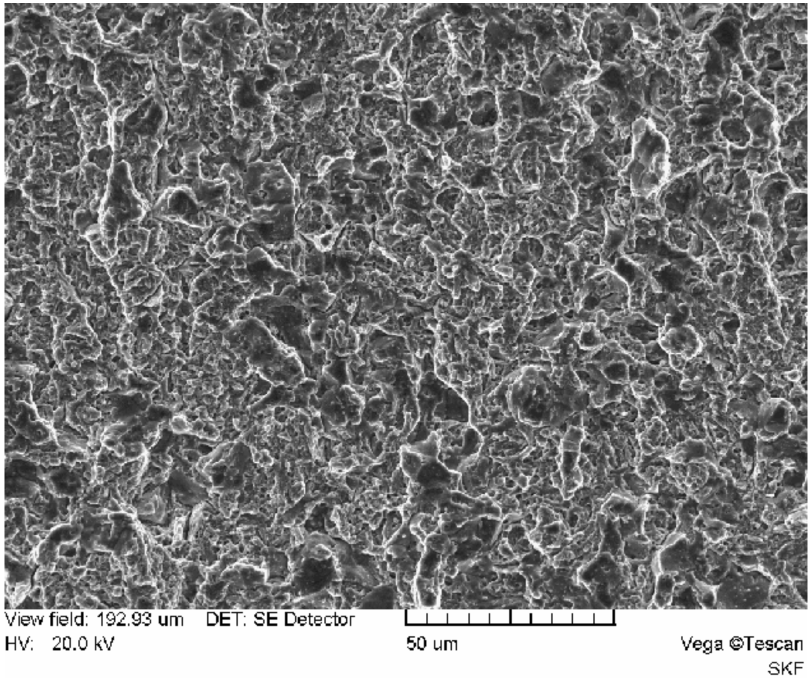

core

SKF®

(Semi-) Circular Brittle Spontaneous Incipient Cracks

2. No Distinct Crack Nuclei

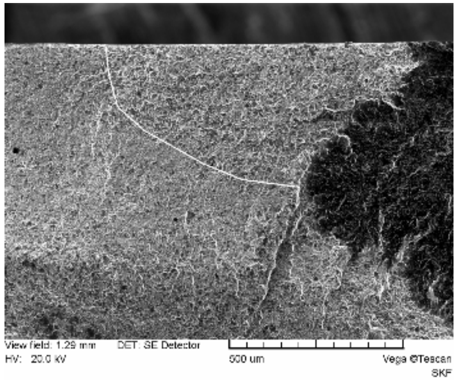

Raceway	2.2 ppm H
Center	1.0 ppm H
Bore	1.0 ppm H

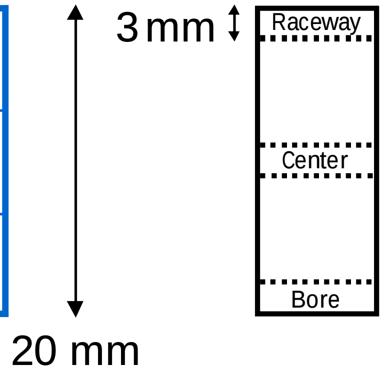

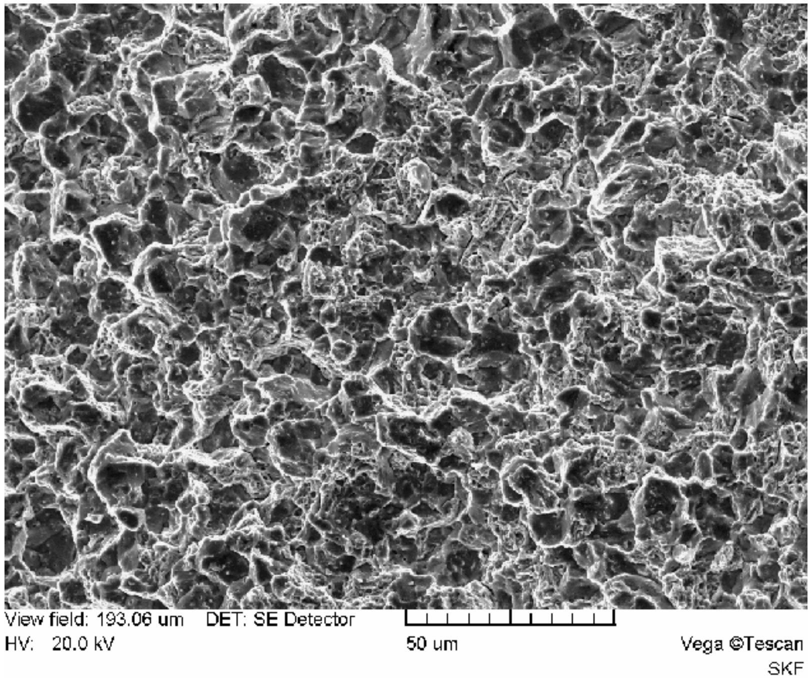

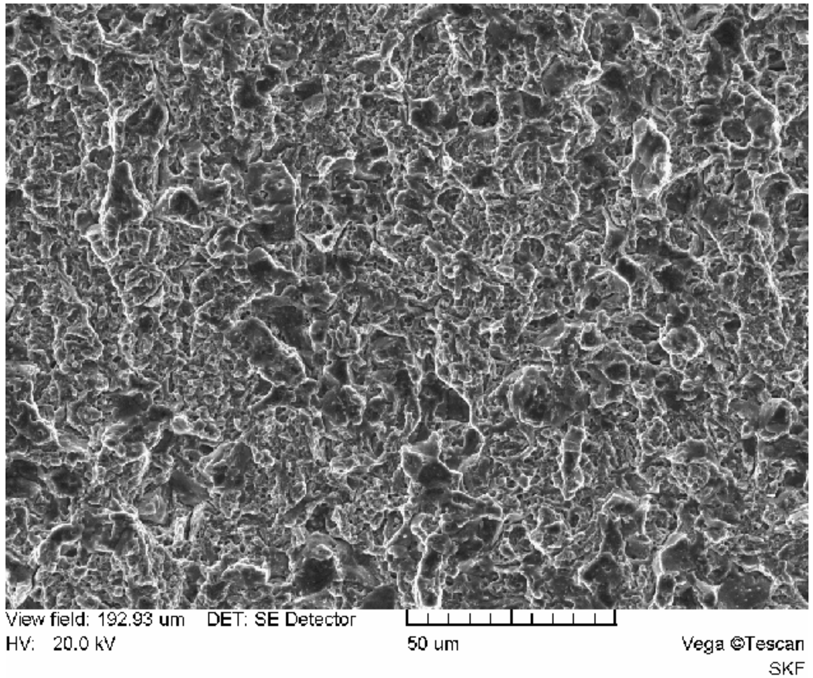

dense surface cracks: H absorption

(Semi-) Circular Brittle Spontaneous Incipient Cracks
2. No Distinct Crack Nuclei

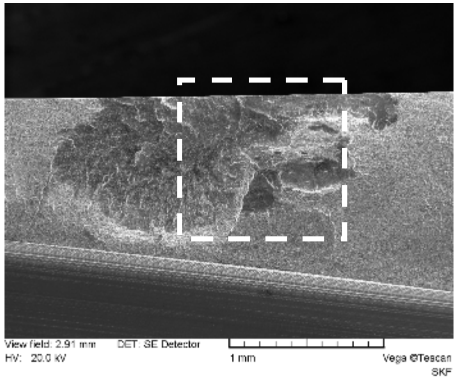

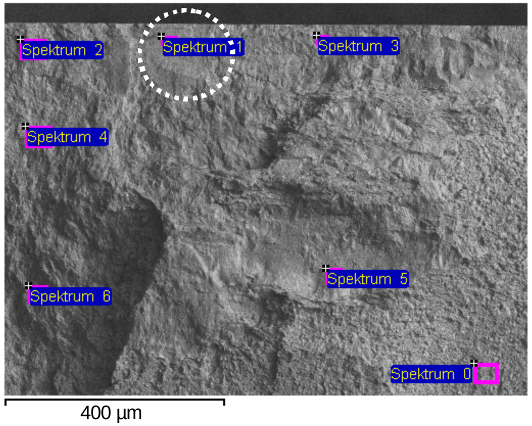

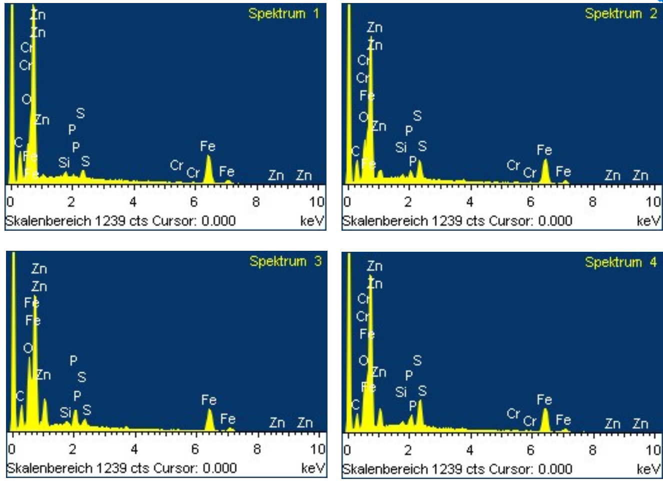

EPMA-EDX (10 kV)

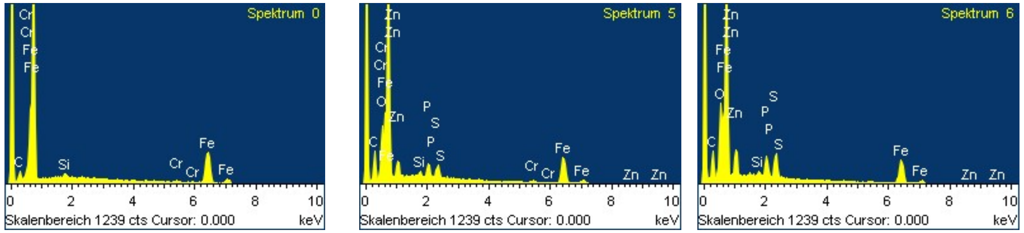

- S1 at incipient *cleavage* crack: only subsequent surface corrosion
- S2-S6 reveal much stronger signals of the typical tracer elements sulfur, phosphor and zinc of the lubricant additives
  - higher tracer enrichment in the (deeper) CFC region due to mixed mechanical-chemical loading

SKF

(Semi-) Circular Brittle Spontaneous Incipient Cracks
2. No Distinct Crack Nuclei

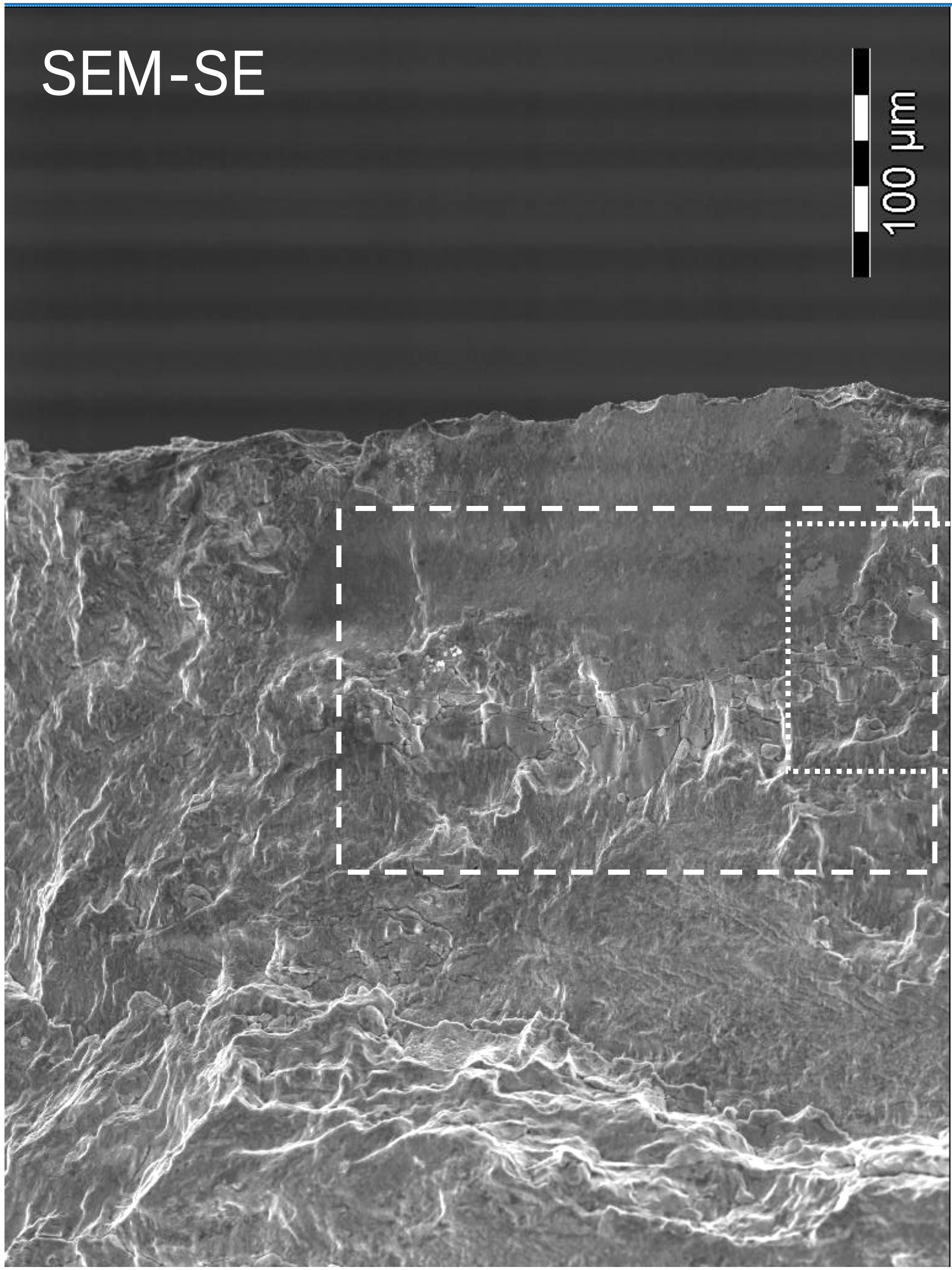

cleavage fracture
as initiation of CFC

different crack mechanisms
inside and outside the flat face

(Semi-) Circular Brittle Spontaneous Incipient Cracks
2. No Distinct Crack Nuclei

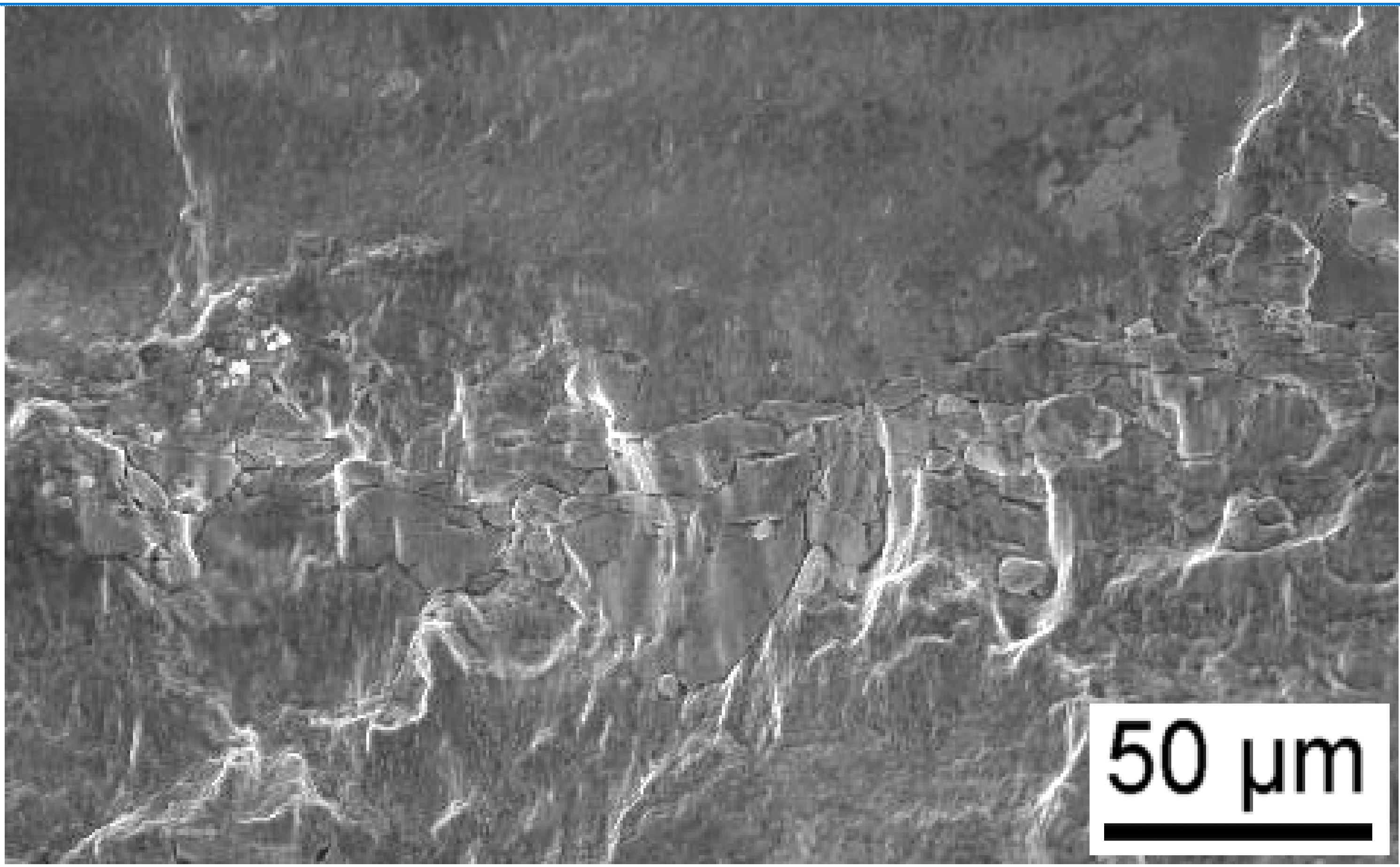

demarcating crack network at the runout of the *cleavage* fracture

detail 1

(Semi-) Circular Brittle Spontaneous Incipient Cracks
2. No Distinct Crack Nuclei

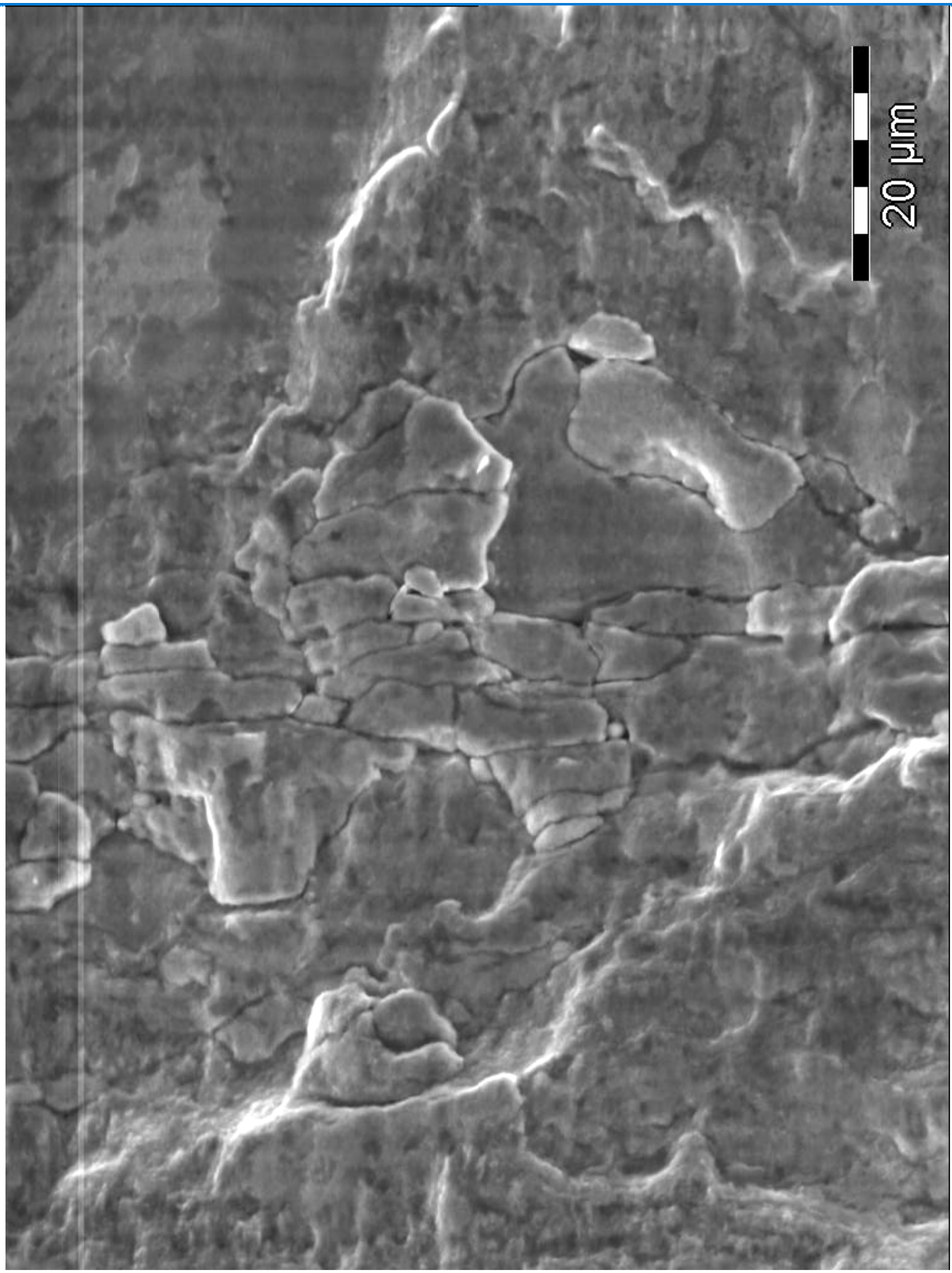

demarcating crack network

- *cleavage* crack occurs first
- temporary crack stop and gradually starting CFC

detail 2

Microstructural Changes around CFC Cracks

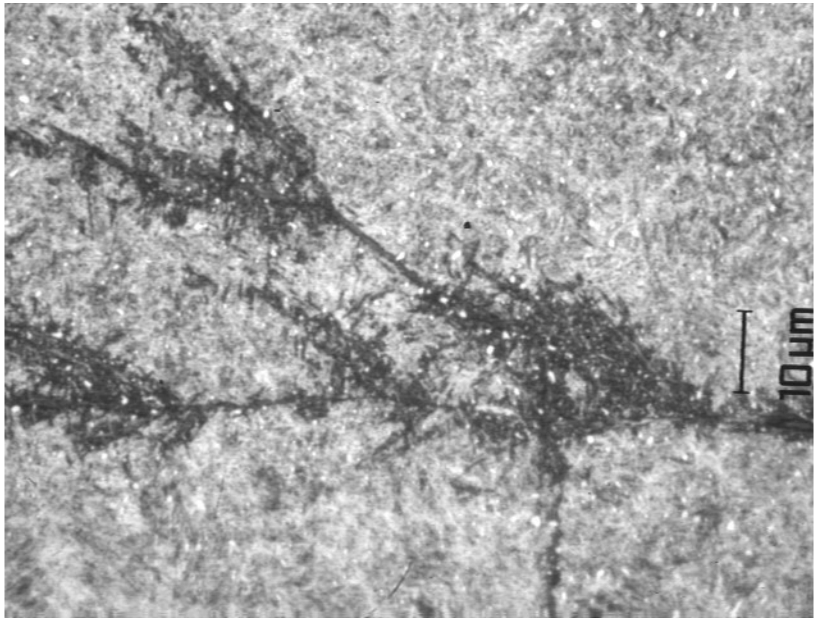

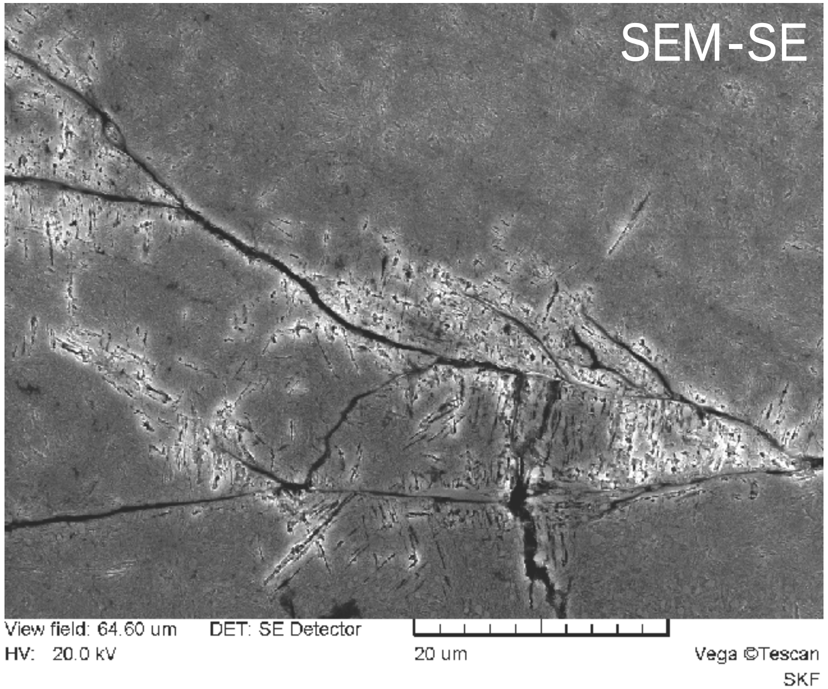

origin of the crack network demarcating the *cleavage* fracture

- embrittled DER precursor of WEA evolution on CFC cracks

ú preparative etching cracks reveal material embrittlement (SEM)

Microstructural Changes around CFC Cracks

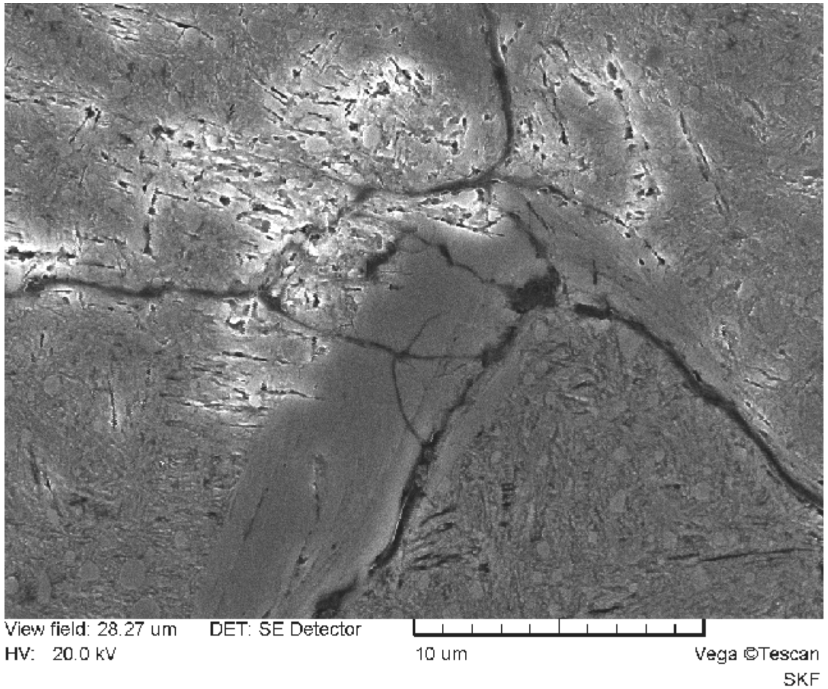

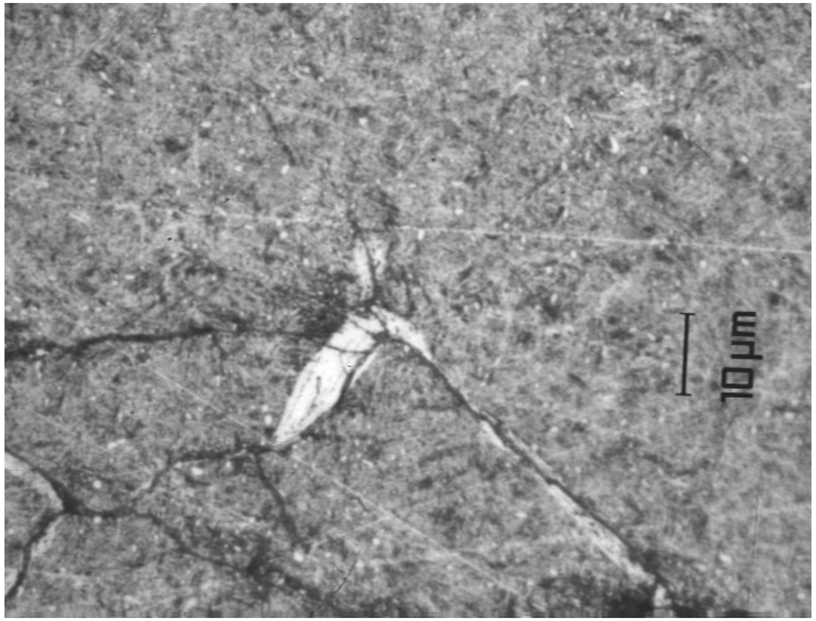

origin of the crack network demarcating the *cleavage* fracture

- hydrogen induced microstructure transformation
  - hydrogen released from decomposition products of the penetrating oil (additives, contaminations) on the rubbing blank metal crack faces/tip

Microstructural Changes around CFC Cracks

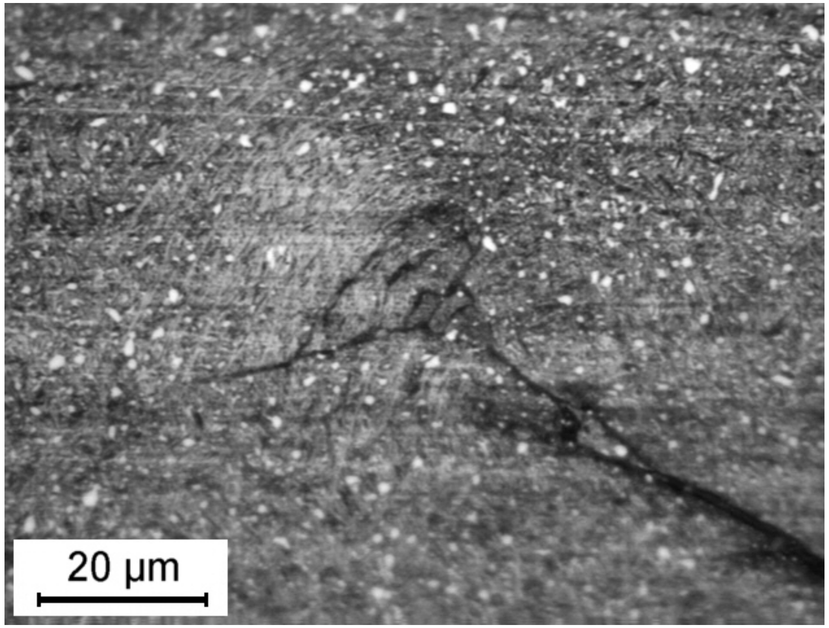

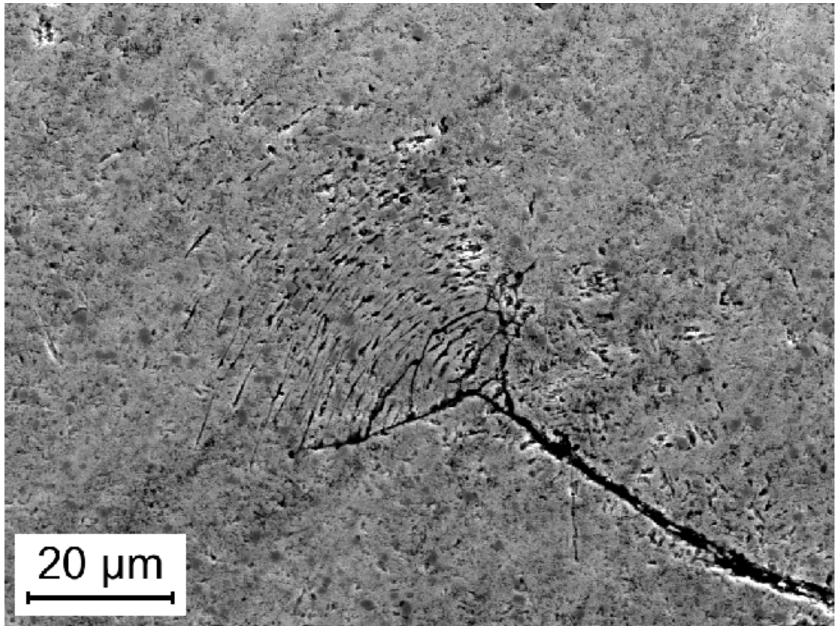

H induced DER: deformation bands as starting crack network

- occasionally visible as topographic feature at fracture faces
- carbide dissolution (DER precursor → WEA by DRX)

ú localized H-RCF (DGSL & HELP)

Microstructural Changes around CFC Cracks

incipient phase transformation (DER) at branching crack tip and crack face

- near CFC cracks: local DER → WEA

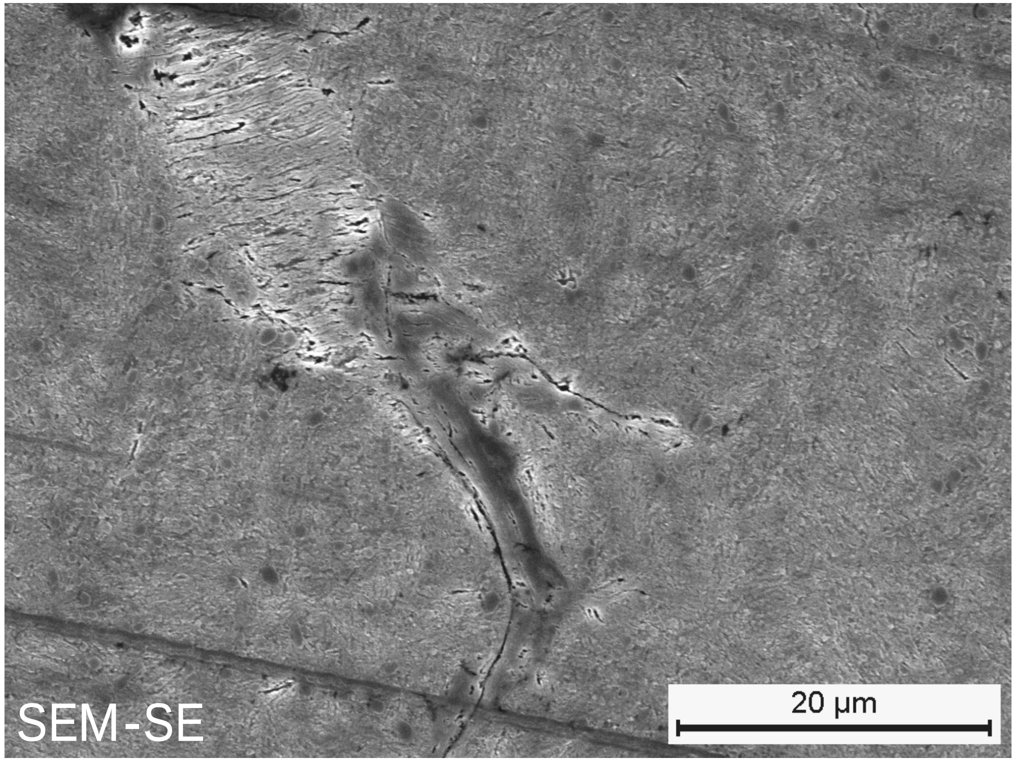

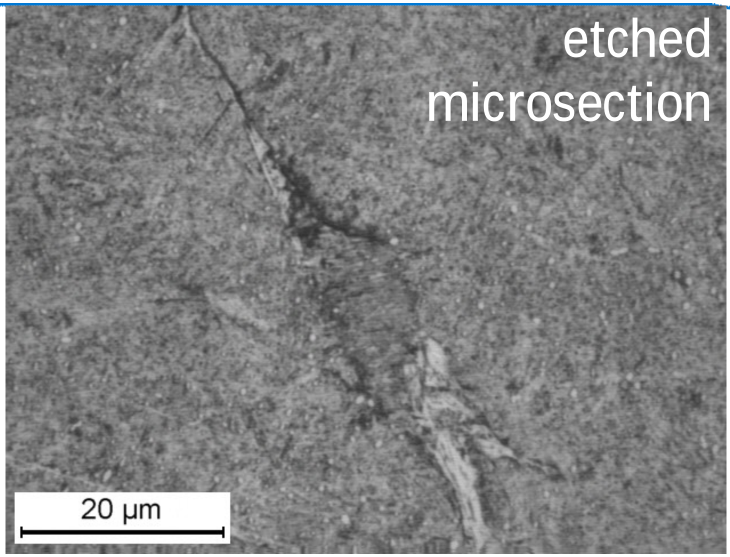

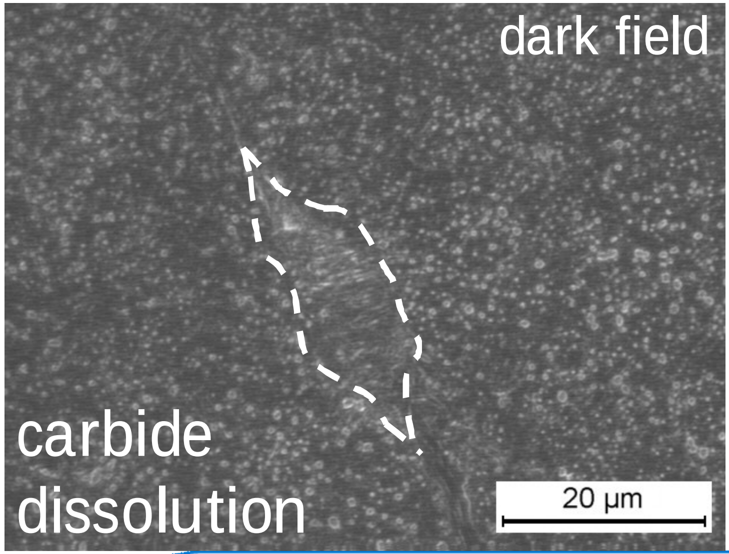

(Semi-) Circular Brittle Spontaneous Incipient Cracks
2. No Distinct Crack Nuclei

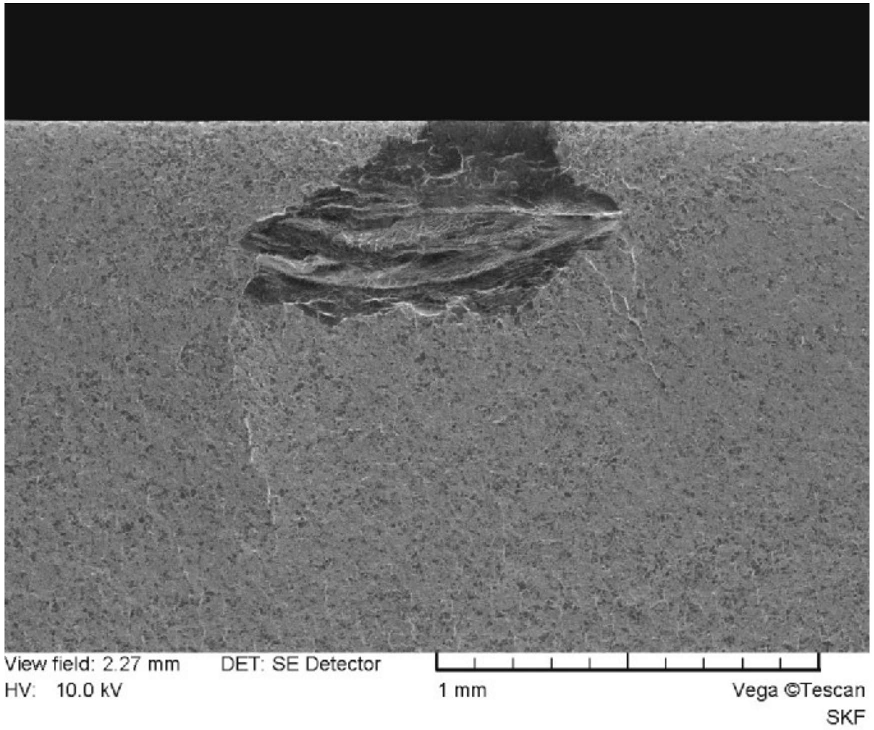

origin of hydrogen sorption

(Semi-) Circular Brittle Spontaneous Incipient Cracks
2. No Distinct Crack Nuclei

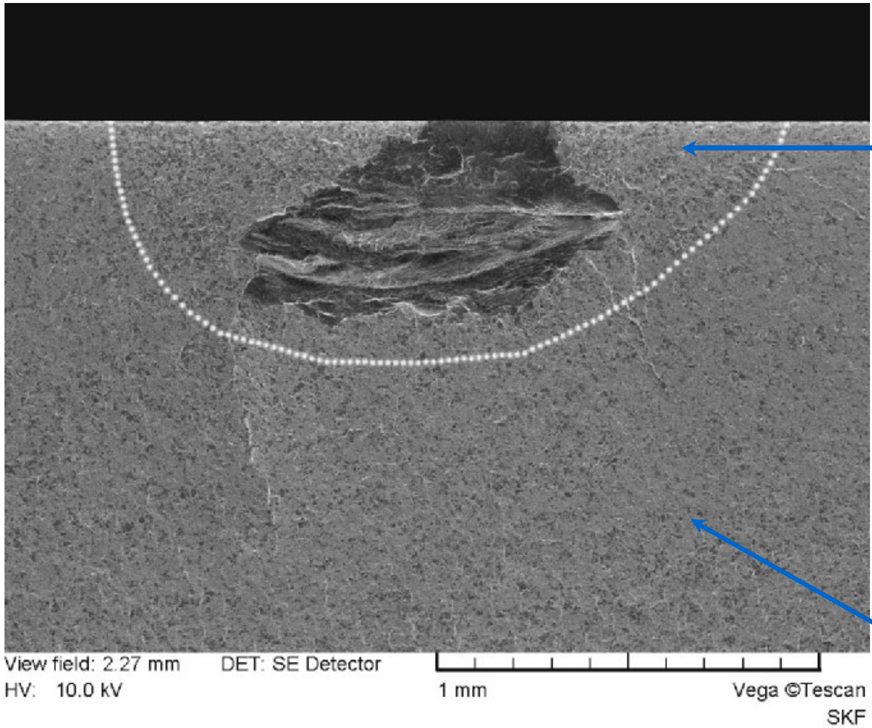

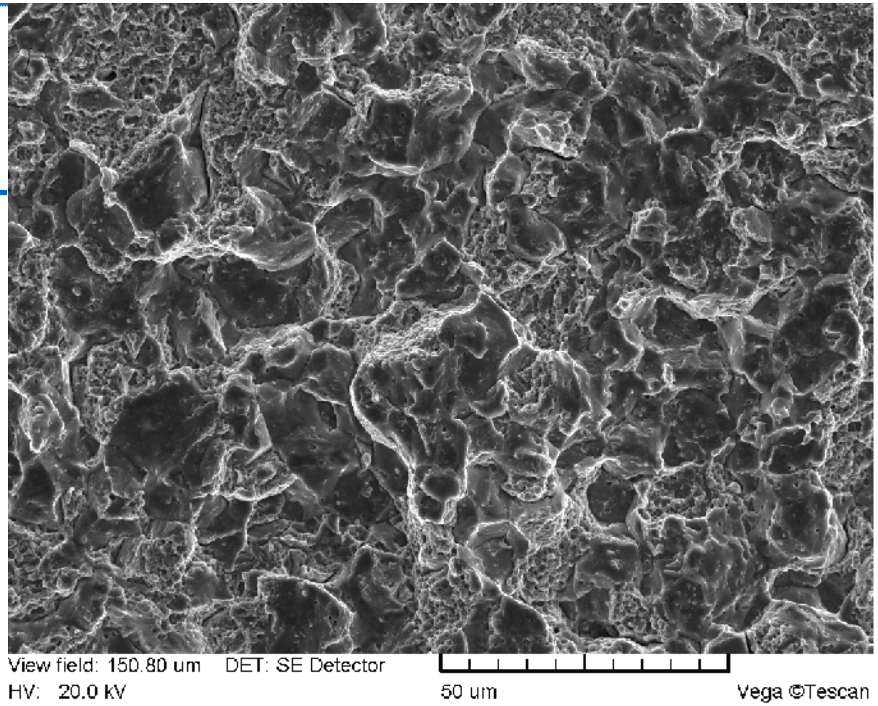

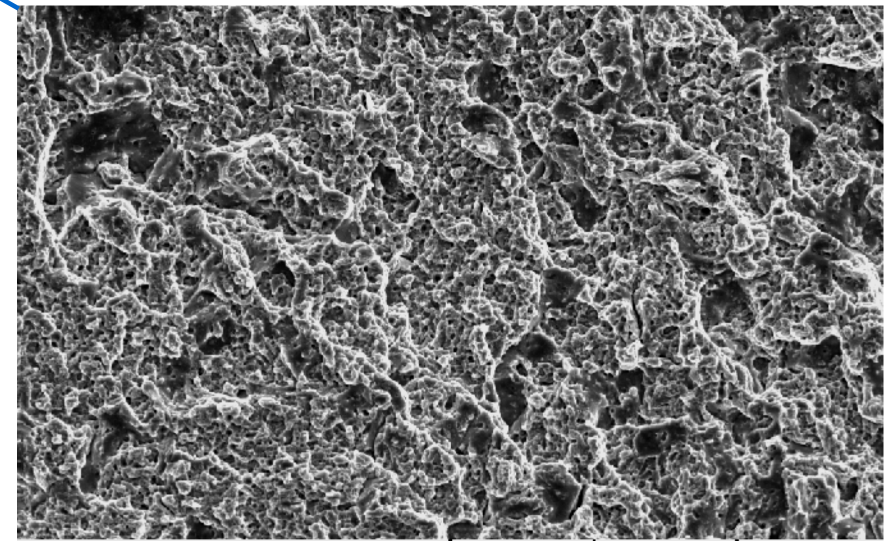

origin of hydrogen sorption

- local H embrittlement

(Semi-) Circular Brittle Spontaneous Incipient Cracks
2. No Distinct Crack Nuclei

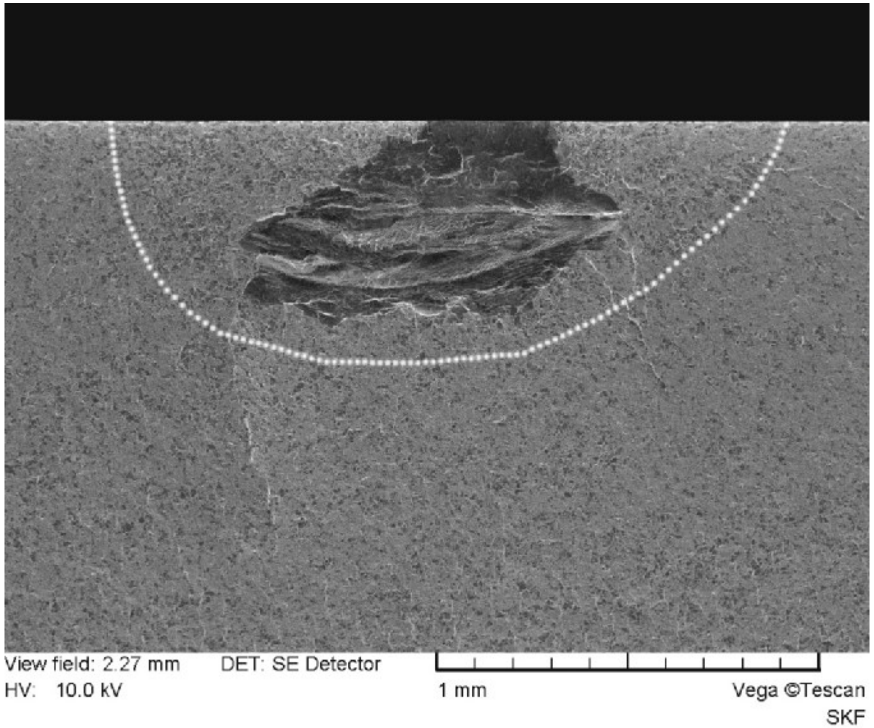

origin of hydrogen sorption

- local H embrittlement

30 mm mean ring thickness

CGHE: ± 0.2 ppm H

3 mm sample height

Raceway	1.8 ppm H
Center	1.4 ppm H
Bore	0.6 ppm H

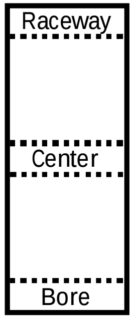

(Semi-) Circular Brittle Spontaneous Incipient Cracks
2. No Distinct Crack Nuclei

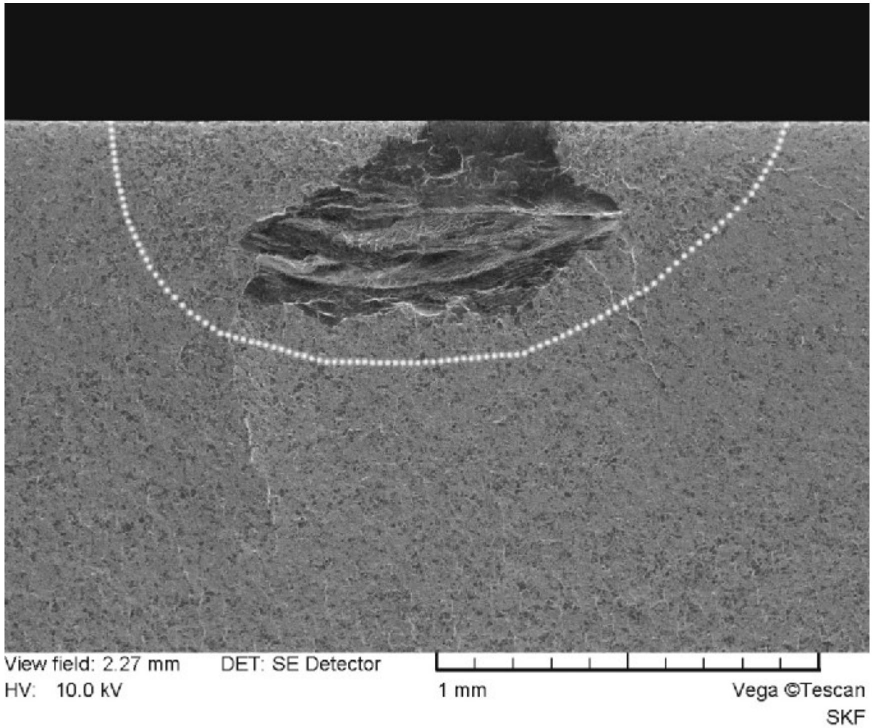

30 mm mean ring thickness

CGHE: ± 0.2 ppm H

3 mm sample height

Raceway	1.8 ppm H
Center	1.4 ppm H
Bore	0.6 ppm H

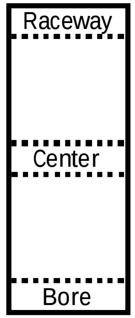

⇒ just several weeks to to few months of hydrogen in-diffusion

origin of hydrogen sorption

- local H embrittlement

is dense *cleavage* surface cracking (penetrating lubricant on CFC cracks)

(Semi-) Circular Brittle Spontaneous Incipient Cracks
2. No Distinct Crack Nuclei

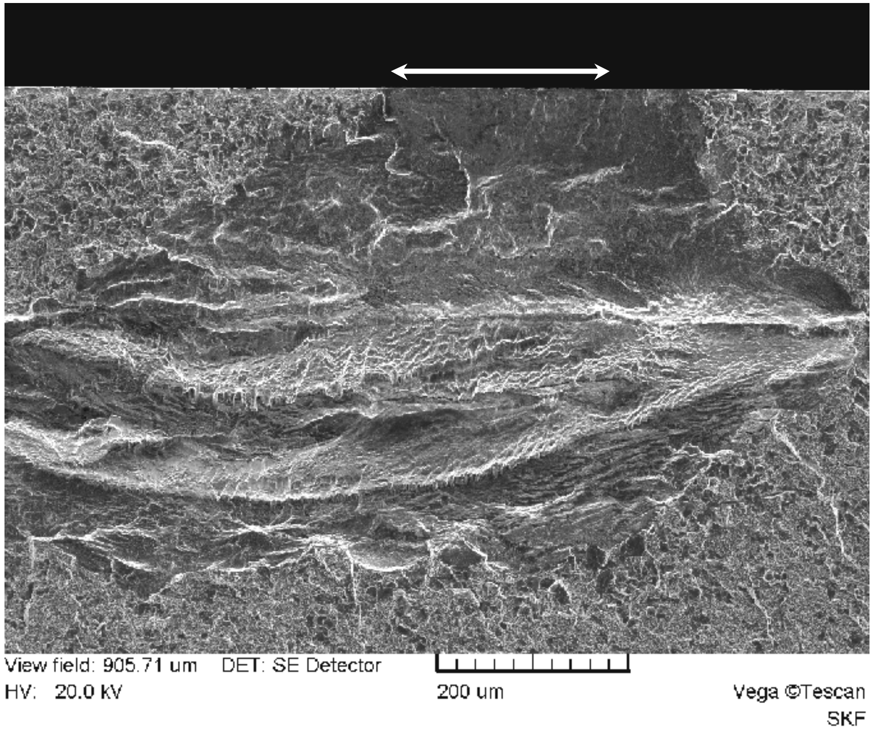

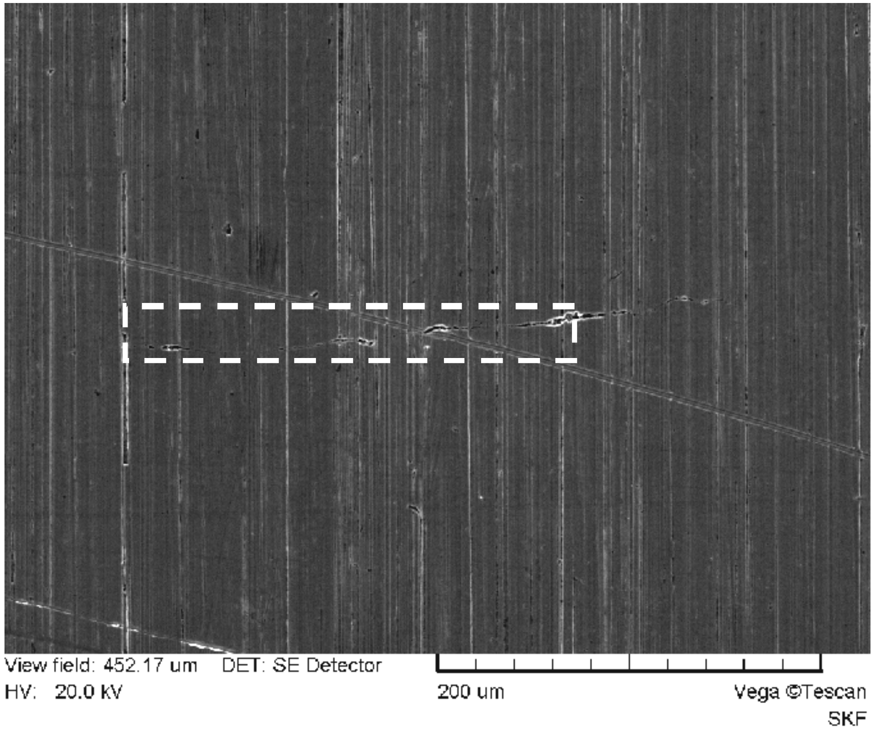

vertical semicircular *cleavage* fracture

- sharp crack edges indicate the incipient hairline *cleavage*

(Semi-) Circular Brittle Spontaneous Incipient Cracks
2. No Distinct Crack Nuclei

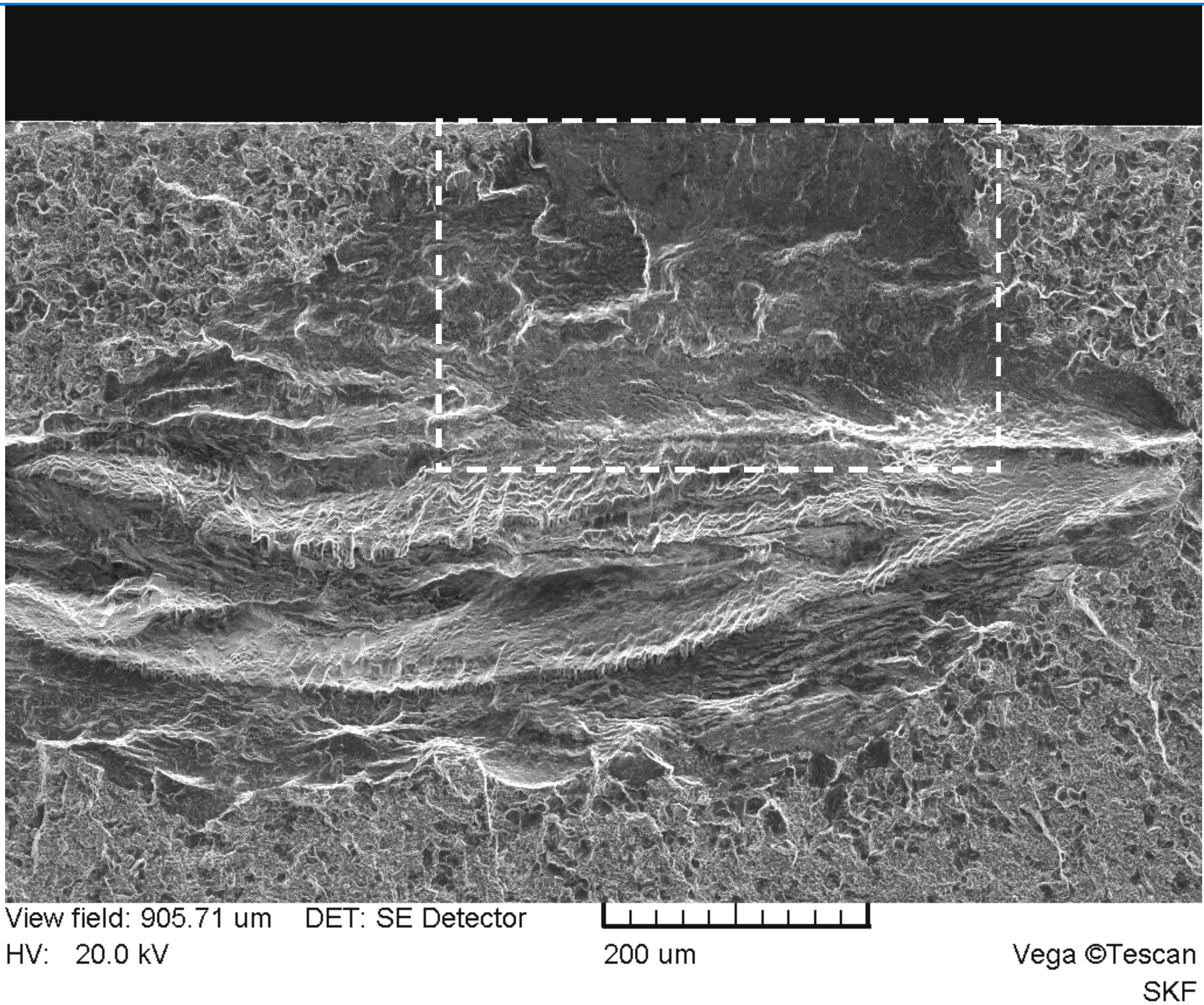

- striations and ...

(Semi-) Circular Brittle Spontaneous Incipient Cracks
2. No Distinct Crack Nuclei

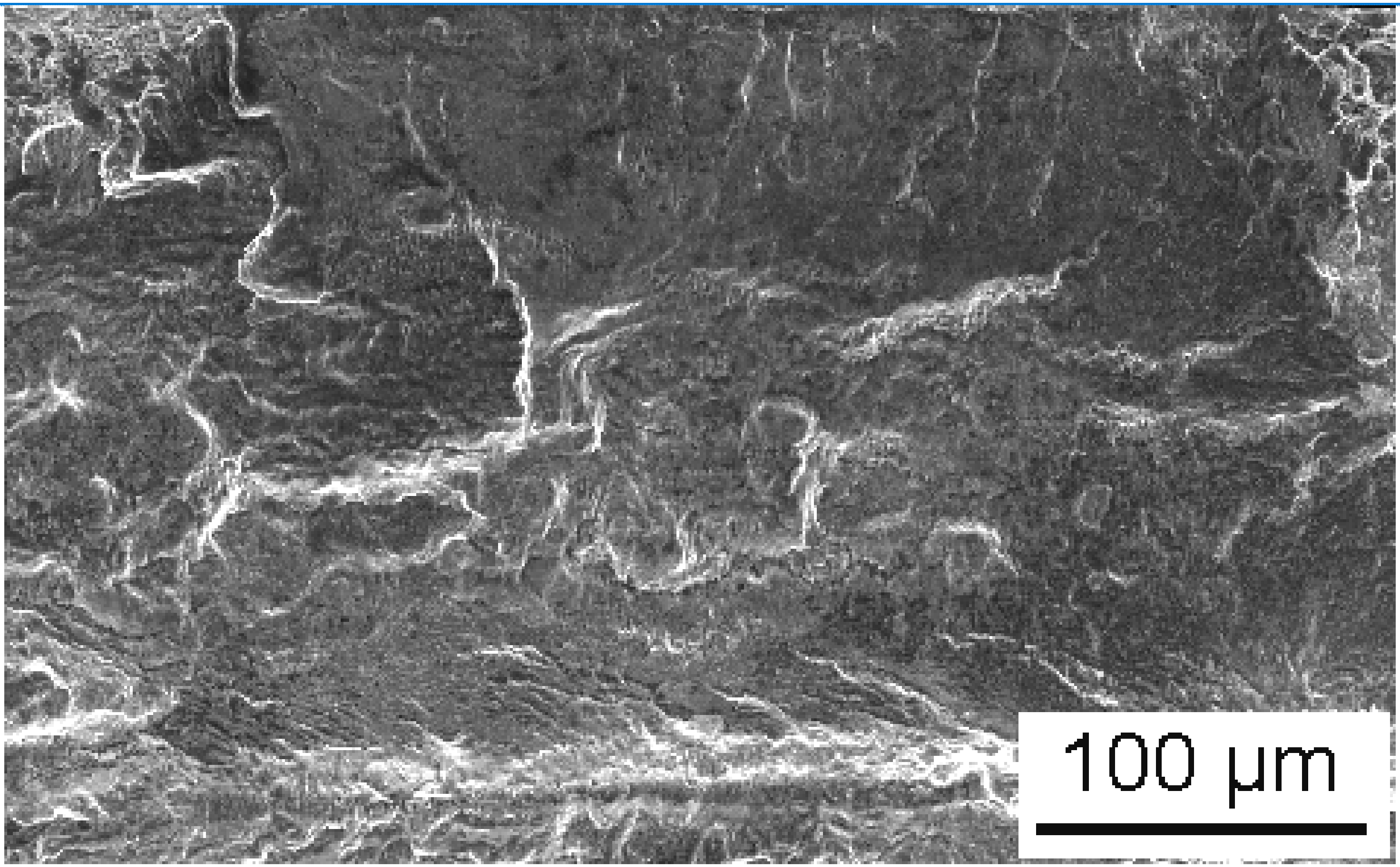

- side cracks and pores at the runout of the *cleavage* fracture

detail

(Semi-) Circular Brittle Spontaneous Incipient Cracks
2. No Distinct Crack Nuclei

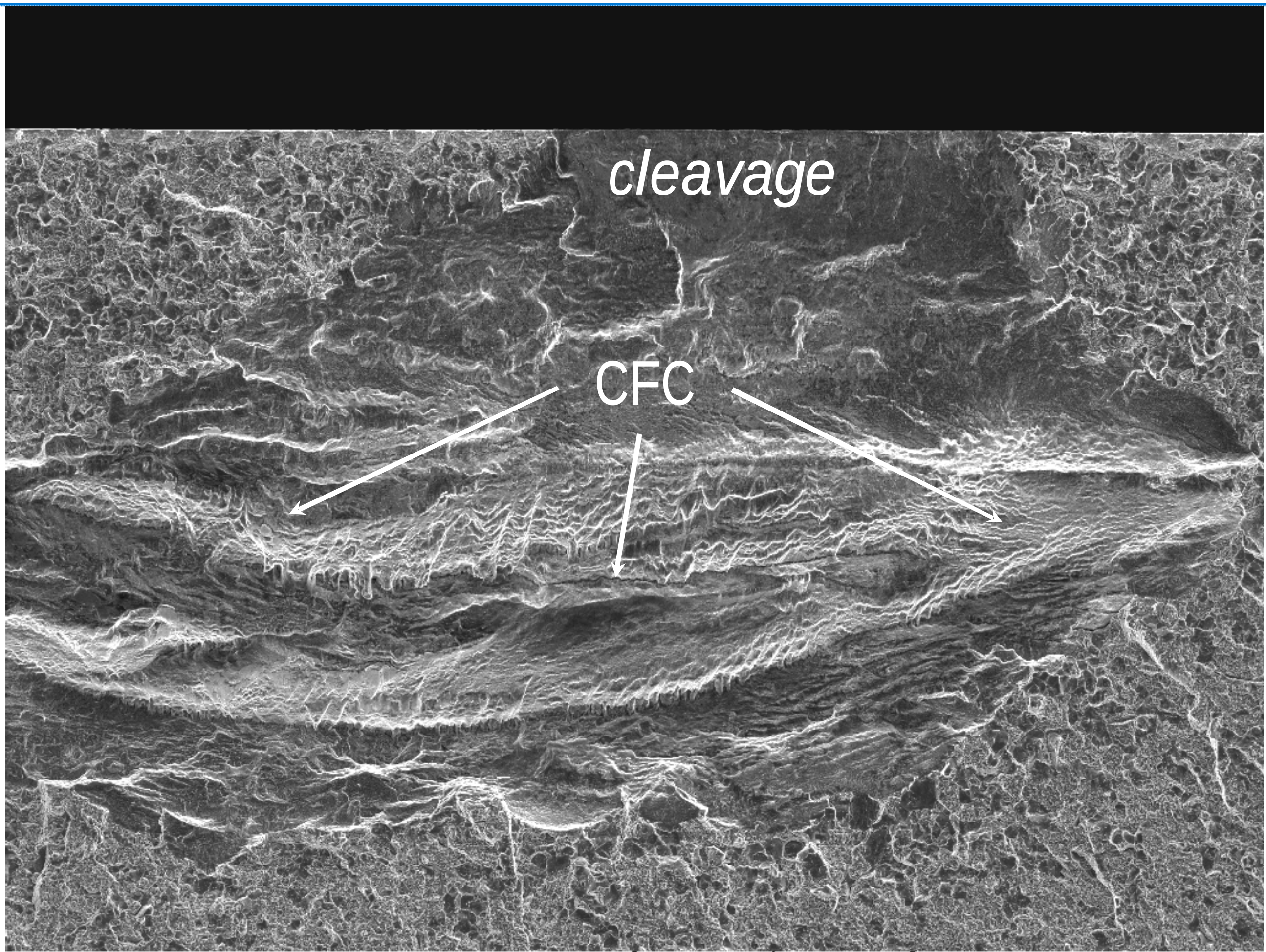

View field: 905.71 um DET: SE Detector
HV: 20.0 kV 200 um Vega ©Tescan
SKF

step 1

step 2

total fracture face is transgranular

- *cleavage* fracture initiates CFC

(Semi-) Circular Brittle Spontaneous Incipient Cracks
2. No Distinct Crack Nuclei

EPMA-EDX (10 kV)

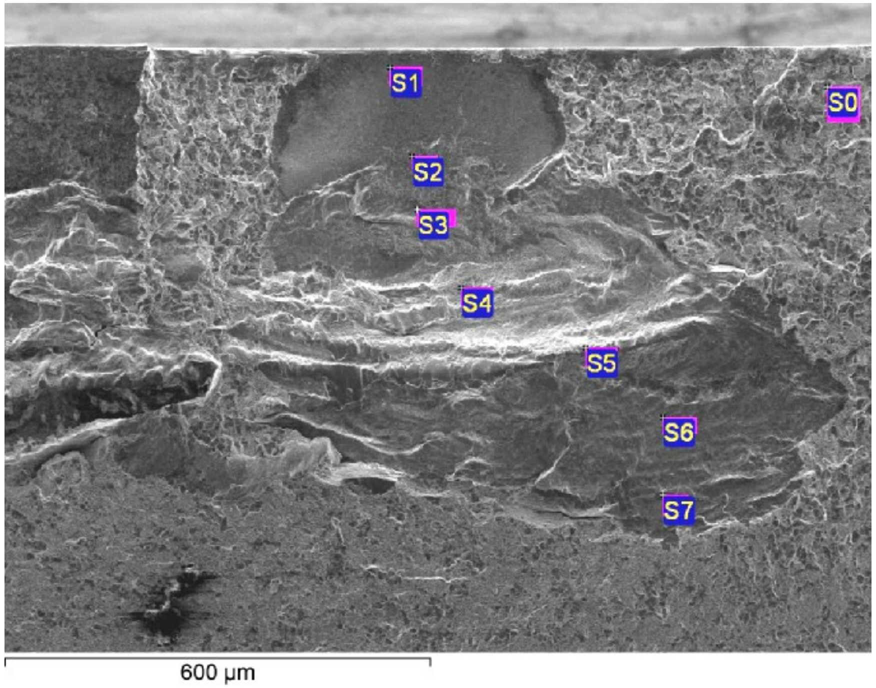

- lens and CFC deep crack

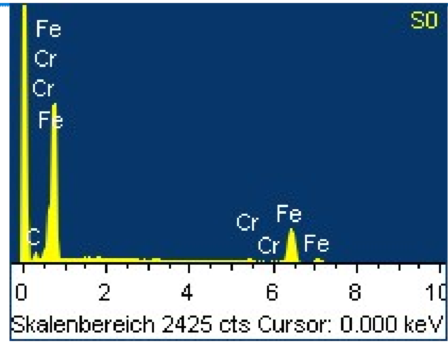

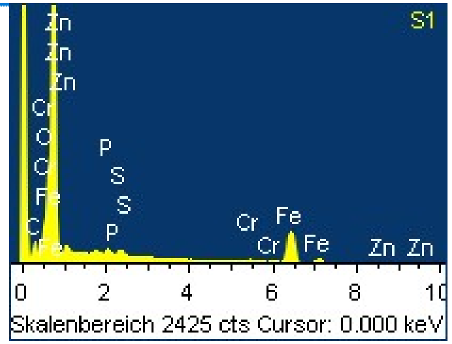

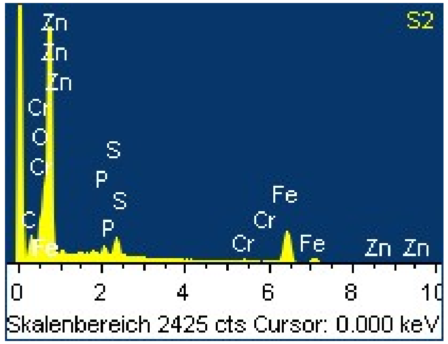

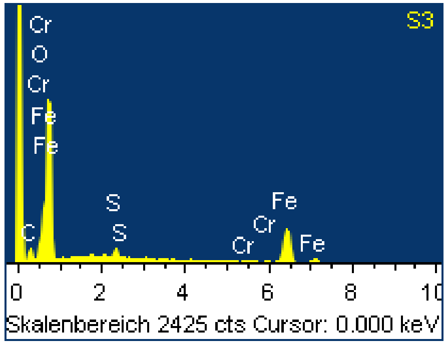

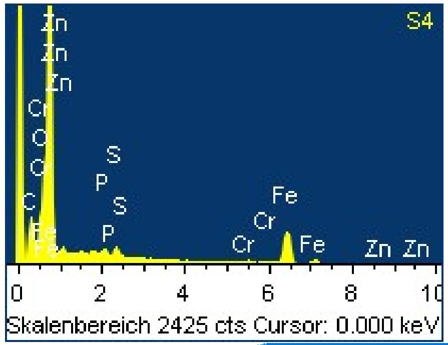

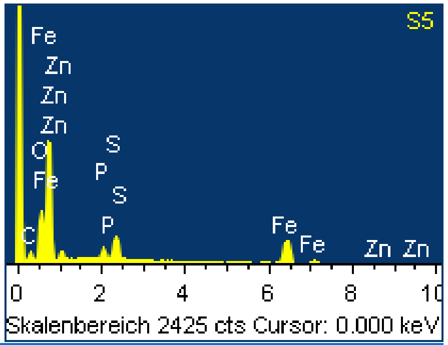

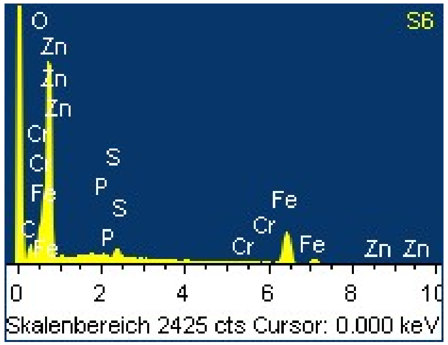

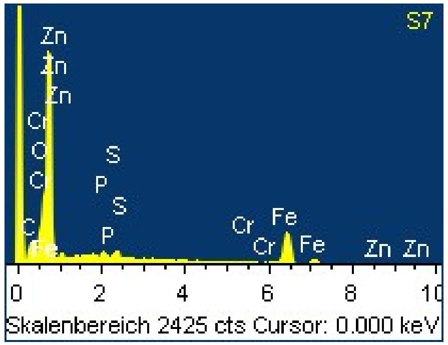

SKF

4

Cleavage Crack Initiation by Frictional Tensile Stresses

Crack Initiation by Frictional Tensile Stresses
1. CRS Buildup near Indentation-Free Raceway Surfaces

material loading by equivalent shear stresses caused by vibrations

Ÿ both types of vibration residual stress pattern occur in WEC cases

ú J. Gegner and W. Nierlich: AXA 52 (2008) 722-731

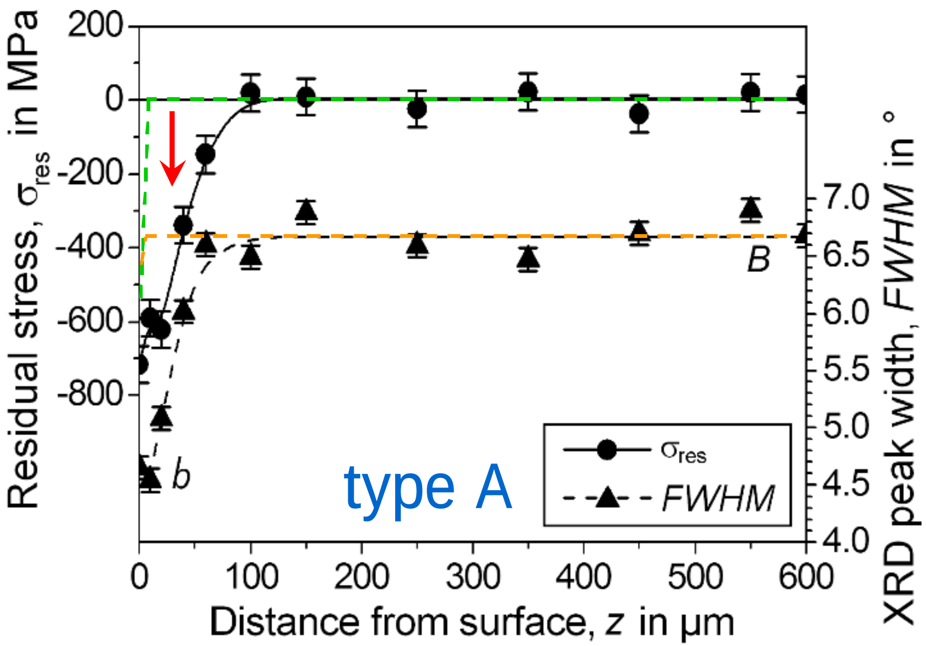

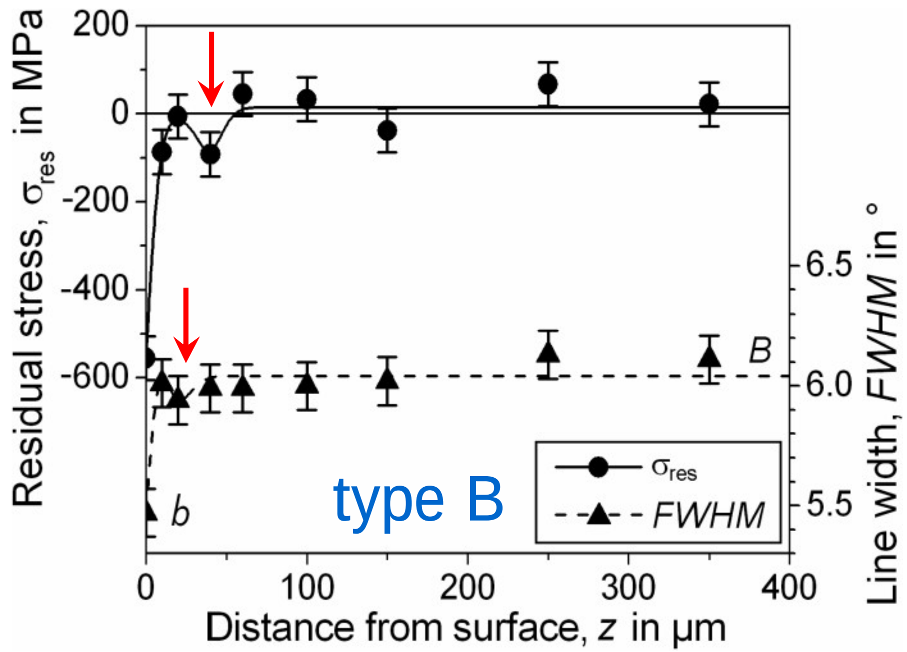

Crack Initiation by Frictional Tensile Stresses
2. Equivalent Stress Distribution in Rolling-Sliding Contact

material loading by equivalent shear stresses caused by vibrations

Ÿ both types of vibration residual stress pattern occur in WEC cases

ú tribological model of localized friction coefficient

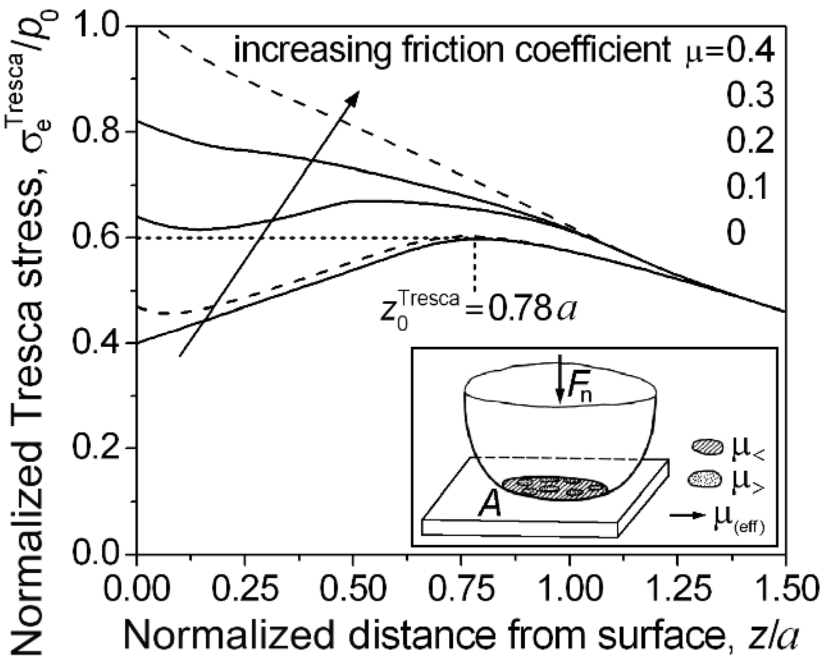

increasing friction shifts the max. equivalent stress to the surface

a semiminor axis of the contact area

Broszeit et al., 1977

Crack Initiation by Frictional Tensile Stresses
2. Equivalent Stress Distribution in Rolling-Sliding Contact

material loading by equivalent shear stresses caused by vibrations

Ÿ both types of vibration residual stress pattern occur in WEC cases

ú tribological model of localized friction coefficient

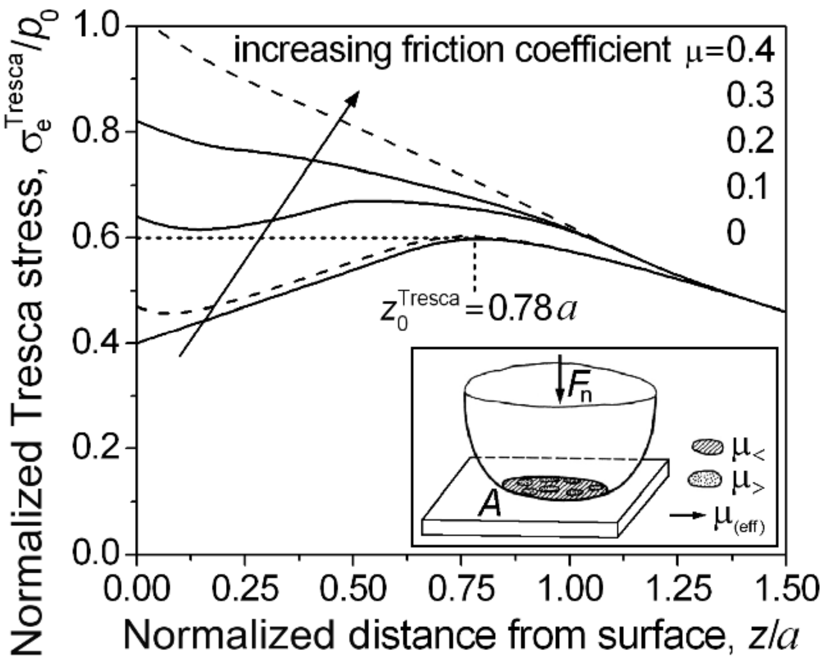

increasing friction shifts the max. equivalent stress to the surface

$\Rightarrow \mu_> \geq 0.4$ occurs

- intermittently varying $\mu_>$ and $\mu_<$

  $\Rightarrow \mu_{(eff)} < 0.1$

- shear sensitive viscosity

Broszeit et al., 1977

Crack Initiation by Frictional Tensile Stresses
2. Equivalent Stress Distribution in Rolling-Sliding Contact

material loading by equivalent shear stresses caused by vibrations

Ÿ both types of vibration residual stress pattern occur in WEC cases

ú tribological model of localized friction coefficient

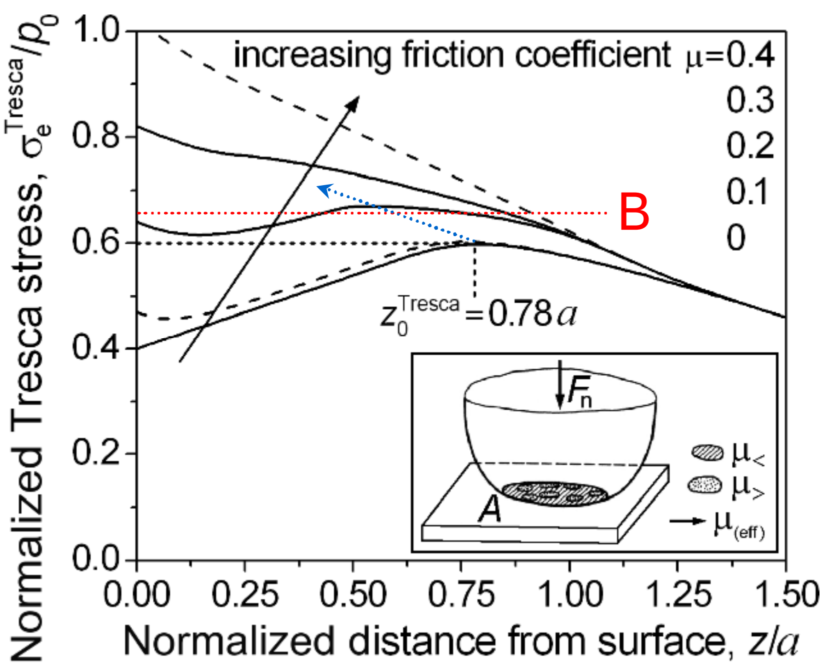

type B $\xrightarrow{\mu_> > 0.25}$ type A

- intermittently varying $\mu_>$ and $\mu_<$

  $\Rightarrow \mu_{(eff)} < 0.1$
- shear sensitive viscosity

Broszeit et al., 1977

Crack Initiation by Frictional Tensile Stresses
3. Tangential Tensile Stresses at the Contact Runout

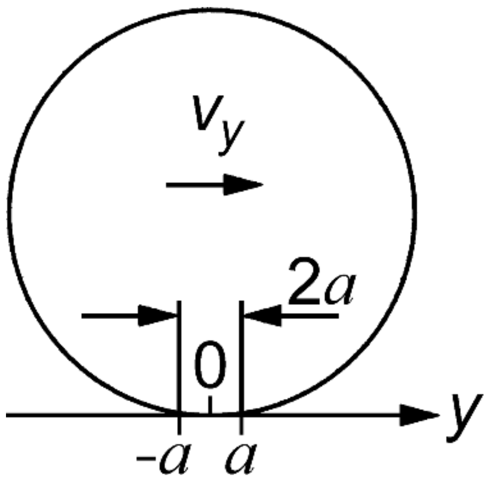

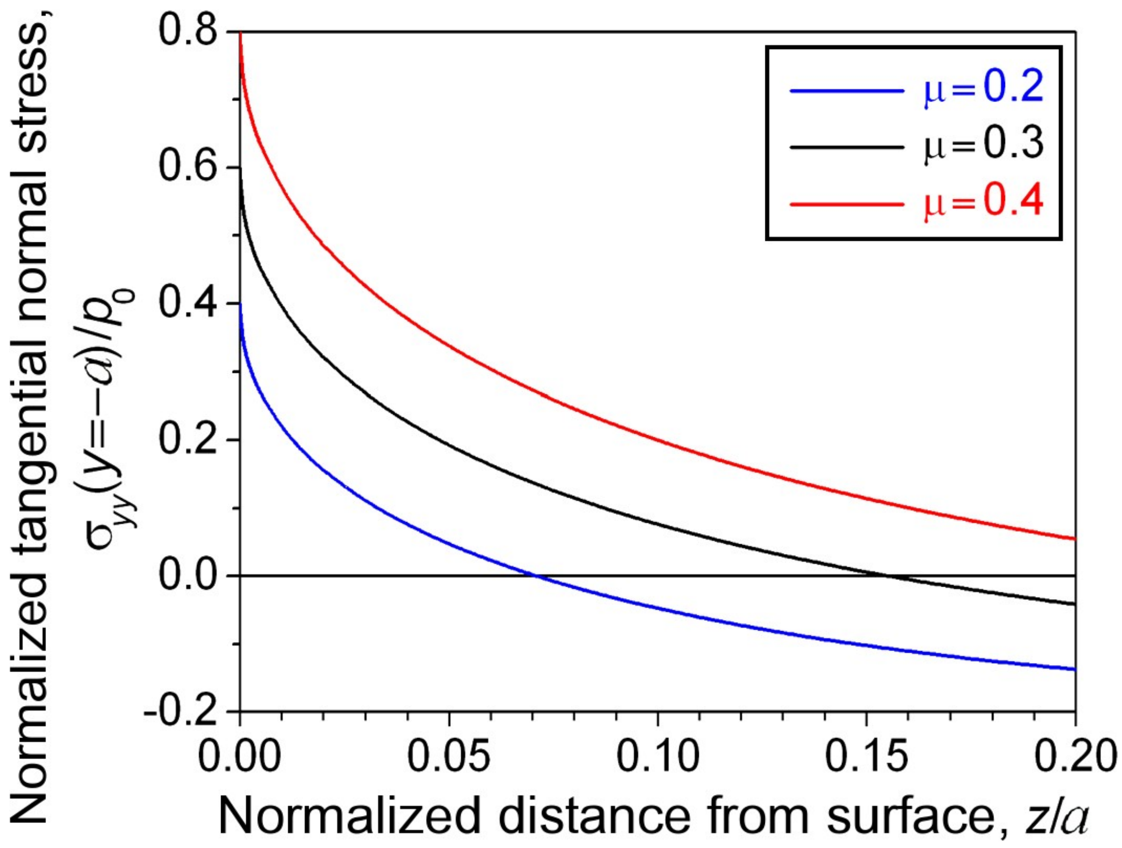

maximum at $z=0$: 2μ

Karas, 1941

Crack Initiation by Frictional Tensile Stresses
4. Normal Stress Hypothesis

Equivalent stress:

$$\sigma_e^{nsh} = \sigma_{yy}(y = -a)$$

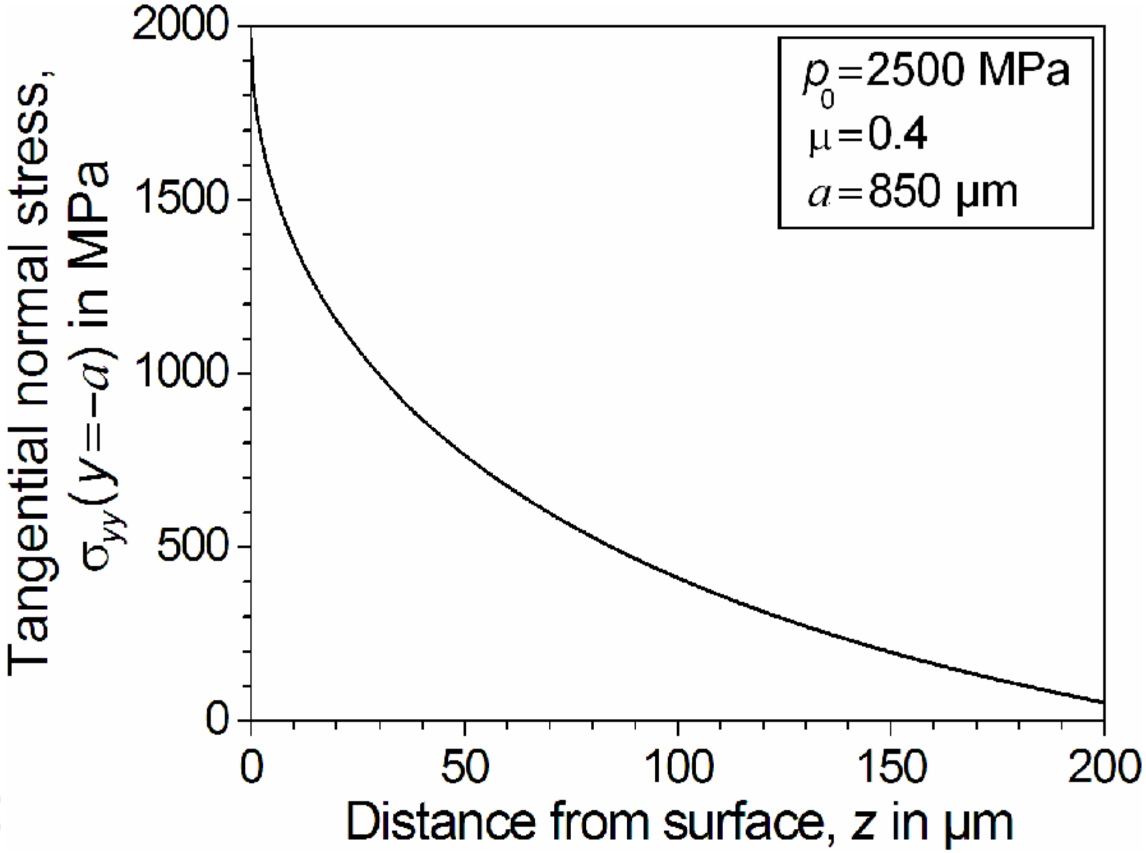

real peak load condition:

spontaneous crack initiation

Ÿ no fatigue

IR-TRB, wind turbine gearbox

Crack Initiation by Frictional Tensile Stresses
4. Normal Stress Hypothesis

Equivalent stress:

$$\boxed{\sigma_e^{nsh} = \sigma_{yy}(y = -a)}$$

Failure range:

$$\boxed{\sigma_e^{nsh}(z) \geq \sigma_{cF}(z)}$$

$\sigma_{cF}(z)$ *cleavage* fracture strength

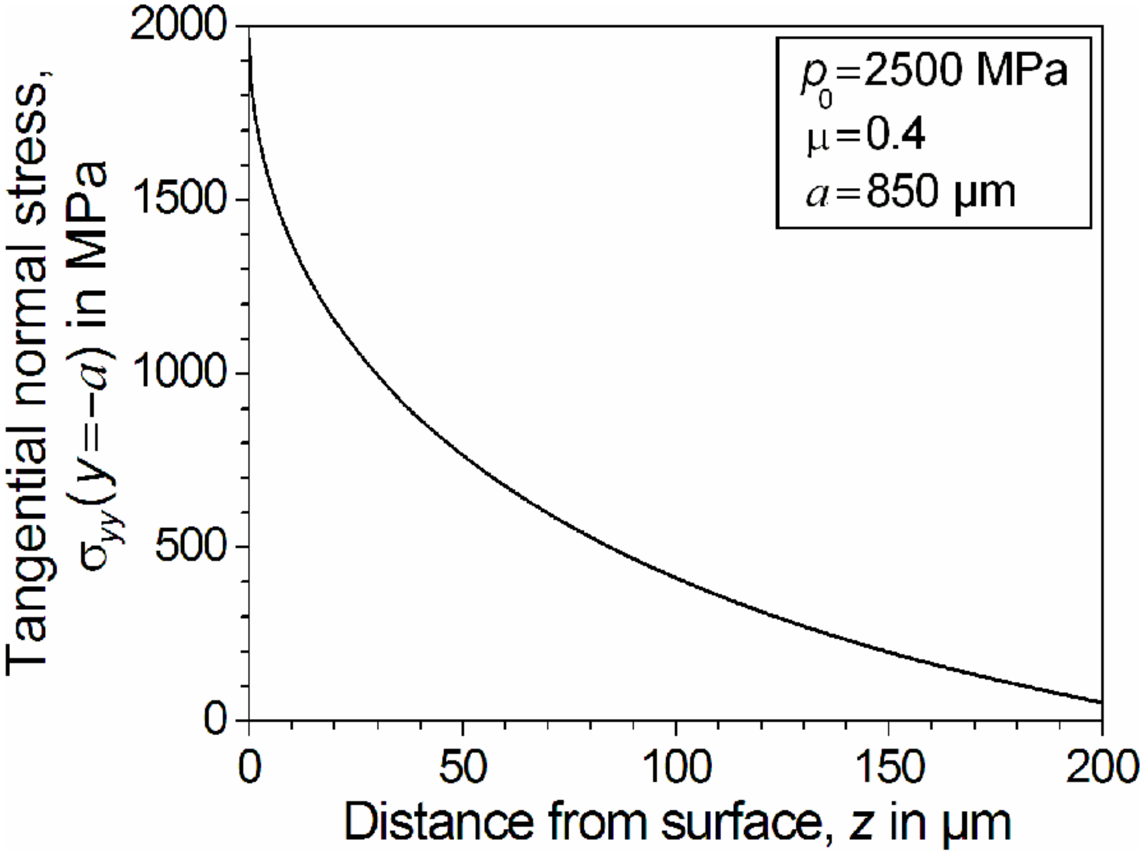

IR-TRB, wind turbine gearbox

Crack Initiation by Frictional Tensile Stresses
4. Normal Stress Hypothesis

Equivalent stress:

$$\sigma_e^{nsh} = \sigma_{yy}(y = -a)$$

Failure range:

$$\sigma_e^{nsh}(z) \geq \sigma_{cF}(z)$$

$\sigma_{cF}(z)$ *cleavage* fracture strength

$$\sigma_{cF} \approx R_e$$

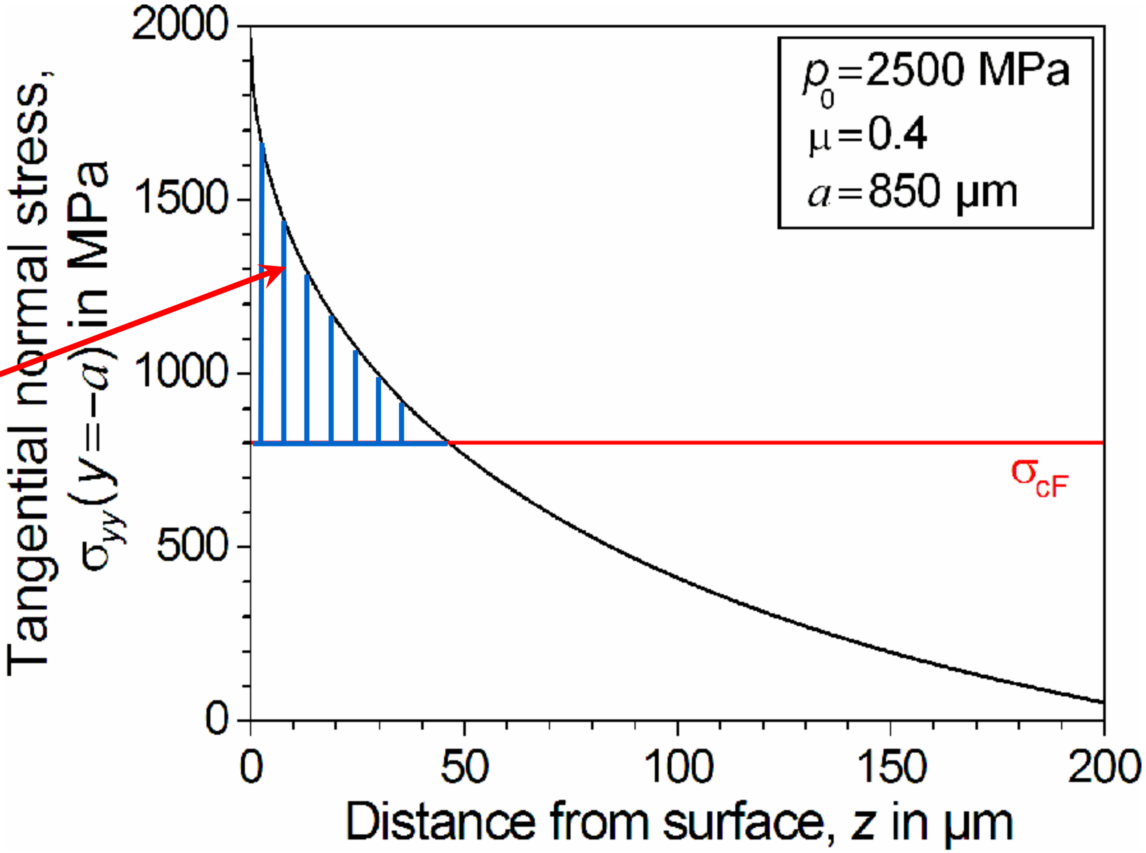

IR-TRB, wind turbine gearbox

Crack Initiation by Frictional Tensile Stresses
4. Normal Stress Hypothesis

Equivalent stress:

$$\sigma_{e}^{nsh} = \sigma_{yy}(y = -a)$$

Failure range:

$$\sigma_{e}^{nsh}(z) \geq \sigma_{cF}(z)$$

$\sigma_{cF}(z)$ *cleavage* fracture strength

$$\sigma_{cF} \approx R_e$$

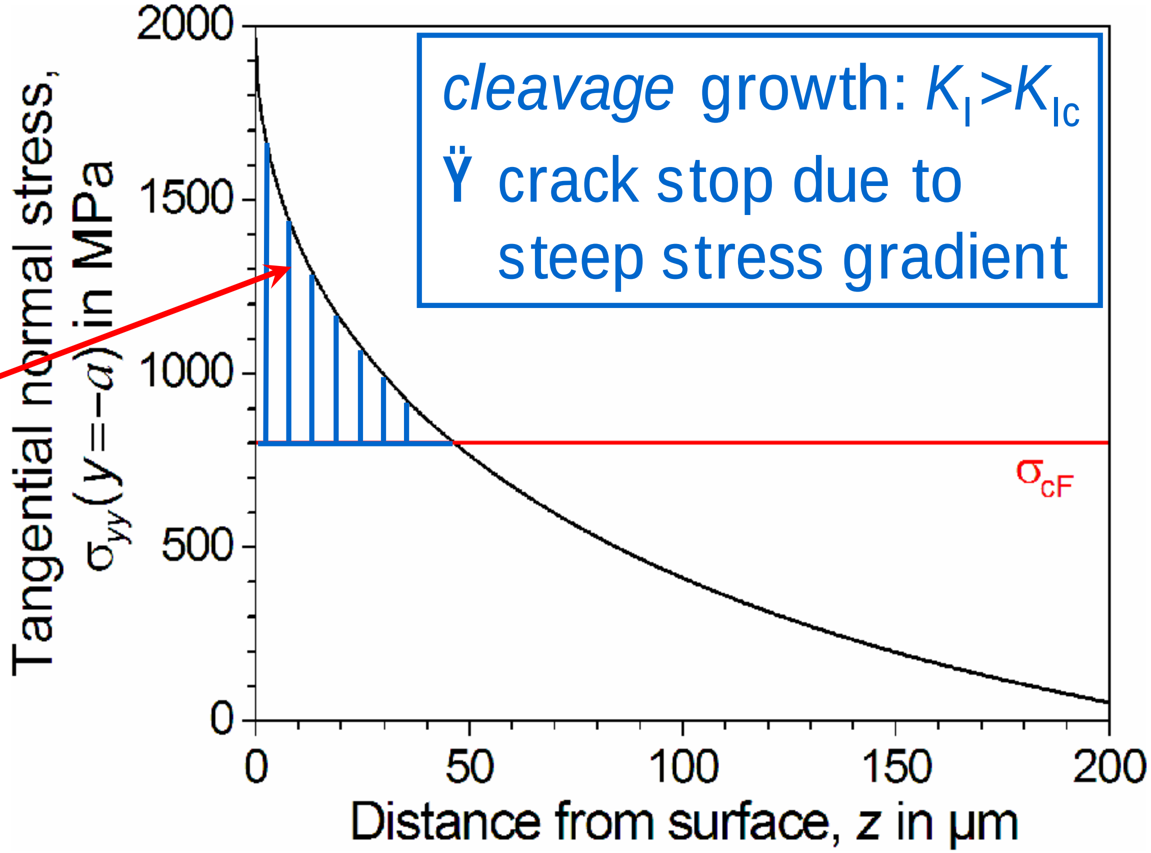

IR-TRB, wind turbine gearbox

SKF

Crack Initiation by Frictional Tensile Stresses
4. Normal Stress Hypothesis

Equivalent stress:

$$\boxed{\sigma_e^{nsh} = \sigma_{yy}(y = -a)}$$

Failure range:

$$\boxed{\sigma_e^{nsh}(z) \geq \sigma_{cF}(z)}$$

$\sigma_{cF}(z)$ *cleavage* fracture strength (surface embrittlement)

$$\boxed{\sigma_{cF} \approx R_e}$$

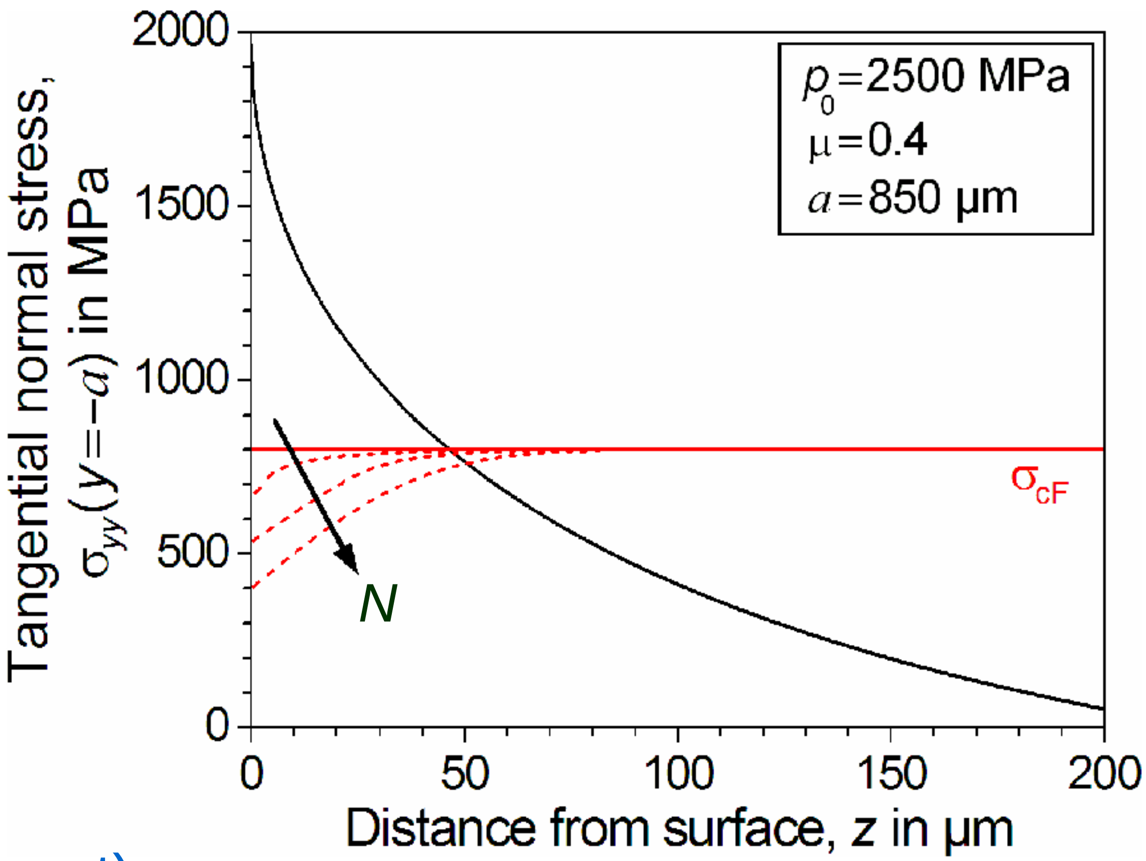

IR-TRB, wind turbine gearbox

N number of ring revolutions

Crack Initiation by Frictional Tensile Stresses
4. Normal Stress Hypothesis

Equivalent stress:

$$\boxed{\sigma_e^{nsh} = \sigma_{yy}(y=-a) + \sigma_{res}}$$

Failure range:

$$\boxed{\sigma_e^{nsh}(z) \geq \sigma_{cF}(z)}$$

$\sigma_{cF}(z)$ *cleavage* fracture strength (surface embrittlement)

$$\boxed{\sigma_{cF} \approx R_e}$$

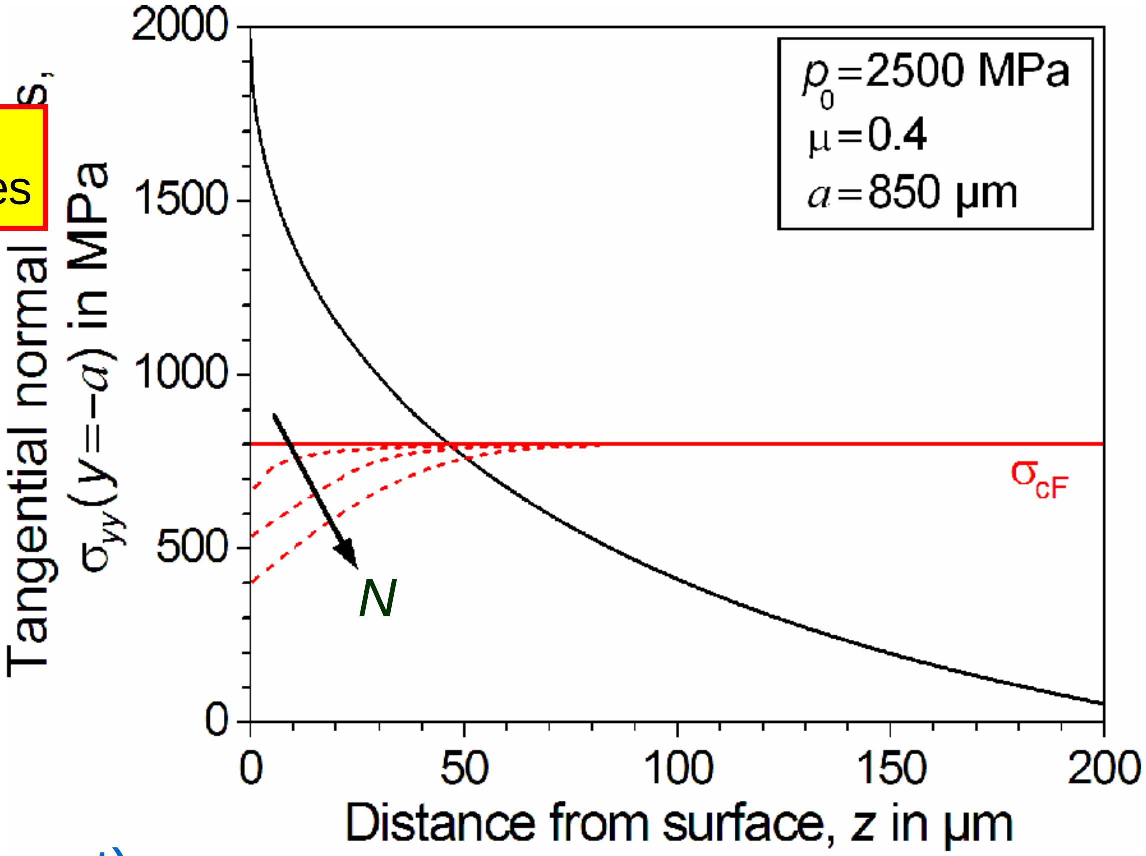

IR-TRB, wind turbine gearbox

Crack Initiation by Frictional Tensile Stresses
4. Normal Stress Hypothesis

Equivalent stress:

$$\sigma_e^{nsh} = \sigma_{yy}(y = -a) + \sigma_{res}$$

Failure range:

$$\sigma_e^{nsh}(z) \geq \sigma_{cF}(z)$$

$\sigma_{cF}(z)$ *cleavage* fracture strength (surface embrittlement)

$$\sigma_{cF} \approx R_e$$

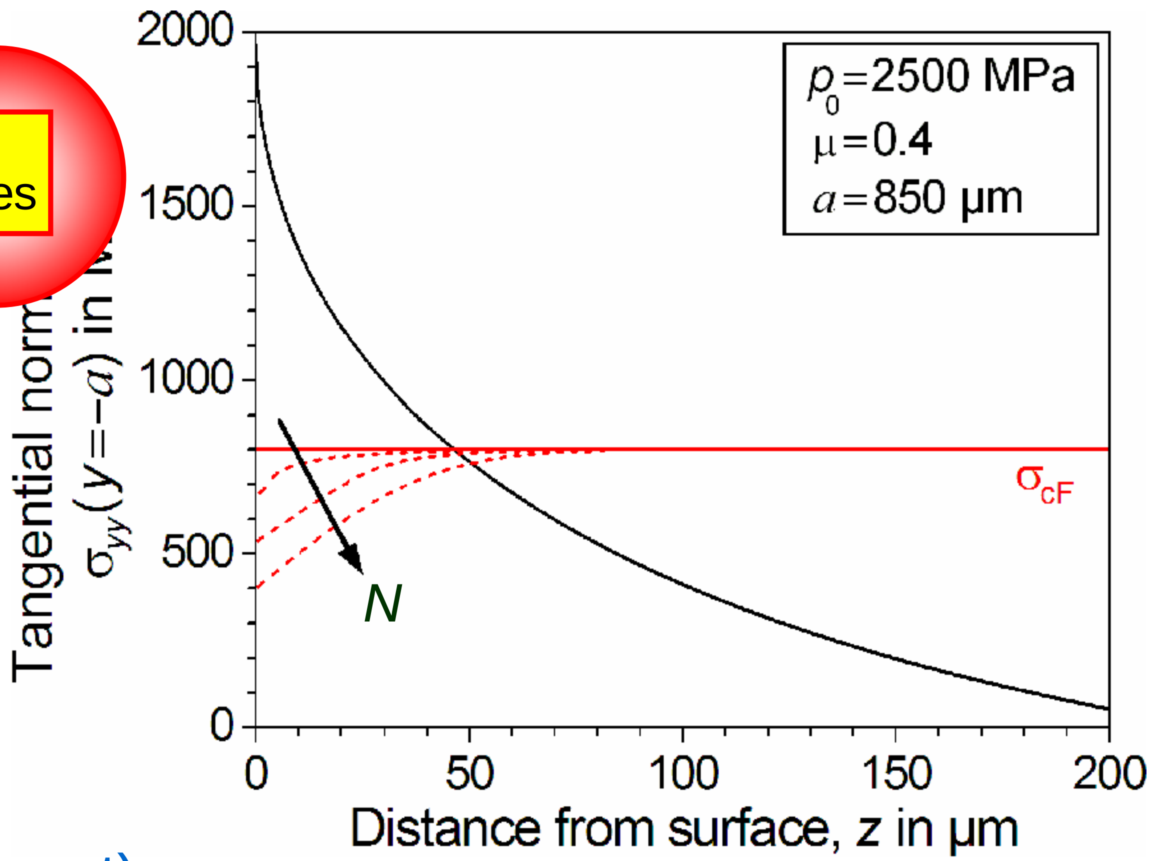

IR-TRB, wind turbine gearbox

5

WEC Early Failure Prevention – Measures against Surface Cracks

Measures against Frictional Surface Cracking

compressive residual stresses by cold working

Ÿ successfully proven in mixed friction loaded rolling contact

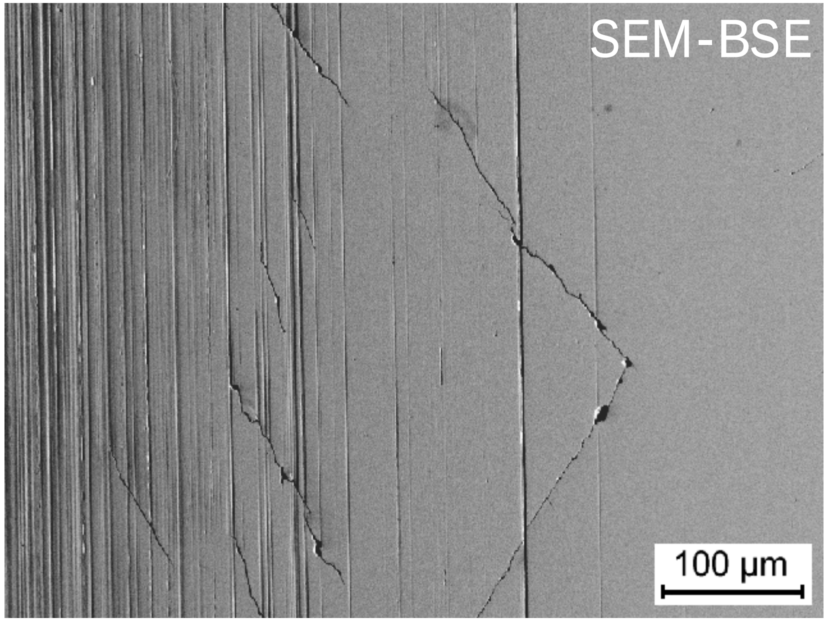

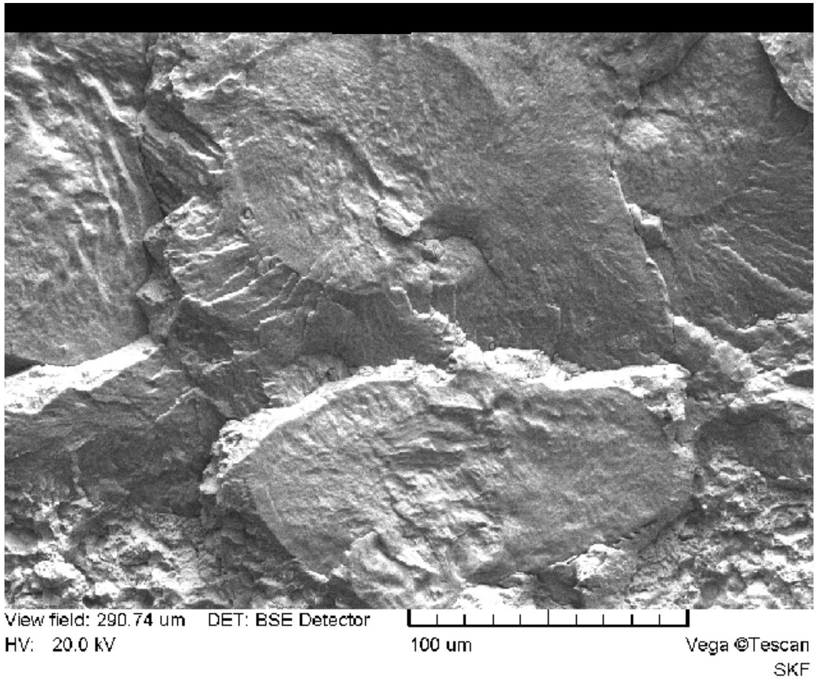

roller-on-disk rig test

Measures against Frictional Surface Cracking

compressive residual stresses by cold working

Ÿ successfully proven in mixed friction loaded rolling contact

ú *cleavage* cracks reproduced

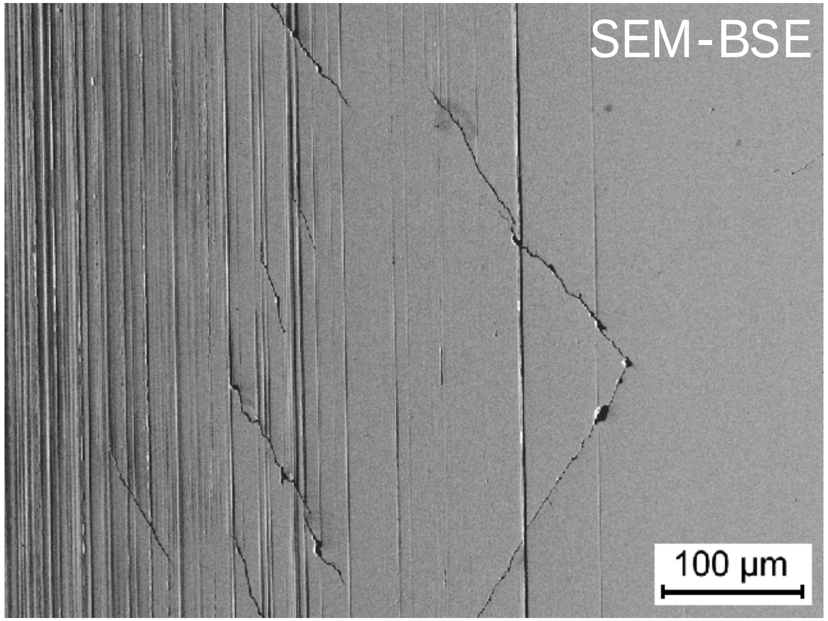

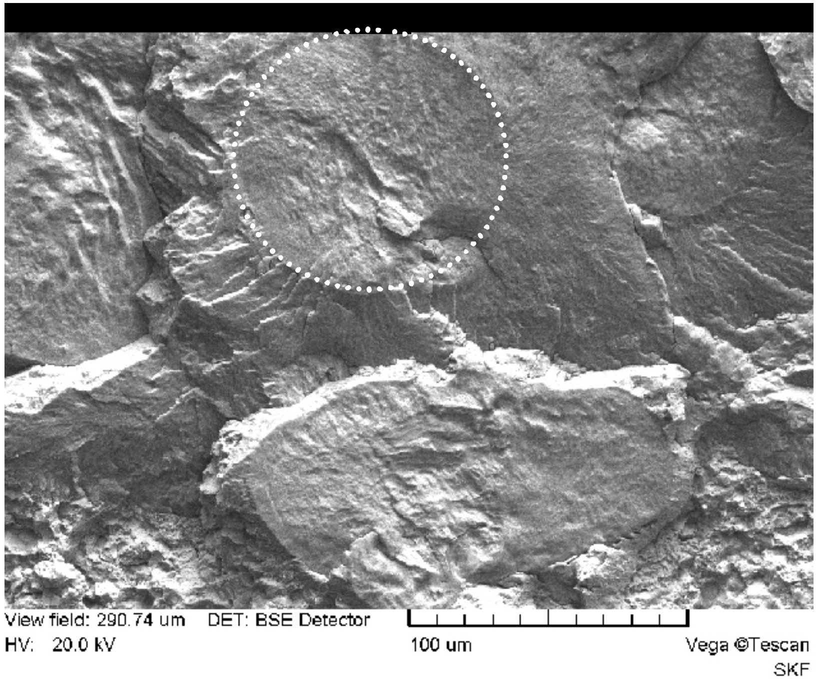

roller-on-disk rig test

Measures against Frictional Surface Cracking

compressive residual stresses by cold working

- successfully proven in mixed friction loaded rolling contact
  - *cleavage* cracks reproduced

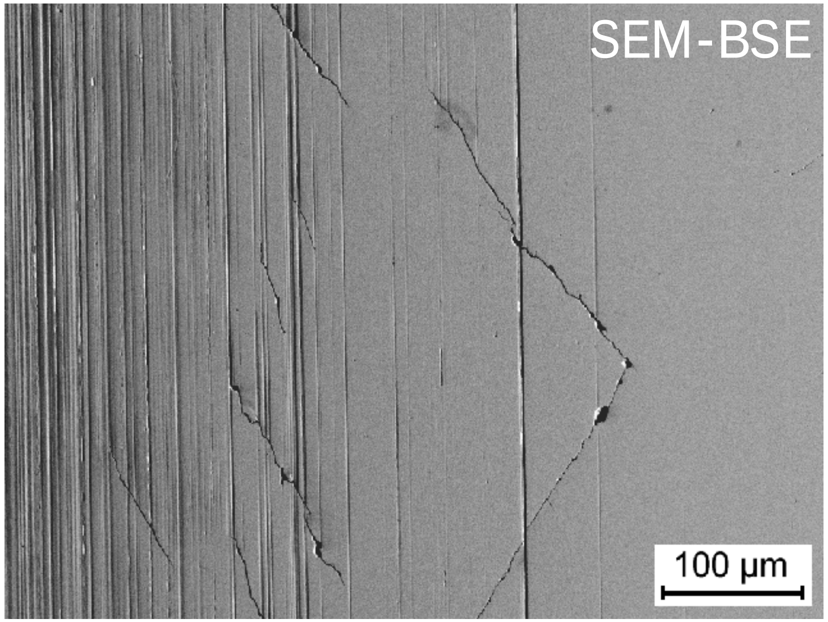

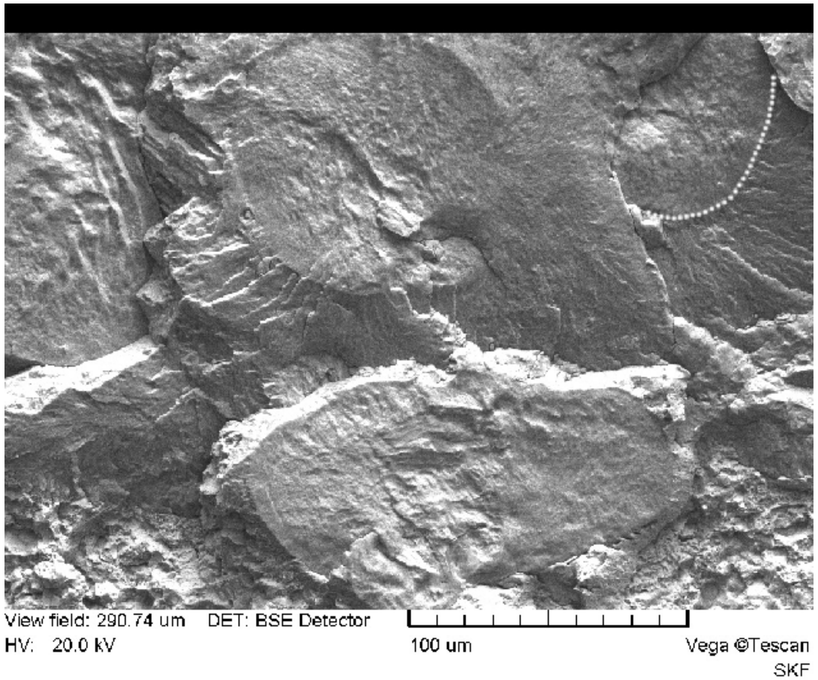

roller-on-disk rig test

Measures against Frictional Surface Cracking

compressive residual stresses by cold working

- successfully proven in mixed friction loaded rolling contact
  - *cleavage* cracks reproduced and prevented by deep rolling

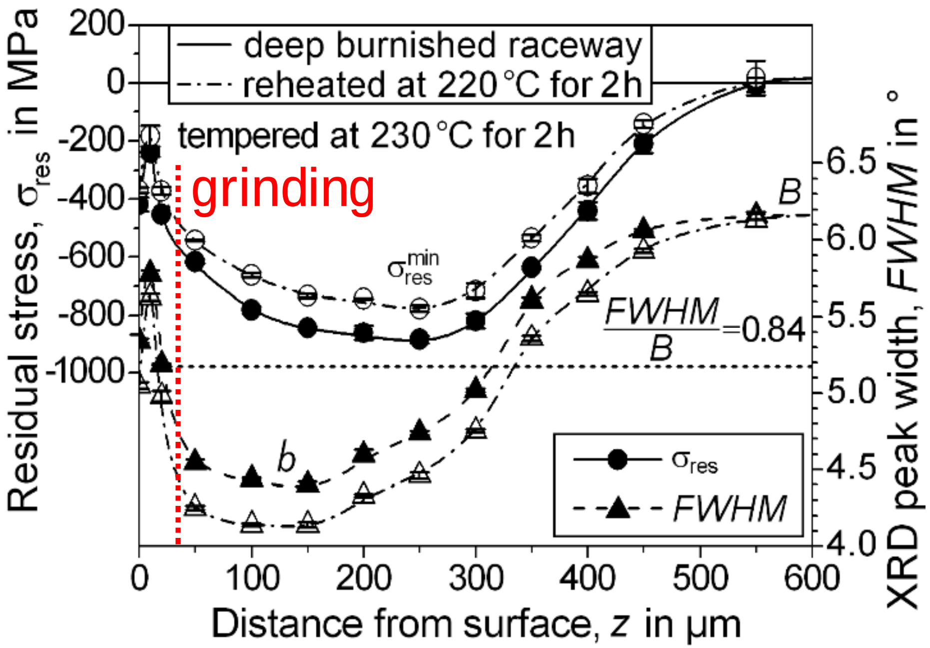

Measures against Frictional Surface Cracking

compressive residual stresses by cold working

Ÿ successfully proven in mixed friction loaded rolling contact

ú *cleavage* cracks reproduced and prevented by deep rolling

\+ black oxidizing: reduced micro friction under peak loading

\+ thermal post-treatment

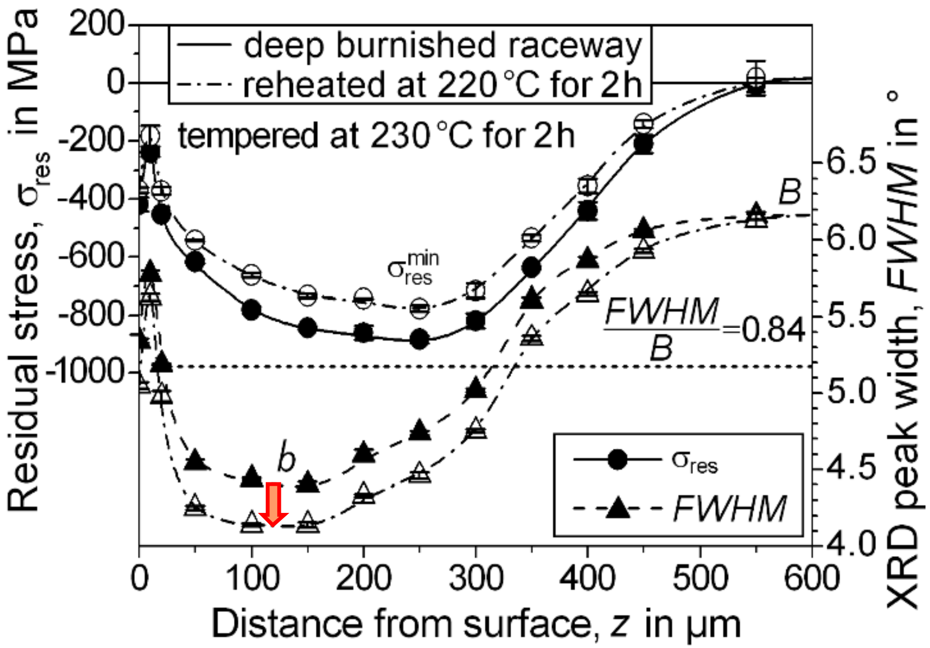

Measures against Frictional Surface Cracking

compressive residual stresses by cold working

Ÿ successfully proven in mixed friction loaded rolling contact

  ú *cleavage* cracks reproduced and prevented by deep rolling

\+ black oxidizing: reduced micro friction under peak loading

\+ thermal post-treatment

  ú reheating below HT tempering/transformation temperature

  ú microstructure stabilization by thermal static strain aging

  ú after grinding reported as full solution against WEC (Luyckx, 2011)

Measures against Frictional Surface Cracking

compressive residual stresses by cold working

- successfully proven in mixed friction loaded rolling contact
  - *cleavage* cracks reproduced and prevented by deep rolling

\+ black oxidizing: reduced micro friction under peak loading

\+ thermal post-treatment
  - reheating below HT tempering/transformation temperature
  - microstructure stabilization by thermal static strain aging
  - after grinding reported as full solution against WEC (Luyckx, 2011)

promising concept for WEC resistant wind turbine gearbox bearings

6

Conclusions

Conclusions

- results of failure analysis and research are presented
- axial raceway cracks in some medium and large size bearings
- root cause hypotheses from the literature are reviewed
- crack initiation by *cleavage* fracture and propagation by CFC
- hydrogen impact due to lubricant reactions at CFC crack tip/faces
- material response in the form of *cleavage* cracking suggests tangential tensile stresses acting, e.g., on weaker strength areas
  - inhomogeneities, near-surface material aging (embrittlement)
- tensile stresses are estimated to be high enough for cracking
- tensile stresses are caused by sliding friction e.g. due to vibrations
- cold working CRS & black oxidizing & reheating is proposed as effective countermeasure

Conclusions

- a textbook chapter on bearing failures & rolling contact tribology is available for free download:
  - http://www.intechopen.com/articles/show/title/tribological-aspects-of-rolling-bearing-failures

SKF®